[Papers in Palaeontology, 2024, e1544]

Late Ordovician and early Silurian virgianid and stricklandioid brachiopods from North Greenland: implications for a warm-water faunal province

by JISUO JIN[1,*], CHRISTIAN M. Ø. RASMUSSEN[2], PETER M. SHEEHAN[3] *and* DAVID A. T. HARPER[4]

[1]Department of Earth Science, University of Western Ontario, London, Ontario N6A 5B7, Canada; jjin@uwo.ca
[2]Globe Institute, University of Copenhagen, Øster Voldgade 5–7, DK-1350 København K, Denmark
[3]Department of Geology, Milwaukee Public Museum, Milwaukee, Wisconsin 53233, USA
[4]Palaeoecosystems Group, Department of Earth Sciences, Durham University, Durham DH1 3LE, UK
*Corresponding author

Typescript received 4 July 2023; accepted in revised form 30 October 2023

Abstract: An unusually rich and diverse suite of virgianid brachiopods, hitherto poorly known, is systematically described here for the first time from the Ordovician–Silurian boundary interval (late Katian – Aeronian) of North Greenland. The Late Ordovician virgianids comprise typical taxa of the warm-water *Tcherskidium* fauna (e.g. *Tcherskidium tenuicostatum*, *Proconchidium schleyi*, *Holorhynchus giganteus* and *Deloprosopus dawesi* sp. nov.). Among the early Silurian taxa, *Virgiana hursti* sp. nov. occurs as abundant shell beds, similar to other congeneric species in Laurentia, but has somewhat larger internal skeletal structures, albeit not as extravagantly developed as in the late Katian virgianids; *Borealoides balderi* gen. et sp. nov. shows extreme thickening of the shell wall and internal structures, approaching the extravagant calcification of Katian virgianids. The highly distinctive mid-Aeronian stricklandioid brachiopod genus, *Kulumbella*, characterized by a shell with criss-cross (divaricate) ribbing, also occurs in North Greenland, represented by *K. heimdali* sp. nov., which has the largest and most strongly biconvex shells for the genus. Palaeogeographically, the Late Ordovician virgianid fauna of Laurentia was highly distinct, confined to the low–mid tropical latitudes north of the palaeoequator. In comparison, the early Silurian (Rhuddanian) *Virgiana* and some related taxa in Laurentia spanned the tropics of both hemispheres, forming extensive shell beds in carbonate basins, although *Borealis* and *Borealoides* gen. nov. remained confined largely to the northern hemisphere, suggesting a certain level of provincialism extending into the earliest Silurian. A palaeoecological preference for warm-water carbonate settings would explain the unusual abundance and richness of the virgianid faunas in North Greenland.

Key words: Virgianidae, Pentamerida, Brachiopoda, Late Ordovician, early Silurian, North Greenland.

THE brachiopod suborder Pentameridina first appeared in the Late Ordovician (late Katian), represented by the predominantly large and strongly convex shells of the family Virgianidae. During its origin and first pulse of diversification in the late Katian, the virgianids were confined largely to the tropical carbonate depositional environments of the Late Ordovician northern hemisphere (Rong *et al.* 1989; Kovalevskiy *et al.* 1991; Jin *et al.* 2022). This is in sharp contrast to the early Silurian when the post-extinction recovery virgianid fauna became nearly cosmopolitan throughout both the northern and southern palaeotropics (for a summary see Boucot *et al.* 1971; Sapelnikov 1985; Rong & Boucot 1998; Boucot *et al.* 2002; Jin *et al.* 2019).

As a part of the tectonic plate Laurentia during the early Palaeozoic, Greenland was located entirely in the tropics during the Ordovician and Silurian, with North Greenland straddling the palaeoequator, and thus hosting a unique warm-water fauna that evolved in a largely hurricane-free climate zone (Jin *et al.* 2013), including a numerically abundant and taxonomically diverse virgianid fauna during the Ordovician–Silurian boundary interval. This unique fauna, however, remains poorly documented, known mainly from faunal lists in geological reports and conference abstracts (e.g. Boucot & Hurst 1979; Peel & Hurst 1980; Hurst & Sheehan 1982).

North Greenland remains one of the most remote regions on Earth (Fig. 1). The land areas closest to the North Pole are located here and, together with northeast Greenland, it constitutes the world's largest national park, stretching from the Kong Oskar Fjord region in central East Greenland (*c.* 71°N) to Hall Land in the northwest

doi: 10.1002/spp2.1544

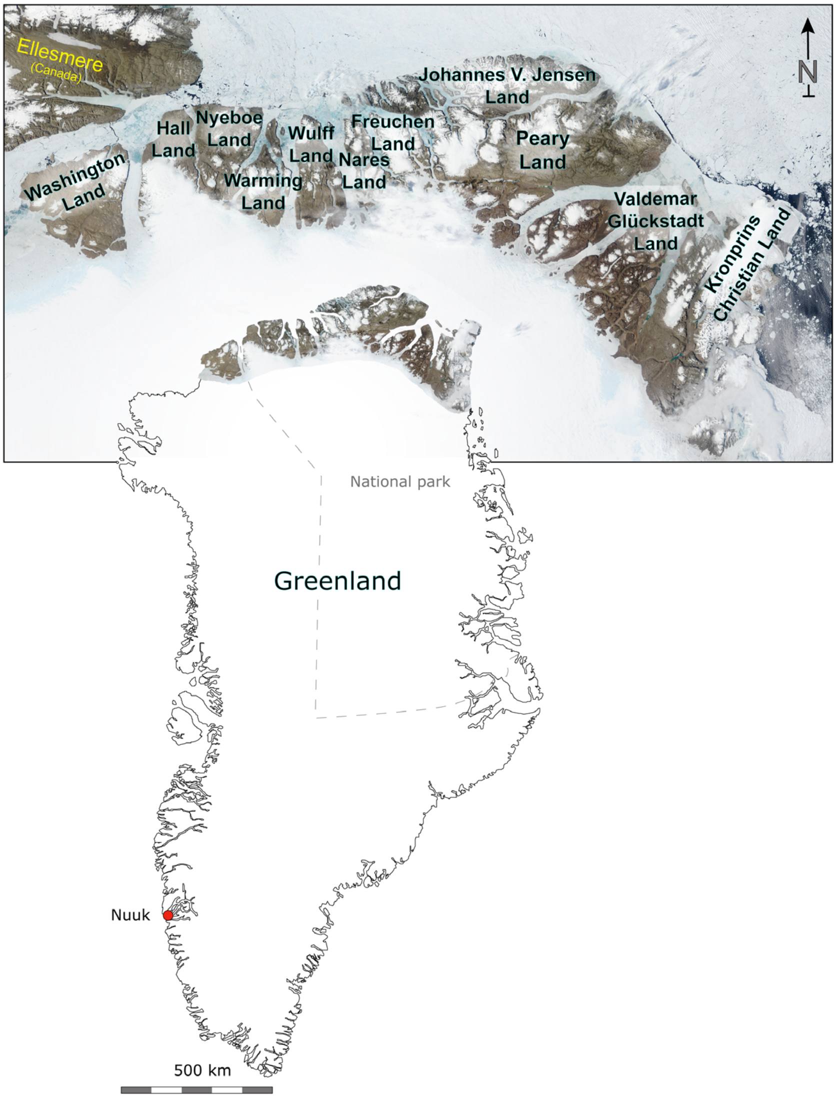

FIG. 1. Major geographical divisions ('Lands') of North Greenland. For outcrop belts of Upper Ordovician to lower Silurian strata and their correlation with the various land masses, see Figures 2 and 3. Satellite image downloaded from https://www.visibleearth.nasa.gov.

(*c.* 82°N). The northernmost coastlines of Greenland were first observed in the far distance in 1875–1876 by Lieutenant Lewis A. Beaumont who, with a party of six expedition members from George S. Nares's British Arctic Expedition, reached what is now known as Beaumont Island (83°20″N). This expedition provided the first collection of pentameride brachiopods from North Greenland (Etheridge 1878). Subsequently, many expeditions have collected material in this remote region and nearly all of that material is now housed in the Natural History Museum of Denmark (NHMD) in Copenhagen. Extensive Ordovician–Silurian brachiopod collections from North Greenland were made primarily by John Hurst and John Peel but several survey geologists contributed to the collections during major geological mapping campaigns carried out by the Geological Survey of Greenland (GGU, now GEUS) in the 1970s–1990s. The NHMD collections also include material from other early expeditions (Fig. 2), such as the Joint Services Expedition (1969), Operation Grant Land (1966), the Danish Peary Land Expedition (1948–1950), the Bicentenary Jubilee Expedition (1920–1923) and the 2nd Thule Expedition (1916–1918), with the latter two expeditions being led by Knud Rasmussen and Lauge Koch.

Some of the Ordovician–Silurian brachiopod collections from the early expeditions have been described in some detail (e.g. Troedsson 1928; Poulsen 1934, 1943). The large number of brachiopod specimens collected during the focused mapping campaigns in the latter half of the 20th century have not been systematically studied or

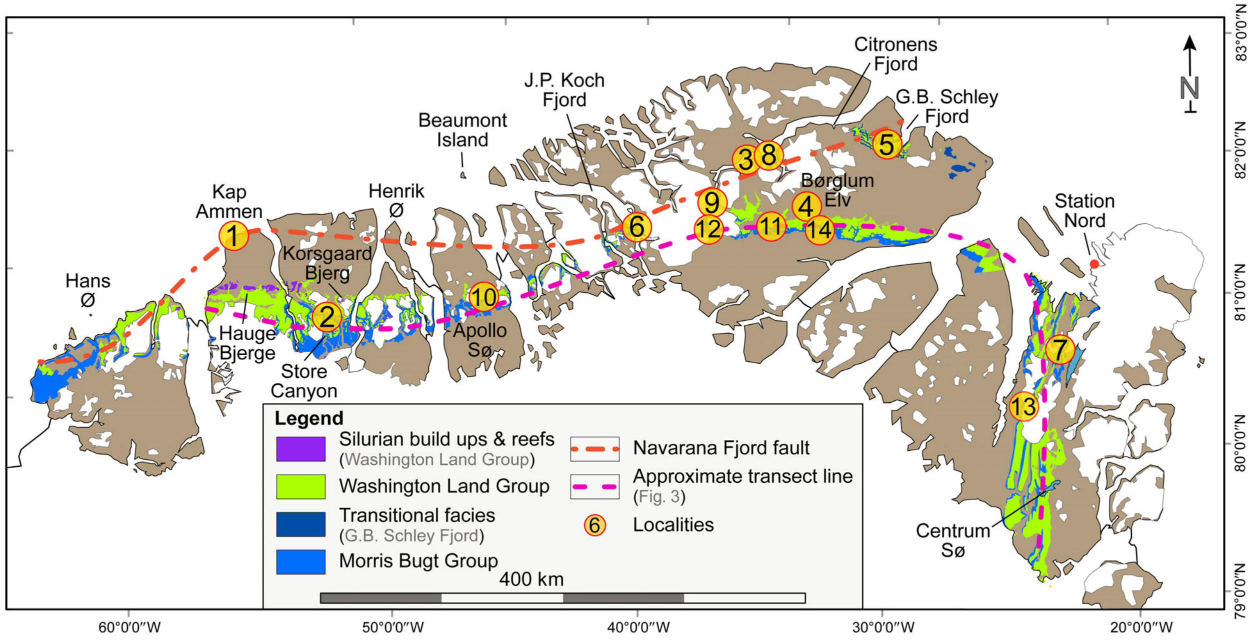

FIG. 2. Major outcrop belt of the Morris Bugt Group (Sandbian to lower Silurian) and Washington Land Group (Silurian). The purple dashed line indicates the approximate transect of the correlated stratigraphic successions in Figure 3 and the red dashed line the location of the Navarana Fjord escarpment line that separates the platform carbonates in the south from deep-water siliciclastic sediments to the north. Locality numbers and mapping expeditions: 1–2, Operation Grant Land, 1965–1966; 1, GGU 82453, 82484–82485; 2. GGU 82178. 3, Joint Services Expedition, 1969; GGU 53498, 53516, 53526. 4, GGU reconnaissance expeditions, 1974; GGU 184102, 184113. 5–13, Peary Land mapping campaign, 1978–1980; 5, GGU 197503, 197536, 197539, 197541; 6, GGU 198860–198861; 7, GGU 225777; 8, GGU 254729; 9, GGU 254760, 254784, 254792, 254795; 10, GGU 254878, 254897; 11, GGU 270631, 270643, 270663, 270664, 270688; 12, GGU 271634; 13, GGU 274963. 14, Peary Land expedition, 2006; DH-02, DH-03, DH-09.

published, except for a few studies on specific genera or faunas (Jin *et al.* 2009, 2022; Rasmussen 2013). In addition, one unpublished PhD thesis described the pentameride faunas of North Greenland with some taxonomic details (Rasmussen 2009). Apart from the aforementioned studies, the only published reports on the pentameroid faunas of North Greenland are a short report (Boucot & Hurst 1979) and a conference abstract (Hurst & Sheehan 1982). The former briefly describes the biogeographical affinities and lists possible genera in the successions, the latter briefly describes the successive evolution of virgianid brachiopods in eastern North Greenland through the Ordovician–Silurian boundary interval, listing *Tcherskidium*, *Proconchidium*, *Virgiana* and *Virgianella*. These preliminary studies recognized approximately nine pentameride genera (with seven new species) from North Greenland, which had a strong palaeobiogeographical link to Siberia (predominantly Kolyma in modern palaeogeography; e.g. Torsvik & Cocks 2013; Cocks & Torsvik 2021).

Notably, nearly all of the pentameride collections examined in this study were assembled before the concept of the Late Ordovician Mass Extinction (LOME) was well established in the literature (Sepkoski 1995; Harper *et al.* 2014a). The LOME, therefore, was not a thematic focus for fossil collection during the mapping campaigns, given that the brachiopods, especially the biostratigraphically useful pentamerides, were sampled mainly to establish biostratigraphical control on predominantly carbonate successions across the Franklinian Basin. Despite this potential collection bias, the great taxonomic richness of the North Greenland pentamerid faunas, of which the virgianids and kulumbellids are treated here, represents a unique window into a vast ecosystem of marine shelly benthos in the palaeoequatorial zone across the LOME interval.

In their study focused on the late Katian virgianids of Alaska, Jin *et al.* (2022) proposed a true warm-water *Tcherskidium* fauna in the palaeoequatorial–northern tropical zone, including the presence of the key taxa *Tcherskidium* and *Proconchidium*, associated with *Deloprosopus* and *Holorhynchus* in North Greenland. The absence of these characteristic taxa from nearly the entire southern palaeotropics during the Late Ordovician may provide some important clues to the causes and processes during the LOME crisis interval. The main purpose of this study, therefore, is to provide a systematic description of 10 adequately preserved taxa from *c.* 20 genera of virgianid and

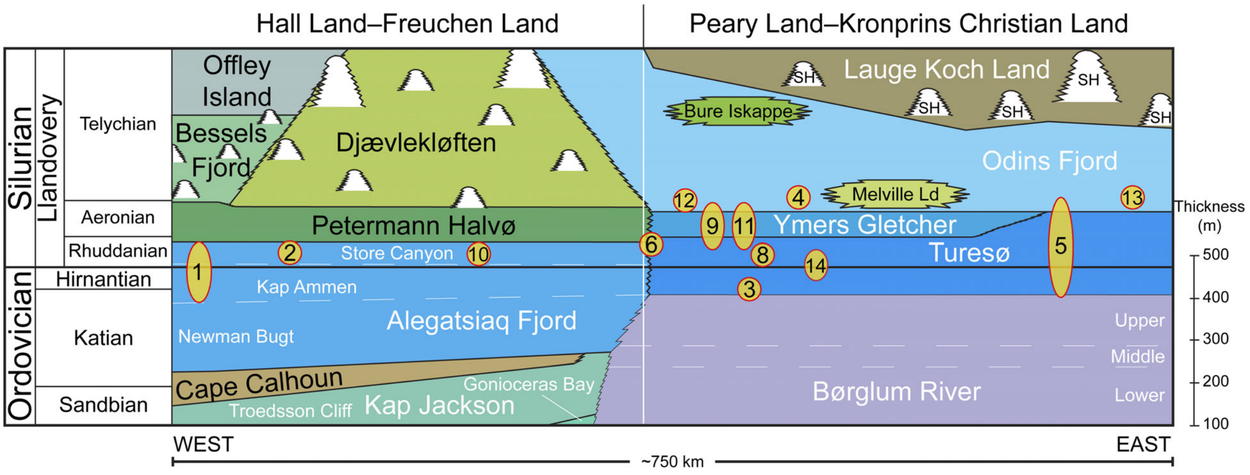

FIG. 3. Stratigraphy of the Upper Ordovician to lower Silurian shallow-water carbonate successions across North Greenland, with emphasis on stratigraphic sections (along the transect shown in Fig. 2) that yielded brachiopods of this study. The carbonates of the Ordovician–Silurian Morris Bugt Group encompass the Kap Jackson, Cape Calhoun and Alegatsiaq Fjord formations to the west of J.P. Koch Fjord, and the Børglum River and the Turesø formations to the east. The lower Silurian (Llandovery) succession consists mainly of the Washington Land Group, a more complex setting to the west but represented mainly by the Ymers Gletcher and Odins Fjord formations in the east. Large font denotes formational unit, whereas small font denotes member names. Locality numbers as in Fig. 2, but here placed according to their approximate geographical position along the transect line, as well as denoting their stratigraphical range. For more details on the Upper Ordovician to lower Silurian stratigraphy, see Rasmussen (2009, 2013). *Abbreviation*: SH, Samuelsen Høj Formation.

kulumbellid pentamerides from North Greenland across the Ordovician–Silurian boundary, ranging from the late Katian to mid-Aeronian, and to explore their palaeoecological and palaeobiogeographical implications, especially in relation to the pentameride biodiversity change through the LOME survival and post-extinction recovery phases.

GEOLOGICAL AND STRATIGRAPHICAL SETTING

The main geological feature of North Greenland is the lower Palaeozoic Franklinian Basin, which is *c.* 2000 km long from east to west, encompassing nearly all of North Greenland, and extending to Arctic Canada to the west, with a total sedimentary succession of *c.* 8000 m in thickness (for details see Higgins *et al.* 1991).

The basin represents a long continental margin facing the Arctic Ocean to the north. It is bordered to the east by the East Greenland Caledonides, which formed during the orogenic processes associated with the gradual reduction and closure of the Iapetus Ocean (from Late Ordovician to the Silurian). The northernmost part the Franklinian Basin, which lies in Johannes V. Jensen Land, is obscured and strongly deformed by the Ellesmere orogenic folding associated with the final closure of the basin (Devonian – early Carboniferous; Higgins *et al.* 1991). In addition, the Carboniferous–Tertiary remnants of the Wandel Sea Basin are found in the northeastern part of the region, as well as the volcanic provinces of Proterozoic–Tertiary age. Farther south, closest to the Inland Ice margin, Proterozoic sediments and volcanics overlie a Precambrian crystalline basement.

The initiation and deposition of the Franklinian Basin has been divided into seven stages of evolution (Surlyk & Hurst 1984; Higgins *et al.* 1991). The upper Katian to middle Aeronian carbonate succession relevant to the current study belongs to Stages 5–6, characterized by a Middle Ordovician to lower Silurian aggregational carbonate platform and a starved siliciclastic slope but with deposition in the trough, with the lower Silurian marked by the development of a ramp and rimmed carbonate shelf and a turbidite trough. The overlying Stage 7 represents the final drowning of the platform with the formation of a Telychian to lower Ludlow reef belt and the expansion of the trough.

The lower Palaeozoic rocks consist predominantly of shallow-water carbonates in the southerly regions, delimited by the Navarana Fjord escarpment that marks a sharp transition into deep-water siliciclastic deposits (Fig. 2), with the exception of Washington Land where a transitional facies belt occurs (Hurst 1981). The carbonates were deposited in equatorial waters as indicated by its fossil faunas and numerous large carbonate build-ups (Hurst 1980, 1984; Sønderholm *et al.* 1987). In addition, a peculiar two-phased sorting of shells in brachiopod coquinas of *Proconchidium schleyi* at G.B. Schley Fjord in northeast Peary Land was interpreted as deposition in the hurricane-free equatorial zone (Jin *et al.* 2013, 2022), constraining the Franklinian Basin to the Equator during the Late Ordovician.

The great extent of Ordovician–Silurian carbonate deposits was noted during pioneer geological mapping of North Greenland (Koch 1920, 1925, 1928), although their faunas were not described until later (Troedsson 1928; Poulsen 1934, 1943). Following the pioneer works of Koch, the stratigraphy of the Ordovician and Silurian rocks has been refined, especially through the studies of Surlyk & Hurst (1984), Smith *et al.* (1989) and Sønderholm *et al.* (1987). A recent update on the Ordovician stratigraphy of the Franklinian Basin can be found in Stouge *et al.* (2023).

The Late Ordovician to early Silurian stratigraphical units of the shelf carbonates

The bulk of the studied material was collected from the inner and outer carbonate shelf succession, through the upper Katian to middle Aeronian interval. This carbonate succession comprises the upper one-third to one-half of the Morris Bugt Group (with a total thickness up to 700 m; Smith *et al.* 1989) and the Washington Land Group (up to 1500 m thick; Hurst 1980). Figure 2 shows the geographical extent of the two groups, and a composite chrono- and lithostratigraphical scheme for the region is provided in Figure 3, as part of the geological setting for pentamerides described in this study.

The Morris Bugt Group. Deposition of the Morris Bugt Group commenced during the Middle Ordovician. From Washington Land in the west to Freuchen Land in central North Greenland, the group is represented by the massive, silty mudstones of the Kap Jackson Formation, overlain by the more recessive unit of the Cape Calhoun Formation of early Katian age (Smith *et al.* 1989). Further upsection is the lowermost unit of the Alegatsiaq Fjord Formation, a 250–360-m-thick succession of dark grey to brown, commonly nodular, burrow-mottled, fossiliferous dolowackestone–dolopackstone (Hurst 1980; Smith *et al.* 1989). The formation is assigned to the *Amorphognathus ordovicicus* conodont Biozone and consists of three members (Smith *et al.* 1989), including, in ascending order, the Newman Bugt, the Kap Ammen and the Store Canyon members. The Newman Bugt Member is 110–170 m thick, probably middle–late Katian in age based on the occurrence of typical taxa of the Red River fauna, such as the giant planispiral gastropod *Maclurites*, favositid corals, a diverse cephalopod fauna, *Fisherites* and auleceridid sponges. In addition, a single graptolite occurrence, *Amplexograptus* cf. *A. inuiti* (now considered a junior synonym of *A. latus*) was reported by Bjerreskov (1989). The middle–late Katian age is further corroborated by the rhynchonellide species *Hiscobeccus gigas*, which is known from the underlying strata of the Cape Calhoun Formation in Washington Land and beds coeval to the Newman Bugt Member farther east in the upper member of the Børglum River Formation in the Peary Land and Kronprins Christian Land regions (Rasmussen 2013). The overlying 40–85-m-thick Kap Ammen Member straddles the Ordovician–Silurian boundary, with clearly Silurian conodont taxa present above a 30-m-thick barren interval (Smith *et al.* 1989). Its lower part is probably latest Katian in age, based on the occurrence of the virgianid genus *Holorhynchus giganteus* (Rasmussen 2009) and many taxa extending from the underlying member, as well as stromatoporoid mounds. The barren interval, which is also seen eastwards, has made it difficult to identify Hirnantian strata in North Greenland. The top of the Alegatsiaq Formation is represented by the 60–113-m-thick Store Canyon Member. The presence of *Virgiana* in the upper part of the member indicates a middle–late Rhuddanian age. In addition, Hurst & Sheehan (1989, unpub. data) reported *Brevilamnulella* (= *B.* cf. *thebesensis* of Rasmussen 2009) from beds probably assignable to the Alegatsiaq Fjord Formation in Fossilbugt, northern Washington Land.

In central and eastern North Greenland (i.e. from Peary Land to Kronprins Christian Land), the Morris Bugt Group is composed of the Børglum River and the Turesø formations. The Børglum River Formation consists generally of dark brown to yellowish-grey lime mudstone, skeletal wackestone and packstone, divided informally into three members. The relatively thick lower and upper members are richly fossiliferous, containing a typical Red River fauna preserved in massive beds with *Thalassinoides*-type burrows (Jin *et al.* 2012, 2013; Rasmussen 2013), whereas the 40-m-thick middle member is unfossiliferous or poorly fossiliferous. The formation ranges from the Sandbian to the mid-Katian. The overlying Turesø Formation is more dolomitic than both the underlying unit and the coeval Alegatsiaq Formation in the west. It is up to 150 m thick in Peary Land but may reach more than 200 m in thickness in Kronprins Christian Land to the southeast (Smith *et al.* 2004). It is composed of dark to light grey banded, medium to thick dolomite to limy dolomite beds. The unit is less fossiliferous than the underlying Børglum River Formation but towards the top coquinas of *Viridita* and *Virgiana* occur, suggesting a Rhuddanian age (Harper *et al.* 2007). Furthermore, *B.* cf. *thebesensis* has been recognized from beds assignable to this formation (Rasmussen 2009). Minor mounds are developed that may be coeval to those observed in the Kap Ammen Member of the Alegatsiaq Formation to the west (Harper *et al.* 2007, 2014b).

In the northeastern part of Peary Land, in the G.B. Schley Fjord region, a transitional facies occurs, characterized by a lesser degree of dolomitization and more abundant nodular wackestone intervals, which resembles more closely the Alegatsiaq Fjord Formation (Hurst 1984; Smith *et al.* 1989). Here major coquinas of *Proconchidium schleyi* occur, reaching a cumulative thickness of up to 350 m (Harper *et al.* 2007; Jin *et al.* 2013, 2022).

The Washington Land Group. The Morris Bugt Group is overlain by a succession of shelf carbonates of the Washington Land Group, which consists of a range of facies from carbonate ramp to intra-shelf mounds and shelf-margin reef complexes (Fig. 3). Sønderholm *et al.* (1987) divided this succession from Freuchen Land to Hall Land into five stratigraphic units that reflect major lithological variations but many more are described from Washington Land (Hurst 1980), which are beyond the scope of this study.

The lower four units of Sønderholm *et al.* (1987) are assigned to the Llandovery Series. The lowermost unit, the Petermann Halvø Formation, consists of generally flat-bedded, light to dark grey skeletal carbonates with a high abundance of corals and stromatoporoids. It is estimated to be 90–120 m thick. The overlying unit 2, the Djævlekløften Formation, consists of massive to irregularly bedded lime mudstones to fine-grained skeletal limestones, also rich in corals and stromatoporoids. The formation occurs as a series of mounds that generally become larger towards the shelf margin. The mounds are located in unit 3, which consists of dark to black back-mound and intermound sediments consisting of thinly bedded lime mudstones interbedded with bioclastic limestones with pebble conglomerates, as well as shaly partings rich in graptolites. The mounds approach 125 m in height whereas the total thickness of the formation may be in the order of 250 m (Sønderholm *et al.* 1987). Unit 4 at the top of the Llandovery succession is variably developed but consists mainly of dark and light coral and stromatoporoid biostromes, interbedded with encrinites that are usually several metres in thickness but locally may reach up to 200 m (Sønderholm *et al.* 1987). The colour difference reflects changes from *in situ* to reworked fossil assemblages. The overall thickness of the unit is *c.* 400 m.

Further west, in westernmost Hall Land (Kap Tyson and Offley Ø) and Washington Land, the Llandovery succession discussed above is coeval to the Petermann Halvø, Bessels Fjord and Offley Island formations. *Pseudoconchidium* has been reported from the lowermost part of the Bessels Fjord Formation, indicating a late Aeronian or early Telychian age (Rasmussen 2009).

From Peary Land eastwards to Kronprins Christian Land, the Washington Land Group is divided into the Ymers Gletcher and Odins Fjord formations, overlain by siliciclastic deposits, in which reef complexes of the Samuelsen Høj Formation occur. The Ymers Gletcher formation is 25–45 m thick, comprising a thin–medium bedded grey lime mudstone unit with algal laminae. It is likely to be early–middle Aeronian in age, and correlates to the upper half of the Petermann Halvø Formation towards the west. Jin *et al.* (2009) reported *Sulcipentamerus* cf. *dorsoplanus* and *Harpidium* sp. from the top of the unit. The formation wedges out towards the south and east, where instead the overlying Odins Fjord Formation rests conformably on top of the Turesø Formation of the Morris Bugt Group. In the Børglum Elv area in central Peary Land, *Sulcipentamerus* and *Harpidium* occur again in another coquina in the lowermost part of the Odins Fjord Formation, characterized by grey to dark blue, medium- to thick-bedded limestone. The lower half of the formation consists of massive, nodular skeletal wackestone. The upper half the formation contains beds of up to 10 m in thickness (Hurst 1984, p. 37), although such massive beds may have been the result of bedding amalgamation through diagenesis. The fauna is rich in trilobites, brachiopods, echinoderms, tabulate and rugose corals. Biostratigraphically, the formation is correlated with the uppermost Aeronian, but it may span the entire Telychian. Hurst (1984) reported *Virgianella* (assigned to *Borealoides* gen. nov. in this study) from the upper 50 m of the formation. This was also confirmed by new material, collected in 2006 (Rasmussen 2009) in the lower part of the formation. Furthermore, *Pseudoconchidium* is recorded from the lower part of the formation, probably assignable to the Melville Land Member (Jin *et al.* 2009; Rasmussen 2009). *Harpidium* is found throughout the formation, and towards the top *Sulcipentamerus* is known from the Bure Iskappe Member and the Samuelsen Høj Formation. These units thicken towards the shelf margin to the North.

The Washington Land Group comprises a complex suite of horizontally stratified carbonates interrupted by mound and reef structures (Hurst 1980). For example, interlaced among the stratigraphic units described above, there are locally developed reef core and flank facies, such as the Samuelsen Høj Formation, which occurs east of J. P. Koch Fjord. These reefs have a wide range of sizes across all of North Greenland, with the largest in Kronprins Christian Land reaching up to 200–300 m in thickness and up to 10 km in circumference (Hurst 1984). Reefs of the Washington Land Group even occur as isolated limestone ‘islands’ within the siliciclastic Peary Land Group (Hurst 1980). The complex setting of the Washington Land Group recognized in Washington Land and Hall Land proved too difficult to separate in the field along the stretch from eastern Hall Land in the west to Freuchen Land in the east. Therefore, the different facies of the Washington Land Group were placed together in the Djævlekløften Formation, as outlined above, although many of the formations of Hurst (1980) may be traced locally in this area (Sønderholm *et al.* 1987).

Last, one locality in the siliciclastic slope facies of the Peary Land Group is of interest to the current study, where massive limestone boulders with abundant shells of *Tcherskidium tenuicostatum* occur as olistoliths, derived from upper Katian carbonates upslope, deposited in a lower Silurian (Rhuddanian) siliciclastic matrix, making up the conglomerates of the Citronens Fjord Member of the Merqujoq Formation (Hurst & Surlyk (1982); Jin *et al.* 2022).

The Ordovician–Silurian boundary itself is positioned in the Morris Bugt Group. West of Peary Land it occurs in the topmost part of the Kap Ammen Member of the Alegatsiaq Fjord Formation, whereas from Peary Land eastwards it is within the dolomitic Turesø Formation. Thus, all over North Greenland it occurs as an intraformational boundary in carbonate facies. The boundary has proven difficult to trace due to the general lack of fossils (Smith *et al.* 1989; Rasmussen 2013). In the Børglum Elv area this barren interval is the narrowest, spanning *c.* 30 m of section (Armstrong & Lane 1981). New palaeontological and sedimentological data have helped to narrow down the interval that contains the Ordovician–Silurian boundary. During field work in 2006 in the Børglum Elv area, at least three peritidal laminite cycles were recognized in strata that occur a few metres below a thick coquina of the virgianid brachiopod *Viridita*. *Viridita* indicates an earliest Rhuddanian age and thus the peritidal cycles are believed to be Hirnantian in age.

MATERIAL AND METHOD

To simplify the lists of brachiopod specimens in the present paper, the following abbreviations are used: dv, dorsal valves(s); vv, ventral valves(s).

This study is based on the following field samples collected by the GGU, with additional field data and samples (DH) made by the authors (CMØR, DATH, JJ) during field work in 2006 (Table 1).

All figured specimens from North Greenland are deposited in the Type and Illustrated Palaeontology Collection of the Natural History Museum of Denmark, Copenhagen. Type specimens of *Kulumbella kulumbensis* examined during this study (for comparison with the Greenland material) are housed in the A.P. Karpinsky All-Russia Institute of Geological Research, Russian Academy of Sciences, St Petersburg. Topotypes of *Deloprosopus jiangshanensis* are housed in the Nanjing Institute of Geology and Palaeontology, Chinese Academy of Sciences.

Institutional abbreviations. GGU, Geological Survey of Greenland; MGUH, Natural History Museum of Denmark, Copenhagen, Denmark; NIGP, Nanjing Institute of Geology and Palaeontology, Nanjing, China; VSEGEI, Russian Academy of Sciences, St Petersburg, Russia.

PALAEOECOLOGICAL AND PALAEOBIOGEOGRAPHICAL IMPLICATIONS

In this study, new data on late Katian brachiopod faunas from the Omulevsk Mountains region, northeastern Siberia (Kolyma terrane), and the accreted terranes of Alaska (Jin *et al.* 2022) and North Greenland were added to the late Katian brachiopod faunal database used in Jin & Blodgett (2020) to update the multivariate analysis to elucidate the palaeobiogeographic relationships of these pre-Hirnantian faunas (Jin *et al.* 2023). The result is similar to that of Jin & Blodgett (2020) in that all brachiopod faunas from shallow-water carbonate platforms in inland seas and continental-margin shelves form a tightly knit cluster (Fig. 4). An additional feature in this updated cluster plot, however, is the differentiation of the *Tcherskidium*-bearing brachiopod fauna of east-central Alaska (northwest margin of Laurentia) and North Greenland, which was confined to the Late Ordovician northern hemisphere (Torsvik & Cocks 2013; Cocks & Torsvik 2021; Jin *et al.* 2022), from the highly homogeneous epicontinental sea brachiopod fauna (Harper *et al.* 2013; Candela 2014; Jin *et al.* 2014) that developed predominantly in the southern tropics.

As proposed in a qualitative sense by Jin *et al.* (2022), the late Katian *Tcherskidium* fauna occurs almost exclusively in palaeoequatorial and northern tropical carbonate depositional environments, with the only exception being in Baltoscandia, where it spread slightly south of the palaeoequator. In Laurentia the *Tcherskidium* fauna has not been found in any of the sedimentary basins south of the palaeoequator, where the Late Ordovician (especially late Katian or Richmondian) brachiopod faunas were usually abundant and diverse. Globally, the eponymous genus *Tcherskidium* was associated with various large-shelled virgianids in different regions, such as with *Proconchidium*, *Deloprosopus*, *Holorhynchus* and/or *Eoconchidium*. The *Tcherskidium* fauna formed a relatively tight cluster among late Katian brachiopods from the Boda Limestone of Sweden (Baltica), upper Tilekhnyakh Subseries of the Omulevsk Mountains region (Kolyma, including the key Mirny Creek locality), and coeval strata in Taimyr (marginal Siberia), and accreted terranes of Alaska (adjacent to Laurentia), where the eponymous taxon *Tcherskidium* occurs. In the Kazakhstan terranes and South China, *Tcherskidium* itself has not been convincingly recognized, but associated key taxa of the fauna, *Proconchidium* and/or *Deloprosopus*, are present. The

TABLE 1. Details of field samples used in this study.

Field sample*	Location	Taxon	Material†	Notes
GGU 53498	82.97893°N 33.60077°W	*Deloprosopus dawesi* sp. nov.	40 vv 11 dv	Peary Land
GGU 53516	Adjacent to GGU 53526	*Deloprosopus dawesi* sp. nov.	10 vv	Peary Land
GGU 53526	82.98222°N 33.51431°W	*Deloprosopus dawesi* sp. nov.	5 vv 2 dv	Peary Land
GGU 82178	81.43469°N 55.83635°W	*Virgiana hursti* sp. nov.	2 vv	Collected by Peter Dawes, 1 July 1966, from 'Store Canyon, Camp 3' in southern Nyeboe Land, Unit 13B of Dawes & Peel (1984); now known as the Store Canyon Member, Alegatsiaq Fjord Fm.
GGU 82453	81.82939°N 61.39812°W	*Holorhynchus giganteus*	1 vv	Collected by Peter Dawes in 1966 from upper Katian strata, Kap Ammen, northern Hall Land
GGU 82484	81.82939°N 61.39812°W	*Virgiana hursti* sp. nov.	10 vv 1 dv	Collected and recorded as '*Kirkidium*?' by Peter Dawes on 28 June 1966, from Kap Ammen, northern Hall Land, Unit 1C of Dawes & Peel (1984, p. 27); now assigned to Rhuddanian strata of the Alegatsiaq Fjord Fm.
GGU 82485	81.82939°N 61.39812°W	*Pleurodium* sp.	1 cs, partly embedded in rock matrix	Collected by Peter Dawes from the Store Canyon Member of the Alegatsiaq Fjord Fm. at Kap Ammen, northern Hall Land
GGU 184102	82.48794°N 30.73547°W	*Borealoides balderi* gen. et sp. nov.	36 vv 1 dv 2 cs	Collected by John Peel (2 July 1974) from the 'Pentamerid bank' at contact between members A and B, Odins Fjord Fm. (40 m above its base), east side of Børglum Elv, Section 30, Peary Land
GGU 184113	Near GGU 184102 82.48794°N 30.73547°W	*Borealoides balderi* gen. et sp. nov.	64 vv 7 dv 4 cs	Collected by John Peel (2 July 1974), 25 m above base of Odins Fjord Fm., east side of Børglum Elv, southern Peary Land
GGU 197503	82.88700°N 25.60600°W	*Tcherskidium tenuicostatum*	Embedded material, exact number of specimens not estimated	Collected by Robert Christie and Jon Ineson (2–4 August 1978) from the Alegatsiaq Fjord facies equivalent in the G.B. Schley Fjord region, eastern Peary Land
GGU 197536	82.88700°N 25.60600°W	*Tcherskidium tenuicostatum*	Embedded material, exact number of specimens not estimated	Collected by Robert Christie and Jon Ineson (2–4 August 1978) from the same area as GGU 197503
GGU 197539	82.88700°N 25.60600°W	*Tcherskidium tenuicostatum*	Embedded material, exact number of specimens not estimated	Collected by Robert Christie and Jon Ineson (2–4 August 1978) from the same area as GGU 197503
GGU 197541	82.88700°N 25.60600°W	*Tcherskidium tenuicostatum*	Embedded material, exact number of specimens not estimated	Collected by Robert Christie and Jon Ineson (2–4 August 1978) from the same area as GGU 197503
GGU 198860	82.486946°N 40.361389°W	*Virgiana hursti* sp. nov.	23 vv 3 dv 1 cs	Collected by John Hurst in 1978 from float on east side of J. P. Koch Fjord, 'Camp Crevasse'
GGU 198861	Same locality as GGU 198860	*Virgiana hursti* sp. nov.	*c.* 44 vv	Collected by John Hurst in 1978 from float on east side of J. P. Koch Fjord, 'Camp Crevasse'
GGU 225777	81.1°N 19.6°W	*Borealoides balderi* gen. et sp. nov.	64 vv 7 dv 4 cs	Collected by John Peel in 1979 in the large N–S-trending valley adjacent to Romer Sø, Kronprins Christian Land. Labelled as 'near the top of the unit, higher than 225774 and 225775'

(continued)

TABLE 1. (Continued)

Field sample*	Location	Taxon	Material†	Notes
GGU 254729	82.97528°N 33.5578°W	*Tcherskidium tenuicostatum*	430 vv 12 dv 3 cs	Collected by John Hurst in 1978, 'Camp 6', Frederick E. Hyde Fjord, central Peary Land; brecciated black shales with slumped limestone boulders/olistoliths, probably the Citronens Fjord Member (Rhuddanian) of the Merqujoq Fm.; the presence of *Tcherskidium* in the limestone boulders indicates that they were derived from upper Katian strata higher up on the carbonate platform, as originally suggested by Hurst & Surlyk (1982)
GGU 254760	82.663055°N 35.878887°W	*Virgiana hursti* sp. nov.	>136 vv 17 dv 1 small block	West-central Peary Land from Odins Fjord, Locality 2 of Hurst (1984), 15 m above base of section, Turesø Fm.
GGU 254784	Close to GGU 254760 82.663055°N 35.878887°W	*Borealoides balderi* gen. et sp. nov.	8 vv 2 dv	Collected by John Hurst in 1978 from the Odins Fjord Fm. at Odins Fjord, west-central Peary Land
GGU 254792	Close to GGU 254760 82.663055°N 35.878887°W	*Borealoides balderi* gen. et sp. nov.	49 vv 3 dv	Collected by John Hurst in 1978 from the Odins Fjord Fm. (Rhuddanian) at Odins Fjord, west-central Peary Land
GGU 254795	Close to GGU 254760 82.663055°N 35.878887°W	*Kulumbella heimdali* sp. nov.	2 vv 1 dv 5 cs	Collected by John Hurst in 1978 from the Odins Fjord Fm. (middle Aeronian), Odins Fjord, west-central Peary Land
GGU 254878	81.82161°N 48.25268°W	*Virgiana hursti* sp. nov.	41 vv 3 dv	Collected by John Hurst in 1978 in southern Wulff Land, labelled as from 'NW Apollo Sø, section 17, 10 m from base above Schuchert [Fm.]'
GGU 254897	81.82161°N 48.25268°W	*Virgiana hursti* sp. nov.	75 vv 6 dv 1 cs	Collected by John Hurst in 1978 in southern Wulff Land labelled as from 'NW Apollo Sø, section 17, 15–20 m above base of unit (middle of unit)'
GGU 270631	Estimated at 82.45220°N 32.26987°W	*Virgiana hursti* sp. nov.	37 vv 9 dv	Collected by Stig Schack Pedersen in central Peary Land at Camp 4 (2 July 1978) from the topmost part of the upper member of the Turesø Fm.
GGU 270643		*Holorhynchus giganteus*	1 dv	Collected by Stig Schack Pedersen from central Peary Land (2 July 1978)
GGU 270663	Estimated at 82.41038°N 32.63502°W	*Borealoides balderi* gen. et sp. nov.	6 vv 1 dv	Collected by Stig Schack Pedersen (11–12 July 1978) at section 30, *c.* 2 km N of 'Lurlangsø', central Peary Land; the specimen was collected from the top of the lower member of the Odins Fjord Fm.
GGU 270664	Exact coordinates and stratigraphic unit unknown, but probably close to GGU 270663	*Borealoides balderi* gen. et sp. nov.	3 vv 1 cs	Collected by Stig Shack Petersen (11–12 July 1978) at section 30, *c.* 2 km N of 'Lurlangsø', central Peary Land
GGU 270688	Estimated at 82.41776°N 33.86313°W probably close to GGU 270664	*Borealoides balderi* gen. et sp. nov.	20 vv 1 cs	Collected by Stig Shack Petersen (15 July 1978) from the Melville Land Member of the Odins Fjord Formation; labelled as 'Pentamerid bank' at contact between members A and B '(24 WS 710 680 32, central Peary Land)'

(continued)

TABLE 1. (Continued)

Field sample*	Location	Taxon	Material†	Notes
GGU 271634	82.5°N 36.4°W	*Borealoides balderi* gen. et sp. nov.	14 vv 1 cs	Collected by J.S. Peel (9 July 1978); labelled as 'Top of Silurian limestone [probably lower Odins Fjord Fm.], hilltop at elevation 850 m, east side of the elongate lake, at its northern end, between Bure Iskappe and Hans Tavsen Iskappe'; west Peary Land
GGU 274963	*c.* 80.7°N 22.4°W	*Virgiana hursti* sp. nov.	2 vv	Collected by J.S. Peel (7 July 1980), *c.* 10 m above base of Odins Fjord Formation, western Kronprins Christian Land, Sjælland Fjelde; labelled as 'Just west of ice cap, lower Silurian'
DH-02	UTM 0532888N 9158178E elevation 318 m	*Brevilamnulella* sp.	*c.* 20, mostly vv, embedded in small blocks of coquina	Børglum Elv section, Peary Land; thick-bedded dolomitic shelly packstone, lower Turesø Formation (Hirnantian); collected in 2006 by the authors
DH-03	UTM 05333067N 9158270E elevation 331–333 m	*Viridita* sp.	*c.* 30, mostly vv, embedded in small blocks of coquina	Børglum Elv section, Peary Land; thick-bedded shelly packstone, middle Turesø Fm. (lower Rhuddanian); the shell packstone unit is *c.* 1.5 m thick, forming a carbonate ledge at the base of a steep slope of very thick-bedded carbonate succession, exposing a *c.* 700-m-long stretch of bedding surface covered by *Viridita* shells; the unit can be traced to a small cliff to the east of the carbonate ledge; collected in 2006 by the authors
DH-09	UTM 0533002N 9158284E elevation 283 m	*Brevilamnulella* sp.	*c.* 30, mostly vv, embedded in small blocks of coquina	Børglum Elv section, Peary Land; thick-bedded dolomitic shelly packstone, with incompletely silicified shells, basal Turesø Fm. (Hirnantian); collected in 2006 by the authors

*GGU, Geological Survey of Greenland; DH, additional samples collected by the authors.
†cs, conjoined shell(s); dv, dorsal valve(s); vv, ventral valve(s).

presence of *Tcherskidium* and *Proconchidium* in the marginal settings of Laurentia (i.e. North Greenland and east-central Alaska) indicates close palaeobiogeographic links between northern hemisphere Laurentia, Alaskan accreted terranes (Farewell and Chukotka), Kolyma, Siberia, the Kazakh blocks (e.g. Chu-Ili), southern Tian-Shan, and South China during the late Katian. By the late Katian standard of virgianid diversity, North Greenland had arguably the most diverse *Tcherskidium* fauna, sharing *Tcherskidium* with Kolyma, Siberia and Alaskan accreted terranes, *Proconchidium* with Baltica (Baltoscandia, Timan), Chu-Ili, Southern Tian-Shan, *Holorhynchus* with Alaskan accreted terranes, Kolyma, Baltica, Kazakh terranes, and North China, as well as *Deloprosopus* now known from North Greenland, the Kazakh terrane of Chu-Ili, and South China. Interestingly, the peculiar and exclusive sharing of the late Katian *Deloprosopus* between North Greenland and South China was mirrored in Aeronian time by the exclusive occurrences of another pentameride, *Sulcipentamerus*, in these two regions. At present it is difficult to explain the shared occurrence of large-shelled pentameride across vast palaeogeographic realms, given that both *Deloprosopus* and *Sulcipentamerus* formed abundant shell beds in relatively shallow-water (BA2–3 equivalent) carbonate platform depositional settings in South China and North Greenland. Similar depositional environments commonly existed in the palaeogeographic regions between South China and North Greenland (where the two genera were absent), such as the Kazakh terranes (except for the presence of *Deloprosopus* in the Chu-Ili terrane recognized in this study), Siberia, Kolyma, northern Baltica, and Chukotka, particularly along the same palaeoequatorial and lower northern palaeotropics during that time interval. Modern palaeogeographic projections for the Late Ordovician indicate that many of the above-mentioned localities were situated on, or close to, the palaeoequator (Torsvik & Cocks 2016). This implies that these regions were probably influenced by westbound warm-water equatorial currents (Pohl *et al.* 2016, 2023). Virgianid brachiopods, therefore, were probably dispersed from South China but this would also imply that one should be able to find genera such as

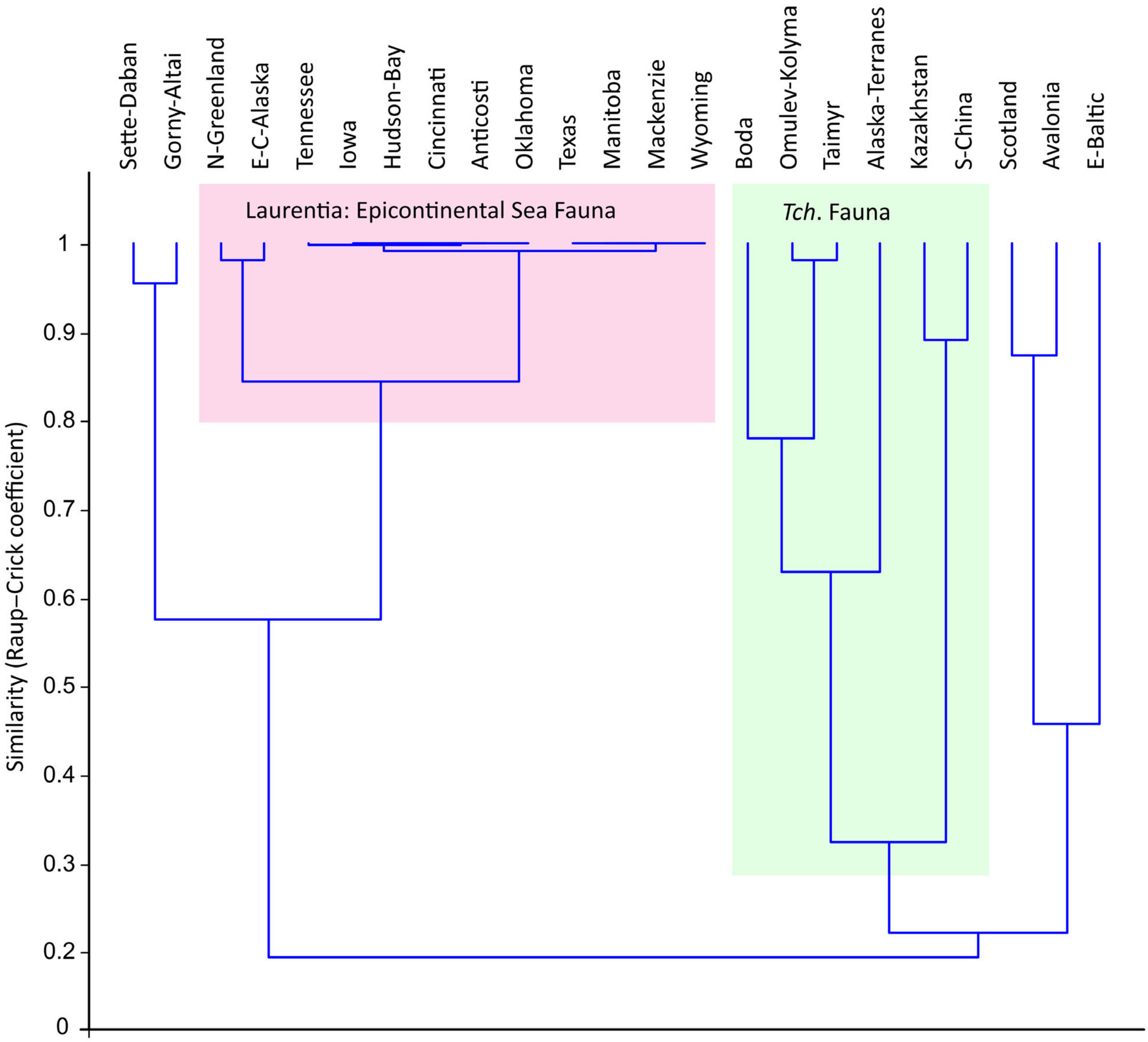

FIG. 4. Multivariate analysis of late Katian brachiopod faunas. See Jin *et al.* (2023) for details of faunal list for each palaeogeographical region. *Abbreviation*: *Tch.*, *Tcherskidium*.

Deloprosopus and *Sulcipentamerus* in the various Kazakh and Siberian terranes. More focused sampling efforts in these regions are needed, however, to test this hypothesis. The recognition in this study of one of the oldest virgianids, *Deloprosopus*, in upper Katian strata of the Chu-Ili terrane (one of the Kazakh blocks), for example, bridges the wide palaeogeographic gaps between its occurrence in South China and North Greenland.

The relatively high degree of cosmopolitanism of the late Katian *Tcherskidium* fauna is in sharp contrast to the epicontinental sea brachiopod fauna from southern hemisphere Laurentia, which is characterized by an extremely high degree of intra-plate homogeneity but extra-plate provinciality (e.g. Jin *et al.* 2014). Newly evolved Katian brachiopod genera typical of southern Laurentia (e.g. *Diceromyonia*, *Nasutimena*, *Hiscobeccus*, *Lepidocyclus* and *Hypsiptycha*) have been found rarely on other tectonic plates, and vice versa (for summaries and examples see: Sheehan & Coorough 1990; Candela 2014; Sproat & Jin 2017).

Causes of the palaeobiogeographic dichotomy in Laurentia: did evolutionary adaptations enable virgianids to exploit a changing environment?

At present it is unclear what palaeoenvironmental and/or palaeobiological factors contributed to the cosmopolitanism of the *Tcherskidium* fauna in northern hemisphere Laurentia, in contrast to the high degree of provincialism of the epicontinental sea brachiopod fauna in southern hemisphere Laurentia. As discussed above, we could point out only two apparent (and possibly superficial) palaeoenvironmental differences between the two hemispheres during the Late Ordovician:

1. Lack of a major landmass in the northern polar regions on which a continental icecap could accumulate.
2. Lack of cold-water upwelling in northern tropics due to the lack of a northern polar icecap to generate major downwelling and psychrospheric flows.

These two factors would favour warmer oceans in the northern tropics rather than in the southern tropics, because the southern tropics would have undergone more frequent incursions of cold-water masses from ice-bearing polar Gondwana, which could have generated an equatorial cold-water tongue as in the modern Eastern Equatorial Pacific (e.g. Jin *et al.* 2018). The relatively cosmopolitan late Katian virgianid fauna of northern Laurentia provides a unique opportunity for a comparative study of late Katian brachiopod faunal endemism versus cosmopolitanism from the perspective of the impact of cool- versus warm-water masses on faunas and biofacies in the palaeotropics (Jin *et al.* 2013, 2018).

Hitherto, the Katian has been thought to be a time of peak Ordovician biodiversity accumulation, reflecting the maximum carrying capacity of the Ordovician ecosystems just prior to the severe Hirnantian extinctions (Sepkoski 1995). The literature convincingly demonstrates that faunal migrations were widespread globally. During the mid–late Katian, warm-water faunas appear to have tracked carbonates facies as far south as 60°S during the Boda warming event (Fortey & Cocks 2005; Colmenar & Rasmussen 2018). In Laurentia, invading taxa are found that seem to have their origins in Baltica and the Iapetus Ocean, driving a faunal change during roughly the same interval, commonly labelled the Richmondian Invasion (Stigall 2023), although the inter-plate migration of typical genera of this invading fauna may have occurred earlier in the Katian. Recently, however, multiclade datasets compiled at different taxonomical levels across vastly different regions and with high temporal resolution, have shown that major biodiversity loss was already underway in some places by the early Katian (Rasmussen *et al.* 2019; Fan *et al.* 2020; Deng *et al.* 2021). This has now led to the hypothesis of an ‘extended-LOME’ phase characterized by at least three major extinction pulses of which the first occurred during the earliest Katian (Rasmussen *et al.* 2023). This new hypothesis is supported when the biodiversity signal is partitioned clade by clade. In the Katian, animal groups, such as the bivalves, bryozoans, gastropods, echinoderms, as well as tabulate and rugose corals, had accelerated origination rates. At the same time, clades that had been successful hitherto either reached a plateau (e.g. the rhynchonelliformean brachiopods due to major intra-clade turnover rates) or began to decline (such as the trilobites and conodonts). This pattern may explain why this first pulse of extinction has been hitherto undetected. However, it also highlights the increased ecologic complexity at this time, which has been recognized for decades (Sepkoski & Sheehan 1983).

The fact that the rhynchonelliformeans did not decline but managed to sustain, and in some places increase, species richness towards the latest Katian, can for the large part be explained by new groups that seem to have been particularly successful in adapting to the new dispersal opportunities. This includes groups such as the atrypides, athyridides, rhynchonellides, spiriferides, triplesiids and the pentamerides (Harper & Rong 2001; Harper *et al.* 2013). Most were associated with carbonate environments. These are the same clades that evolved into the bulk of the dominant brachiopod fauna following the LOME (Harper & Rong 2001; Rasmussen 2014; Rong *et al.* 2020).

Considering most of the Katian as part of a protracted extinction phase would imply a much more spatiotemporally heterogenic climate history, which may have been partly associated with increased volcanism (Rasmussen *et al.* 2023). Rather than a unidirectional trend associated with the onset of glaciations from the Katian to the Hirnantian (e.g. Saltzman & Young 2005; Finnegan *et al.* 2011), there may have been episodes of extreme temperature fluctuations, such as those observed during the Boda and Richmondian events, when Laurentia experienced large-scale marine transgressions. Such temperature extremes are likely to have forced rapid evolutionary adaptations in order to cope with the changing climate and environment. Globally intense volcanism in the Late Ordovician is indicated by thick and widespread bentonite deposits, such as the Millbrig and Deicke bentonites in Laurentia, the Kinnekulle event in Baltica (Bergström *et al.* 2003), and upper Katian bentonites on the western Yangtze Platform of South China (Ling *et al.* 2019). In addition, a large igneous province may have existed in high-latitude Gondwana (present-day northern Iran; Derakhshi *et al.* 2022), although this magmatic event within a microplate may have been temporally protracted and thus the severity of its impact on Late Ordovician climate remains to be studied (Álvaro *et al.* 2022). In general, a geological episode of heightened volcanism and related magmatic events would have altered climatic and environmental conditions through massive, repeated outgassing of greenhouse gases into the atmosphere. Apart from the physical evidence as observed from the rock record, a characteristic step change is also evident in the ^{13}C-record (Bergström *et al.* 2009), further supporting a fundamental change in atmospheric and ocean temperature and other related conditions.

Many brachiopod lineages have been shown to have evolved through drastic climate fluctuations in the Late Ordovician and some continued into the Silurian to become dominant groups of the shelly benthos. Examples are the Hirnantian rhipidomellid progenitor *Mendacella* (Jin & Zhan 2008), hindellid *Hindella* (Copper & Jin 2017), strophodontoid *Eostropheodonta* (Huang *et al.* 2023) and others (Rong *et al.* 2020). This suggests that the Hirnantian was an interval of moderate speciation and diversification in many regions, thus representing a much more dynamic phase than the classic extinction scenario. This is illustrated by the origin and radiation of the giant-shelled virgianids during the late Katian, which then reduced in size to the dwarf *Brevilamnulella* during the Hirnantian, and then eventually re-radiated immediately after the LOME to evolve into the ubiquitous pentameride brachiopod faunas that became a signature of the Silurian. The virgianid fauna evolved through drastic swings of greenhouse–icehouse–greenhouse episodes, suggesting their particularly successful adaptability to shallow warm-water carbonate settings. Jin *et al.* (2022) identified the *Tcherskidium* fauna, which seem to be confined to this setting during the latest Katian. This fauna is characterized by virgianid genera that have unusually enlarged and thickened shells, with excessive calcification in the ventral posterior part of the shell.

During the late Katian episode of greenhouse climate, especially in the northern palaeotropics and equatorial regions, shallow, moderately agitated, persistently warm sea waters over shallow-water carbonate platforms would reduce dissolved CO_2 and promote $CaCO_3$ precipitation due to supersaturation with respect to the $HCO_3^- + Ca^{2+} = CaCO_3 + H^+$ system. This would have favoured the building of thick shells by virgianids and required minimal metabolic energy in a sea-water chemical system favouring $CaCO_3$ precipitation. In an equatorial climate zone devoid of severe storms, virgianids would become environmental opportunists, growing a large, rostrate, and extremely thickened (and thus heavy) ventral valve to assume a stable, stationary, recumbent life position, where the risk of smothering by large, storm-generated mud plumes was greatly reduced, whereas the much smaller and lighter dorsal valve functioned like a rotating lid to open and close the shell, using minimal energy (e.g. Jin *et al.* 2013, 2023). Additionally, excess calcification would provide better protection against predators. During the Hirnantian glaciation, these large shells became extinct, and the entire virgianid lineage was represented by the small and relatively thin-shelled *Brevilamnulella*. Shell enlargement and thickening resumed during the re-radiation of virgianids in the early Silurian, especially during episodes of global warming and marine transgressions.

SYSTEMATIC PALAEONTOLOGY

Order PENTAMERIDA Schuchert & Cooper, 1931
Suborder PENTAMERIDINA Schuchert & Cooper, 1931
Superfamily PENTAMEROIDEA M'Coy, 1844
Family VIRGIANIDAE Boucot & Amsden, 1963

Genus TCHERSKIDIUM Nikolaev & Sapelnikov, 1969

Type species. Conchidium (?) *unicum* Nikolaev, 1968 (see also Nikolaev 1974). Iryuda Formation (upper Katian), Ina River, near junction with Mirny Creek, Omulevsk Mountains, northeast Siberia (Kolyma terrane).

Tcherskidium tenuicostatum Jin & Blodgett, 2020
Figures 5–8

2020 *Tcherskidium tenuicostatum* Jin & Blodgett, p. 637.
2020 *Tcherskidium tenuicostatus* Jin & Blodgett, p. 647, figs 7.1–7.8.
2022 *Tcherskidium tenuicostatum*; Jin *et al.*, p. 1466, fig. 3.1–3.11.

Holotype. By original designation, GSC 131829 (Jin & Blodgett 2020, fig. 7.1, 7.2), unnamed stratigraphic unit, upper Katian, Black River D-1 1:63 360 scale quadrangle, east-central Alaska.

Material. GGU 254729, 430 ventral, 12 dorsal and 3 articulated shells.

Description. (Greenland material) Shell moderate to relatively large for Late Ordovician virgianids, attaining a maximum preserved length of 36 mm and width 31 mm, elongate oval with maximum shell width located anterior of mid-length, ventribiconvex with strongly convex ventral valve approximately twice as deep as dorsal. Hinge line short, curved latero-anteriorly, reaching less than one-third shell width, merging smoothly into lateral contour of shell. Costae simple, strong, evenly spaced (e.g. Figs 5A, E, 7A, C), with sub-rounded to subangular crests, well-developed except in apical and posterolateral areas of shell (Figs 5B, C, F, I, 6B–D, 7B, C, F, G), ranging from 10 to 16 per 10 mm in middle portion of shell. Growth lines sharply defined (visible in well-preserved specimens), uniformly and rhythmically spaced (Figs 5D, 6I), punctuated by stronger growth lamellae (Figs 5A, C, 6G, 7G). Ventral umbo obtuse, high, strongly and uniformly arched (helmet shaped); beak prominent, strongly in-curved (Figs 5B, C, 7B, G) in relatively large shells. Ventral sulcus weakly developed anterior of umbo, beginning *c.* 20 mm from beak, becoming slightly better developed anteriorly (Figs 5H, I, 6A, D). Delthyrium open, with apical angle *c.* 60°

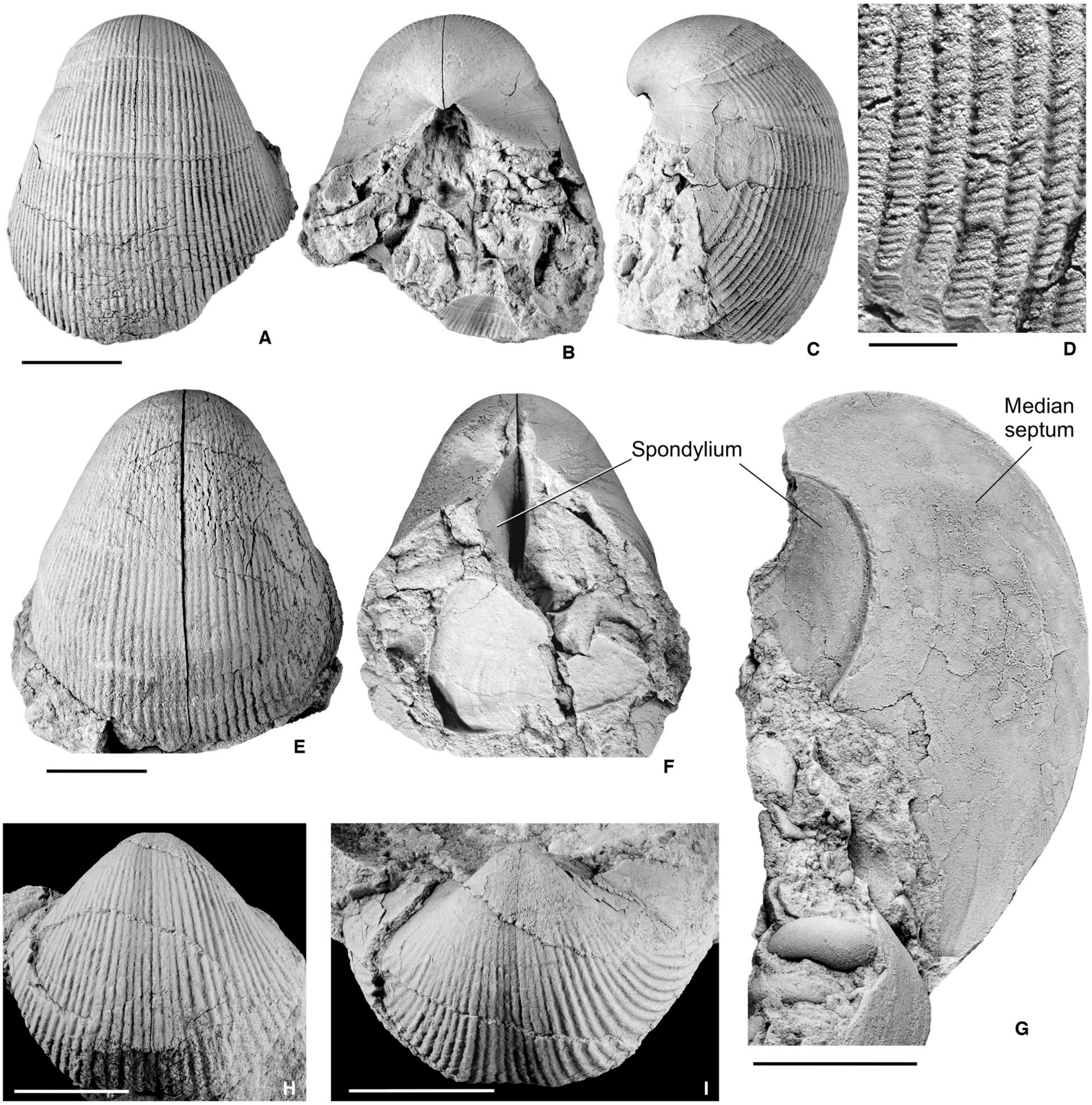

FIG. 5. *Tcherskidium tenuicostatum* Jin & Blodgett, 2020, three specimens from GGU 254729, from coquinitic boulders and olistoliths of late Katian age, embedded in the Citronens Fjord Member (Rhuddanian), Merqujoq Formation. A–D, MGUH 34213, exterior, interior, lateral views, and enlarged growth lines of anteriorly damaged ventral valve. E–G, MGUH 34214, exterior, interior, and medially split views of ventral valve, showing long and high median septum. H–I, MGUH 34215, ventral and posterior views of ventral valve, showing variant with gentle sulcus. Scale bars represent: 10 mm (A–C, E–I); 2 mm (D).

(Figs 5B, F, 6B, 7F). Dorsal umbo notably lower, narrower, and of much lower convexity than the ventral, with weakly in-curved to suberect beak (Fig. 6E, G). Dorsal valve evenly and moderately convex, without fold or sulcus.

Ventral interior. Spondylium large, broadly V shaped but with narrow and rounded basal portion (*c.* 1.5 mm wide along entire length), extending to about mid-length of shell, supported along its entire length by a median septum that extends further to the anterior margin of shell (Figs 5F, G, 6B, 7D, F, H). Median septum high, reaching more than two-thirds of ventral valve depth (achieving a maximum height of 15 mm in a relatively large shell), but receding ventrally from the junction with the distal end of spondylium to the anterior margin (Figs 5G, 7D, H).

Dorsal interior. Inner socket ridges well developed. Inner hinge plates low, short, confined to apical area, extending

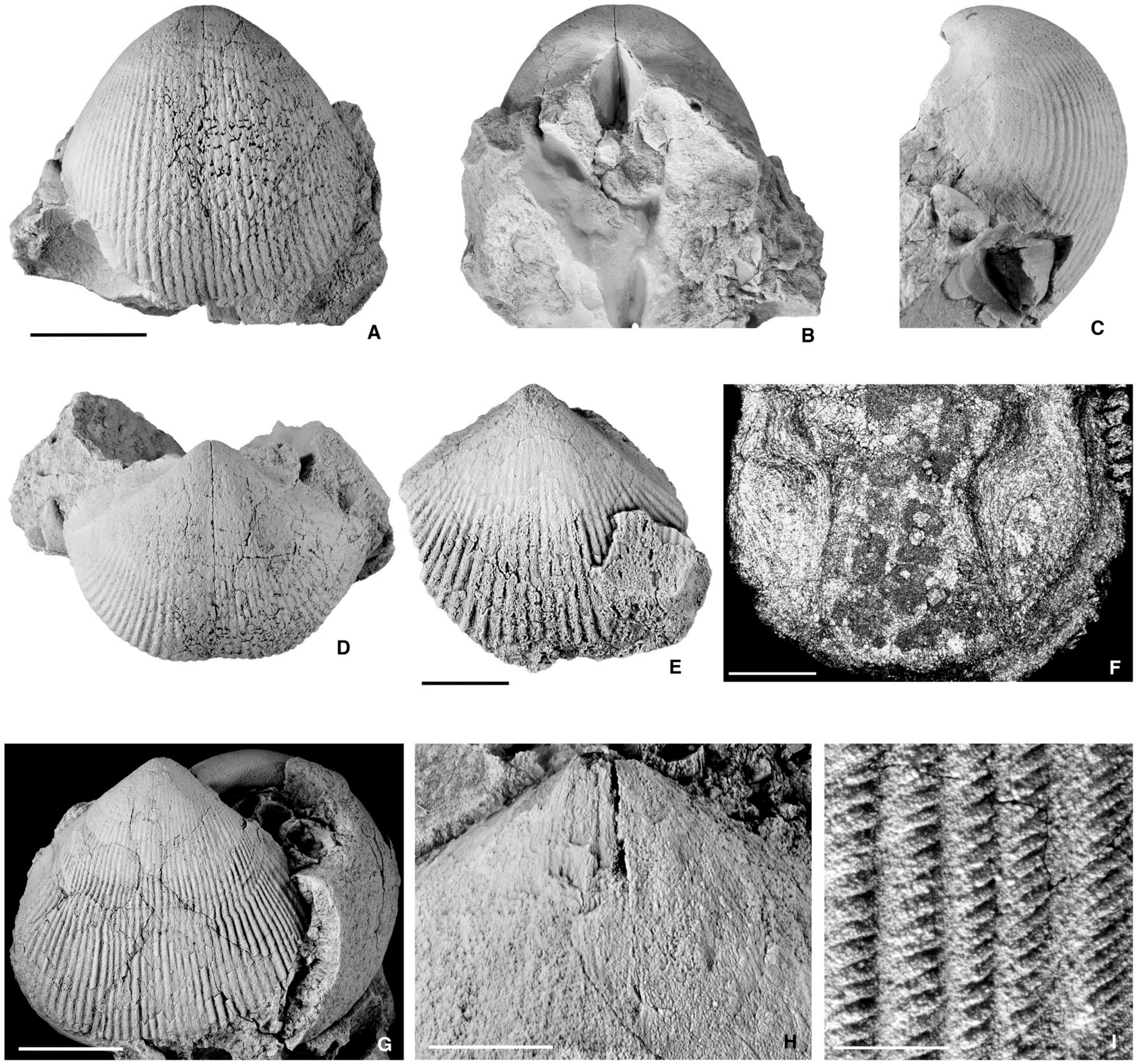

FIG. 6. *Tcherskidium tenuicostatum* Jin & Blodgett, 2020, one ventral valve and two dorsal valves from GGU 254729. A–D, MGUH 34216, exterior, interior, lateral, and posterior views of anteriorly damaged ventral valve, with weakly developed ventral sulcus. E–F, MGUH 34217, exterior and cross-section (F, 0.6 mm from apex; Fig. 8) of dorsal valve, showing basolaterally divergent inner hinge plates. G–I, MGUH 34218, exterior, apical views (note short inner hinge plates) of dorsal valve, and local enlargement (I) showing rhythmic growth lines in the lateral part of the valve. Scale bars represent: 10 mm (A–D, G); 5 mm (E, H); 1 mm (I), 0.5 mm (F).

anteriorly from beak for *c.* 3 mm in an average-sized valve (Fig. 6E–H), diverging basolaterally from each another towards valve floor (Fig. 8). Outer hinge plates longer and more robust than inner hinge plates. Junction of crural base with outer and inner hinge plates smooth, without formation of flanges, extending anteriorly into free, rod-like crura for up to 7 mm in length.

Remarks. The Greenland material is assigned to *Tcherskidium* based mainly on the dorsal internal structures, especially the short and low inner hinge plates (Fig. 8). According to the original definition by Nikolaev & Sapelnikov (1969; see also Nikolaev 1974; Sapelnikov 1985), *Tcherskidium* is indistinguishable from *Proconchidium* in their ventral internal structures, but they differ in that *Tcherskidium* has reduced inner hinge plates that are much lower and shorter than the outer hinge plates, whereas *Proconchidium* has long and high inner hinge plates. The Greenland shells resemble those of *T. tenuicostatum* in having fine, simple (non-branching) costae, averaging 14 per 10 mm, and lacking ventral interarea. *Tcherskidium lonei* Jin et al., 2022 from the upper Katian of Alaska (accreted terrane) is

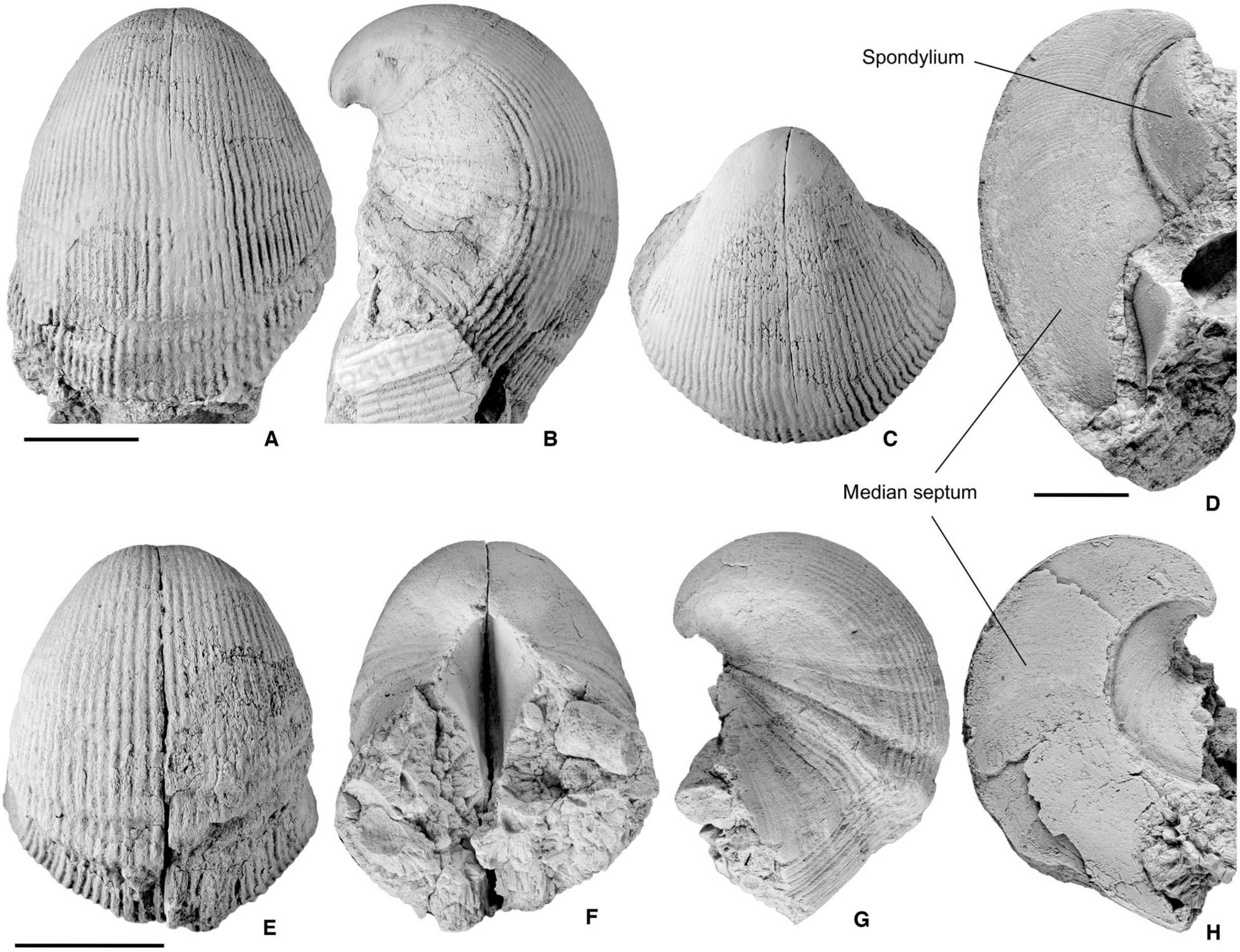

FIG. 7. *Tcherskidium tenuicostatum* Jin & Blodgett, 2020, three ventral valves from GGU 254729. A–C, MGUH 34053, ventral, lateral, and posterior views of ventral valve, variety without notable sulcus. D, MGUH 34054, medially split ventral valve; note the long and high median septum with finely rhythmic growth lines and relatively short spondylium. E–H, MGUH 34055, exterior, interior, and lateral views of ventral valve showing drastic changes in growth direction (G), and medially split view (H) showing prominent median septum extending to anterior margin of valve. Scale bars represent: 10 mm (A–C, E–H); 5 mm (D).

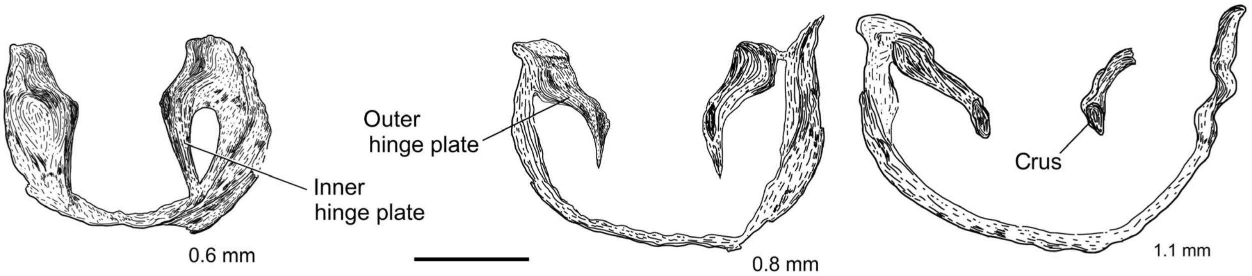

FIG. 8. *Tcherskidium tenuicostatum* Jin & Blodgett, 2020. Three selected (out of a total of nine) serial sections (at 0.6 mm, 0.8 mm and 1.1 mm from valve apex) of dorsal valve (MGUH 34217, same specimen as Fig. 6E, F) showing short, basolaterally divergent inner hinge plates, and somewhat longer outer hinge plates. Note smooth junction of crural base with inner and outer hinge plates. Scale bar represents 1 mm.

similar to *T. tenuicostatum* in nearly all of its morphological characteristics except for the sharply defined ventral interarea. *Tcherskidium unicum* from Siberia has notably coarser costae than *T. tenuicostatum* or *T. lonei* (for morphological details and comparisons see: Nikolaev & Sapelnikov 1969; Nikiforova 1989; Modzalevskaya 2018; Jin *et al.* 2022).

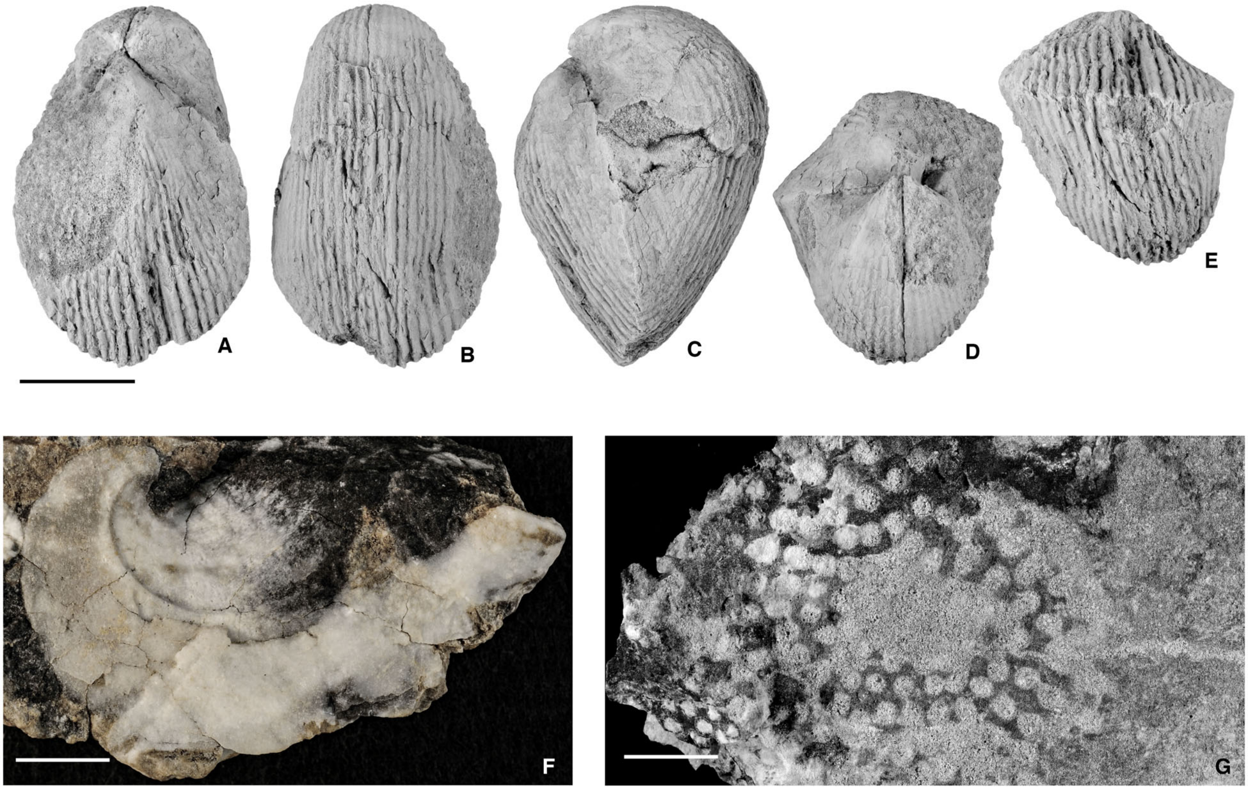

FIG. 9. *Proconchidium schleyi* Jin *et al.*, 2022, and associated *Fisherites* sp. from upper Katian strata that are correlative to the lower Turesø and Alegatsiaq Fjord formations, G.B. Schley Fjord, North Greenland. A–E, MGUH 34049, dorsal, ventral, lateral, posterior and anterior views of holotype. F, MGUH 34051, paratype, medially split view of large ventral valve; note long median septum extending to anterior margin of valve, and relatively large spondylium with a depth approximately equal to height of median septum. G, MGUH 34219, *Fisherites* sp. (common alga in middle–upper Katian of Laurentia) from the same coquinitic unit as MGUH 34049. Scale bars represent 10 mm.

Genus PROCONCHIDIUM Sapelnikov *in* Nikolaev & Sapelnikov, 1969

Type species. *Conchidium muensteri* St. Joseph, 1938.

Remarks. Precise locality and stratigraphic horizon unknown for the original type specimens in the Kiær Collection, which includes the following material: P.M.O. 15.132–42, 16.644–52, 16.665–74, and 20.821, all from Vestre Svartøy, a small island in Ringerike, southern Norway. The holotype (P.M.O 20.821a) and two paratypes (P.M.O 20.821b, c), originally embedded together in a small block, were selected by St. Joseph, (1938, pl. 6, figs 10, 11). Kiær's original specimens, collected as loose material from the shoreline of Vestre Svartøy, were labelled as from 'Etage 5b', which is Hirnantian in modern terminology. At Kiær's (1897, p. 7, fig. 3) section of Vestre Svartøya, the lower unit of 'gastropod limestone' (Gastropodenkalk) was assigned to Etage 5a, which would be upper Katian in modern terminology, attributed by Hanken *et al.* (2016) to the upper Bønsnes Formation, consisting of bioclastic carbonate concretions embedded in shales. Worldwide, *Proconchidium* has not been recorded so far from Hirnantian strata. It is thus likely that the type specimens of *P. muensteri* came from the limestone concretions in the upper Bønsnes Formation, which was described by Hanken *et al.* (2016, p. 193) to be rich in calcimicrobes, brachiopods, bryozoans, gastropods, trilobites, ostracods and crinoids.

Proconchidium schleyi Jin *et al.*, 2022
Figure 9

2022 *Proconchidium schleyi* Jin *et al.*, p. 1472, figs 7, 8.

Holotype. MGUH 34049 (Jin *et al.* 2022, fig. 7.6–7.11), unnamed upper Katian strata, G.B. Schley Fjord, North Greenland.

Material. In addition to the material reported in Jin *et al.* (2022) from G.B. Schley Fjord in Peary Land, disarticulated valves occur in earlier collections at the Natural History Museum of Denmark (Copenhagen): GGU 197503, 197536, 197539, 197541. The exact number of specimens is difficult to estimate because most of the shells are embedded tightly in carbonate matrix.

Remarks. We refer to Jin *et al.* (2022) for descriptions and discussion of the North Greenland species. The holotype of

P. schleyi is illustrated here, plus an image of the co-occurring *Fisherites* sp. (Fig. 9G) in the same coquinitic unit. *Fisherites*, commonly regarded as a large globular alga, was exceptionally common in upper Katian carbonate rock of the Williston Basin, Hudson Bay Basin, Mackenzie Mountains, and other regions of Arctic Canada.

Genus DELOPROSOPUS Jin *et al.*, 2006

Type species. Eoconchidium jiangshanensis Liang *in* Liu *et al.*, 1983, Changwu Formation (upper Katian), western Zhejiang Province.

Species included. In addition to the type species, *Deloprosopus* includes two species: *Tcherskidium ulkuntasensis* Rukavishnikova & Sapelnikov, 1973; Tolen horizon, *Holorhynchus giganteus* zone (= Ülkentas Limestone, Şoqpar Regional Stage, *Paraorthograptus pacificus* Zone of modern terminology; LE Popov, pers. comm. 2023), upper Katian, Chu-Ili Mountains, southern Kazakhstan; and *Deloprosopus dawesi* sp. nov. (see below).

Remarks. Jin *et al.* (2006) initially distinguished *Deloprosopus* from *Tcherskidium* by its somewhat shorter ventral median septum that does not extend near the anterior margin, and the presence of a ventral interarea. Up until this study, *Deloprosopus* was known only from South China, and was initially reported as *Eoconchidium* or *Tcherskidium* (Liu *et al.* 1983; Zhan & Cocks 1998) because of their external similarity, especially in their elongate, strongly ventribiconvex, ribbed shell with a high, strongly arched ventral umbo. Compared with the typical *Tcherskidium* from northeastern Siberia, the shells of *Deloprosopus* have a notably smaller average or maximum size, and the costae tend to be uneven in size, unlike the neat, equal-sized costae in *Tcherskdium*. The well-defined ventral interarea, initially regarded by Jin *et al.* (2006) as a unique character in Late Ordovician virgianids, has been observed also in the late Katian species of *Tcherskidium lonei* Jin *et al.*, 2022 from accreted terranes of Alaska. It is notable that the new species of *Deloprosopus* from North Greenland share with the type species such characters as the relatively small shell size with uneven costae, well-delimited ventral interarea, and a relatively long ventral median septum extending beyond mid-length (although not extending near the anterior margin) of the shell. The Greenland new species is the first known occurrence of *Deloprosopus* outside of South China.

Deloprosopus dawesi sp. nov.
Figures 10, 11

LSID. https://zoobank.org/nomenclaturalacts/7EB173FF-2252-48A6-AF5F-8E84541C6B32

1973 *Virgiana* cf. *decussata* Poulsen *in* Bjerreskov & Poulsen, p. 13

1982 *Tcherskidium* sp.; Hurst & Sheehan, p. 48.

2009 *Tcherskidium* sp.; Rasmussen, p. 51, pl. 3, figs 1–3.

Derivation of name. After Peter Dawes, who made significant contributions to the geology of North Greenland.

Holotype. MGUH 34223 (Fig. 10P–S); ventral valve.

Paratypes. Five specimens (3 vv, 2 dv), MGUH 34220–34222, 34224, 34225 (Figs 10F–O, 11).

Material. GGU 53498 (40 vv; 11 dv); GGU 53516 (10 vv); GGU 53526 (5 vv; 2 dv).

Type locality and stratum. The holotype and paratypes are from GGU 53526, Merqujoq Formation (upper Katian), south coast of Frederick E. Hyde Fjord, east of Thors Fjord, northern Peary Land.

Diagnosis. Medium-sized, commonly asymmetrical, strongly ventribiconvex shell with highly arched ventral umbo. High and narrow ventral interarea. Long and wide spondylium extending beyond mid-length, supported by similarly long median septum not reaching anterior margin. Inner hinge plates short and low, discrete.

Description. Shell small to medium in size for late Katian virgianids, with average length *c.* 20 mm, and largest shell reaching 39 mm in length and 26 mm in width, oval to pear shaped in outline, commonly asymmetrical in ventral view to various degrees, strongly elongate (average width/length ratio = 0.68 in shells larger than 20 mm long) and laterally compressed in relatively large forms, resulting in shell being notably thicker than wide (Fig. 10P–S). Lateral profile strongly ventribiconvex, with a much larger and more strongly convex ventral valve and weakly convex dorsal valve. Costae strong, with subangular to subrounded crest, unequal in size (coarseness) and spacing (width of interspaces), commonly 10–12 per

FIG. 10. *Deloprosopus* from North Greenland and South China. A–E, two topotypes of *Deloprosopus jiangshanensis* (Liang *in* Liu *et al.*, 1983), Xiazhen Formation (upper Katian), Yushan, eastern Jiangxi, South China: A–D, NIGP 139301, dorsal, ventral, lateral and posterior views; note presence of ventral interarea; E, NIGP 203273, ventral view of relatively small shell. F–S, *Deloprosopus dawesi* sp. nov., four specimens from GGU 53526, upper Katian strata, Peary Land: F–J, MGUH 34220, paratype, exterior, interior, lateral, posterior and enlarged apical area of posteriorly abraded ventral valve; note presence of ventral interarea (G, J); K–M, MGUH 34221, paratype, ventral, lateral and posterior views of ventral valve with strong costae; note valve outline similar to that of other specimens (B, E and F); N–O, MGUH 34222, paratype, ventral and lateral views of relatively large ventral valve, with some contorted costae; P–S, MGUH 34223, holotype, exterior, interior, lateral and posterior views of relatively large ventral valve; note external mould of prominent spondylium (its shell substance is not preserved). Scale bars represent: 5 mm (A–M); 10 mm (N–S).

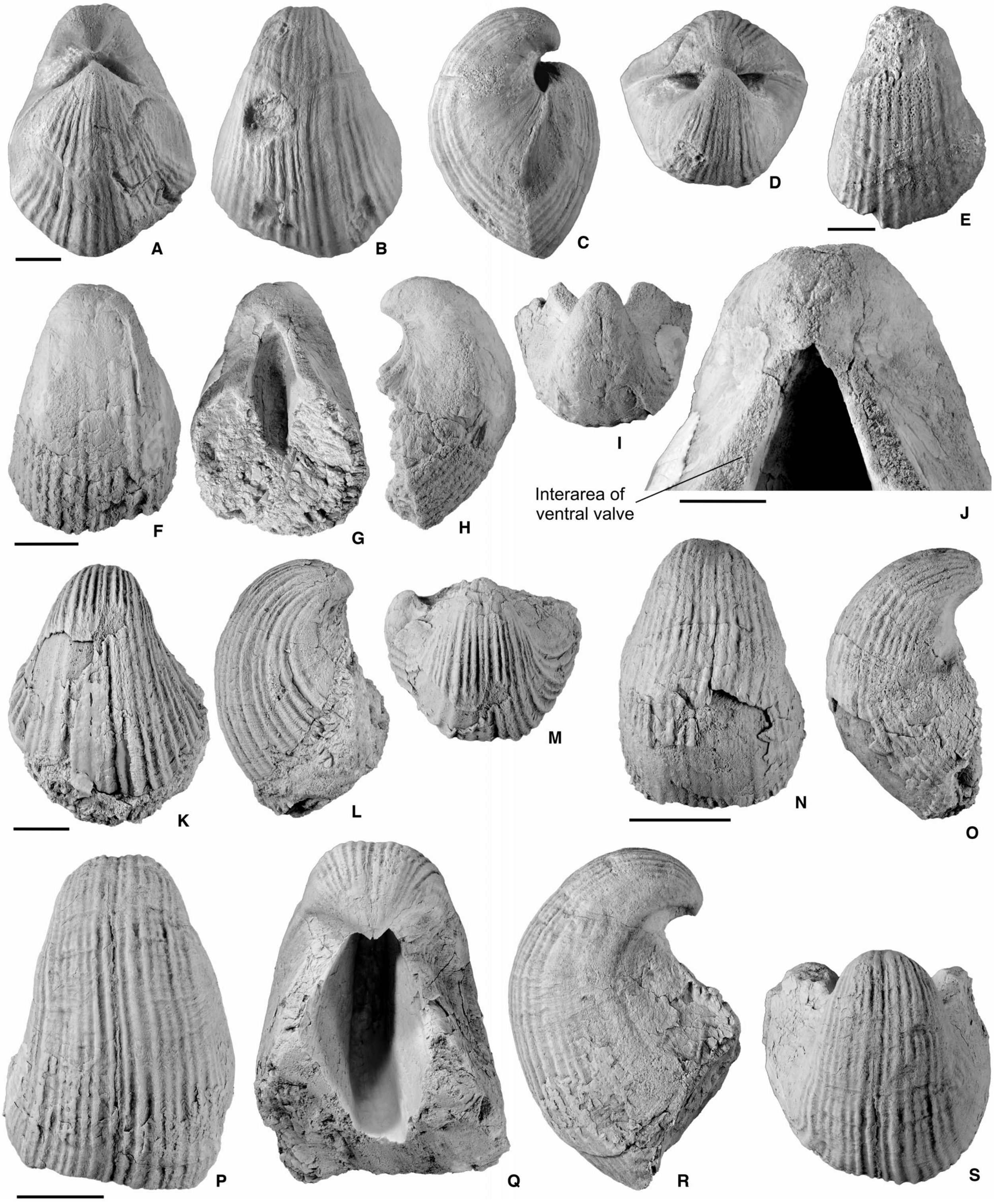

10 mm in anterior part of shell, with occasional bifurcation in anterior one-third of shell (Fig. 10K, L). Fine growth lines well developed, evenly spaced at *c.* 5 per 1 mm, but only apparent on well-preserved parts of shell (Fig. 10L), superimposed on much coarser and irregularly spaced growth lamellae. Curvature of anterior commissure difficult to determine because of rare shells without damage to anterior margin.

Ventral umbo broad, high, strongly convex and arched, with prominent, pointed, in-curved beak (Fig. 10H, R). Relatively narrow and gentle sulcus present in umbonal area, usually

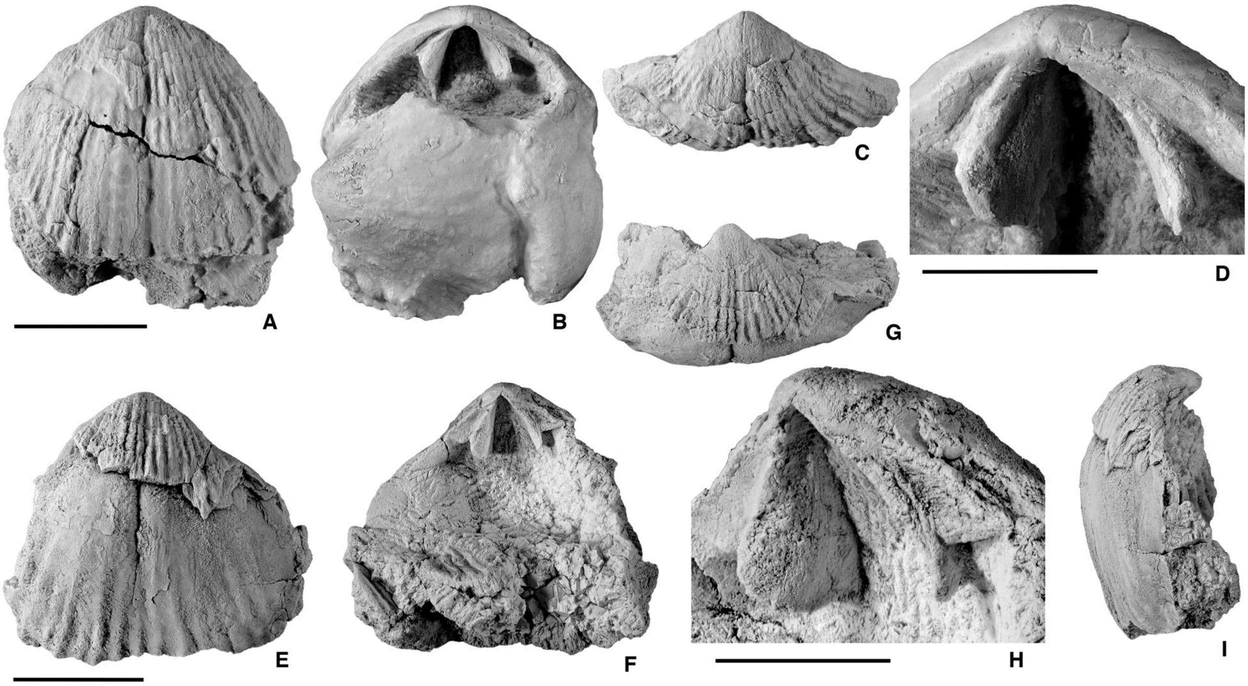

FIG. 11. *Deloprosopus dawesi* sp. nov., two dorsal valves from GGU 53526, upper Katian strata, Peary Land. A–D, MGUH 34224, paratype, exterior, interior, posterior views of dorsal valve, and enlarged apical area (D) showing relatively short hinge plates. E–I, GUH 34225, paratype, exterior, interior, posterior, enlarged hinge plates, and lateral views of partly exfoliated dorsal valve. Scale bars represent: 10 mm (A–C, E–G, I); 5 mm (D, H).

bearing two costae, extending anteriorly into weak medial furrow in some specimens (Fig. 10P). Ventral interarea sharply defined, developed as narrow platform along each side of high delthyrium (Fig. 10G, J, Q), then transitioning abruptly into steep posterolateral side of shell.

Dorsal umbo weakly to moderately convex (Fig. 11A, C, E, I), with inconspicuous beak bending slightly in ventral direction. Dorsal interarea well developed, oriented along the commissural plane. Sulcus-like medial furrow developed a few millimetres anterior of valve apex, narrow and generally shallow.

Ventral interior. Apical area of shell thickened during growth by secondary shell substance on both sides of spondylium. Spondylium long, extending beyond mid-length, reaching about half of shell width at its widest middle part (Fig. 10G, Q) and more than half of valve depth; narrow U-shaped basal portion with rounded bottom, deflected dorsolaterally into overall V-shaped cross-section. Median septum long, extending beyond mid-length, but not reaching anterior margin, supporting entire length of spondylium.

Dorsal interior. Hinge sockets represented by narrow, relatively shallow grooves along each side of notothyrial cavity. Inner hinge plates very low, discrete, weakly divergent anterolaterally along valve floor, and divergent dorsolaterally in cross-section at *c.* 25°, confined to apical area, shorter than outer hinge plates. Outer hinge plates higher and wider than inner hinge plates, ventrolaterally divergent from each other at *c.* 80° (Fig. 11B, D, F). Junction of crural base with outer and inner hinge plates smooth, lacking any prominent flanges.

Remarks. The North Greenland new species resembles the type species, *D. jiangshanensis* (Fig. 10A–E), in its overall shell size and shape, varying degree of asymmetry, uneven and occasionally bifurcating costae, presence of ventral interarea, and internally in a long median septum that extends beyond mid-length but is short of reaching the anterior margin. In the late Katian ribbed virgianids it is common to see that the generally strong costae fade or disappear in posterolateral areas close to the lateral commissure (compare *D. dawesi* in Fig. 10R with the type species in Fig. 10C). The Greenland species differs from the type species in having a more commonly developed shell asymmetry, a higher and more strongly arched ventral umbo and thus a higher delthyrium, and a notably longer and wider spondylium relative to shell size (Fig. 10G, Q). Whereas the type species commonly has a moderately developed ventral sulcus and dorsal fold, *D. dawesi* has a sulcus-like medial furrow in both the ventral and dorsal valves.

Tcherskidium ulkuntasensis Rukavishnikova & Sapelnikov, 1973 from the upper Katian of southern Kazakhstan is assigned to *Deloprosopus* in this study because of its generally small shell size (usually <25 mm in length) and the presence of a 'pseudo-interarea' in the ventral valve (Sapelnikov & Rukavishnikova 1975, p. 69). The Kazakhstan species differs from *D. jiangshanesis* and *D. dawesi* in having a longer median septum that nearly (but does not) reach the anterior margin, and extends anterior beyond the distal end of the spondylium. *Deloprosopus dawesi* differs from *D. ulkuntansensis* in reaching a much larger maximum size. Small specimens of the Greenland species differ from the Kazakhstan species in having a narrower shell with a more in-curved beak and a better defined, narrower ventral sulcus. The shells of *D. ulkuntansensis* are nearly equidimensional, ranging from slightly elongate to slightly transverse.

Genus VIRGIANA Twenhofel, 1914

Type species. *Pentamerus Barrandi* [sic] Billings, 1857, p. 296. Becscie River Bay, middle to upper Becscie Formation (middle Rhuddanian), Anticosti Island, Quebec (for details on the type material see Twenhofel 1928 and Jin & Copper 2000).

Virgiana hursti sp. nov.
Figures 12–14

LSID. https://zoobank.org/nomenclaturalacts/BA9698FC-69A0-4037-A13F-0E54AD69CDDD

1982 *Tcherskidium* sp.; Hurst & Sheehan, p. 48.

2009 *Virgiana* cf. *decussata* Whiteaves; Rasmussen, p. 81, pl. 1, figs 1–4.

2009 *Virgiana* n. sp.; Rasmussen, p. 81, pl. 1, figs 6–9.

Derivation of name. After John Hurst, in recognition of his substantial work on Ordovician and Silurian brachiopod faunas of North Greenland.

Holotype. MGUH 34226 (Fig. 12A–C), ventral valve.

Paratypes. 10 specimens (1 incomplete conjoined shell, 6 vv, 4 dv), MGUH 34227–34236 (Figs 12D–L, 13).

Material. GGU 82178 (2 vv); GGU 82484 (10 vv, 1 dv); GGU 198860 (1 conjoined shell; 41 vv; 3 dv in coquina); GGU 198861 (44 vv); GGU 254760 (236 vv; 17 dv); GGU 254878 (40 vv, 3 dv); GGU 254897 (1 shell, 75 vv, 6 dv); GGU 270631 (37 vv, 8 dv); GGU 274963 (2 vv).

Type locality and stratum. The holotype and serially sectioned paratype are from GGU 254760, Odins Fjord, Turesø Formation (Rhuddanian), and other figured paratypes from GGU 254897, ‘middle unit’ of Hurst (1984), also of Rhuddanian age.

Diagnosis. Relatively large *Virgiana*, with strong convex ventral valve and high, arched ventral umbo, and moderately strong ribbing. Median septum long for genus, reaching about one-third of valve length. Inner hinge plates long for genus, parallel to each other in transverse cross-section, fused to valve floor without forming wedged junction, extending to level of hinge line; outer hinge plates slightly longer than inner hinge plates.

Description. Shells medium to very large, reaching a maximum length of *c.* 80 mm, and width of 63 mm; subcircular in outline at early growth stage, becoming elongate oval in large shells (Figs 12, 13); position of maximum shell width varying from near mid-length to anterior third of shell; ventribiconvex, with strongly convex ventral valve twice as deep as dorsal valve in large shells. Hinge line short and anterolaterally curved, not forming distinct cardinal extremities. Anterior commissure not well preserved in available specimens. Costae generally strong, with rounded crests, but faint or absent in umbonal and posterolateral portions of shell (e.g. Figs 12B–F, I–K, 13I, K), increasing anteriorly by bifurcation, commonly 7–9 per 10 mm. Fine growth lines better preserved in anterior part of shell, punctuated by strong, irregularly spaced growth lamellae (Figs 12A, C, D, J, 13G, H). Ventral umbo varying from narrow and posteriorly tapering in relatively small valves to broadly rounded and strongly arched in larger forms (compare Fig. 12A, B with 13J), with a correspondingly developed beak from moderately (pointing to dorsal direction) to strongly in-curved (pointing anteriorly). Sulcus present posteriorly, narrow and well-delimited in ventral umbonal area, bearing one or two costae on its floor, becoming broader and shallower anteriorly (with costae on its floor increasing to as many as 14), until it disappears and merges into a uniformly convex contour of shell at distance of 15–20 mm from beak (Figs 12A, C, E, I, J, 13E, F, K). Dorsal valves usually not exceeding one-half of depth of ventral valve; with moderately convex dorsal umbo and small beak buried under ventral beak area (Fig. 12G, H). Dorsal fold present posteriorly in some specimens, narrow and devoid of ribbing in umbonal area, widening and flattening anteriorly, disappearing anterior of umbonal area (Fig. 12D); poorly defined in others (Fig. 13G–I).

Ventral interior. Hinge teeth weak, delimited by groove on lateral margin of each tooth. Spondylium broadly V shaped but with narrow and rounded floor, extending for about one-third of shell length, tilting in anterodorsal direction (Figs 12K, L, 13A). Median septum very high, supporting the entire length of the spondylium, with a slightly concave-arched anterior edge (Fig. 12L).

Dorsal interior. Valve floor moderately thickened. Inner hinge plates relatively long for genus, extending along valve floor for *c.* 5 mm in average-sized valves (reaching level of hinge line); diverging at very low angle from each other along their junctions with valve floor, mostly parallel to each other in transverse cross-section (Fig. 14, 2.8 mm and 3.0 mm from apex), or diverging very slightly in basolateral direction at their distal ends (Fig. 14, 3.5 mm). Outer hinge plates somewhat stronger but lower (in cross-section) than inner hinge plates, deflected from each other ventrolaterally in their anterior portions, showing robust lamellar layers. Crura rod like, oval in transverse cross-section, forming a relatively smooth junction with inner and outer hinge plates, or forming only an inconspicuous inner ridge (Fig. 14, 2.8–3.5 mm from apex).

Remarks. Of all the known species of *Virgiana*, the new species from North Greenland has the most prominent ventral median septum and dorsal hinge plates in proportion to shell size. For example, the median septum of *V. hursti* sp. nov. extends nearly twice as far anteriorly as that in *V. barrandei* and *V. mayvillensis* from Anticosti Island and Wisconsin (Jin & Copper 2000; Jin *et al.* 2019). The relatively small shells of *Virgiana hursti* resemble the type species, *V. barrandei*, in the dorsal fold and ventral sulcus developed in the umbonal areas, and the gentle relief of costae (e.g. compare Fig. 12A–D with

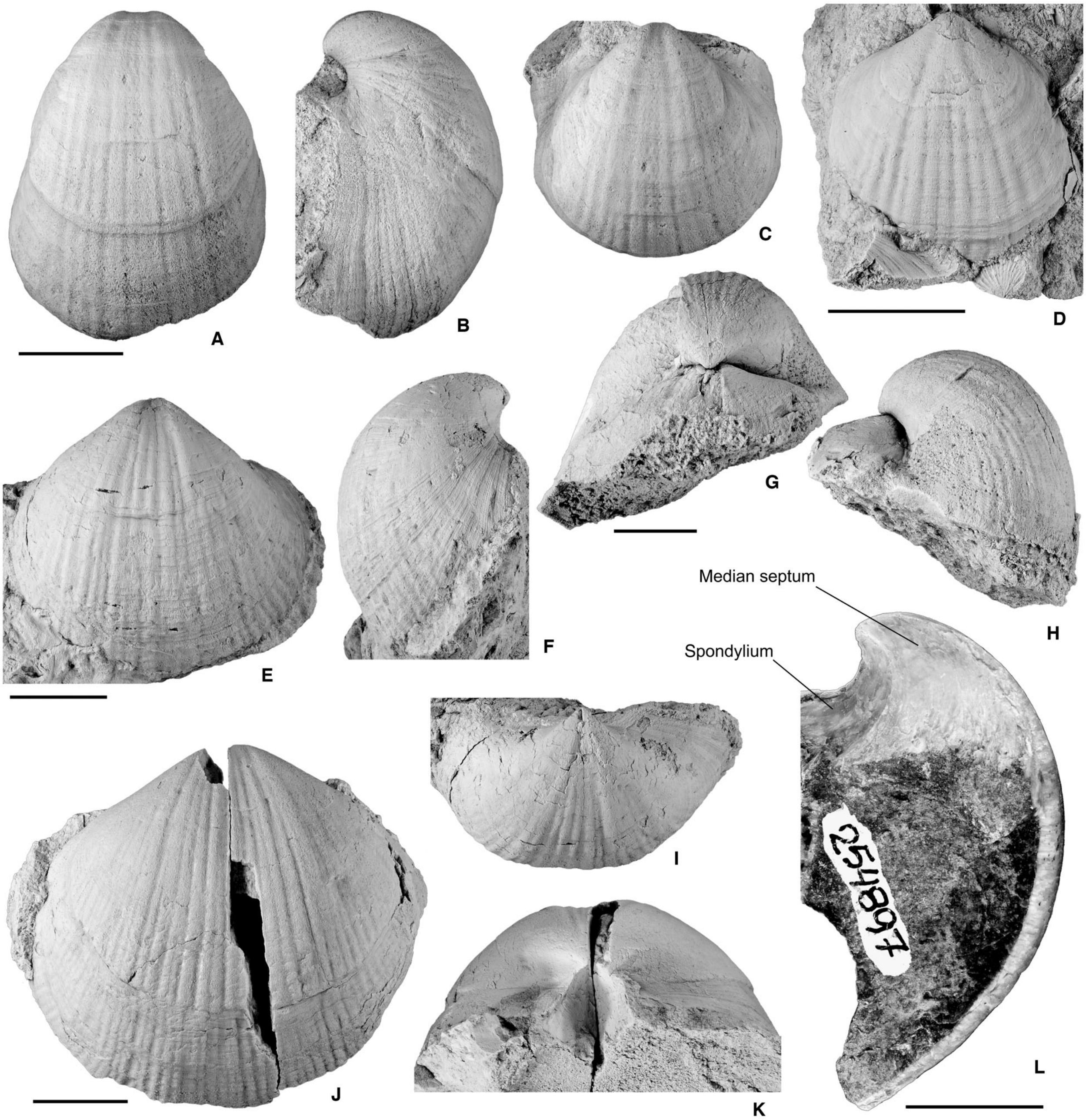

FIG. 12. *Virgiana hursti* sp. nov. A–C, MGUH 34226, holotype, ventral, lateral and posterior views of ventral valve, showing well-delimited sulcus in umbonal area, GGU 254760, Odins Fjord, Turesø Formation (Rhuddanian). D, MGUH 34227, paratype, nearly complete dorsal valve showing clearly defined fold but lack of costae in umbonal area; GGU 254760. E–F, I, MGUH 34228, paratype, ventral, lateral and posterior views of transversely extended ventral valve, with gentle and broad sulcus in posterior half of valve; GGU 254897, NW Apollo Sø, section 17 (close to GGU 254760). G–H, MGUH 34229, paratype, posterior part of conjoined shell, showing strongly biconvex profile; note partly exposed traces of short inner hinge plates; GGU 254897. J–L, MGUH 34230, paratype, ventral and posterior–interior views (J, K) of relatively large and wide ventral valve, with short and shallow spondylium, which is supported by a relatively long and high median septum well preserved along medially split plane (L); GGU 254897. Scale bars represent 10 mm.

Jin & Copper (2000, pl. 6, figs 11–14) and Jin & Copper (2010, fig. 5K–O)). The new Greenland species, however, differs in having a much larger maximum shell size (up to 80 mm in length, compared with 50 mm for *V. barrandei*), finer but more consistently developed costae, and the ventral median septum in the new species is notably longer than in all other congeneric species, reaching about one-third of the valve length. In comparison, the median septum in

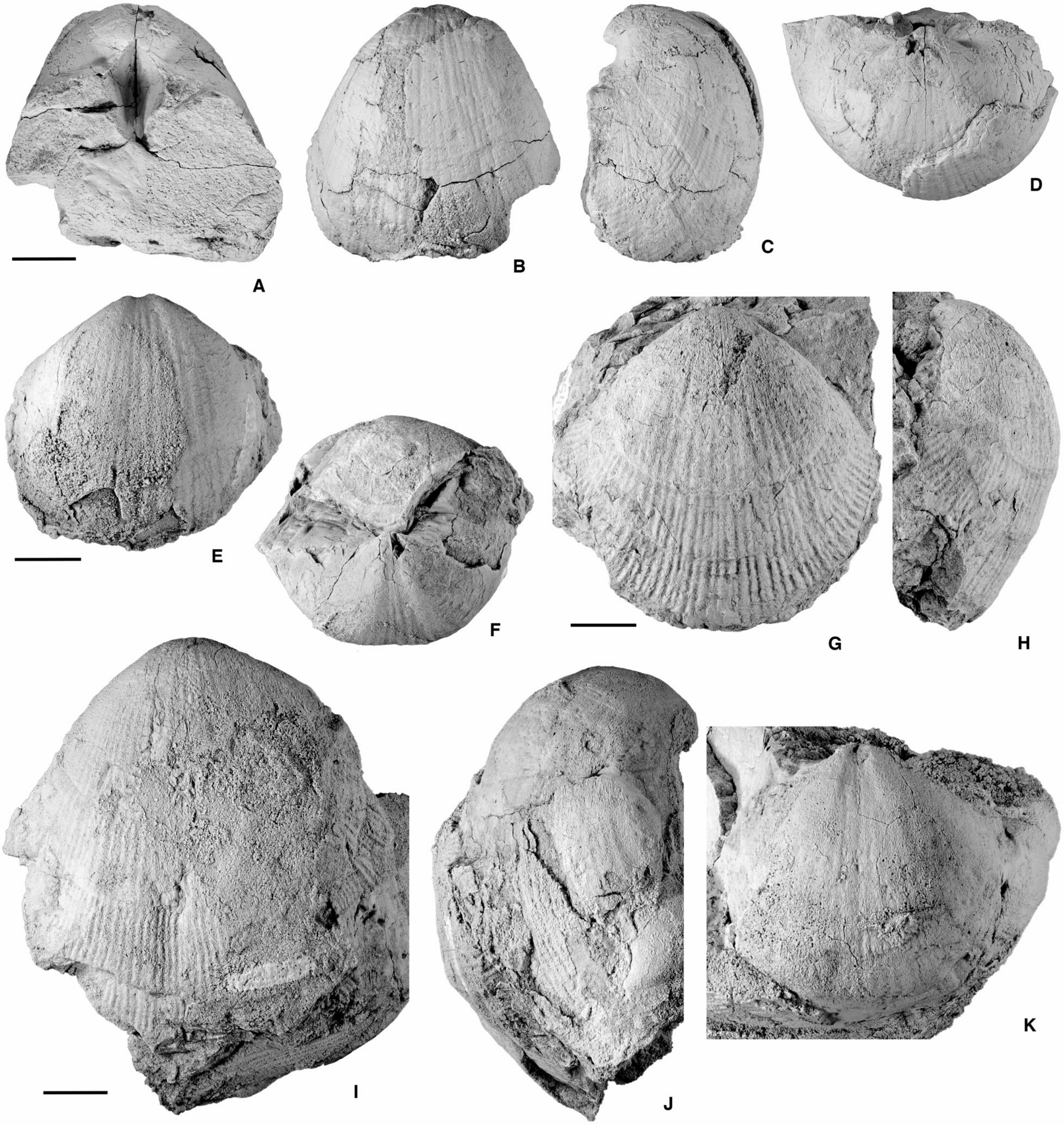

FIG. 13. *Virgiana hursti* sp. nov. Four specimens from Rhuddanian strata of the Store Canyon Member, Alegatsiaq Formation (equivalent to the Turesø Formation), GGU 254897, Apollo Sø area, Wulff Land. A–D, MGUH 34231, paratype, interior, ventral, lateral and posterior views of ventral valve showing small and shallow spondylium (A) and cracked trace of relatively long median septum (D). E–F, MGUH 34232, paratype, ventral and posterior views of anteriorly damaged ventral valve; note umbonal sulcus with costate floor. G–H, MGUH 34233, paratype, dorsal and lateral views of relatively large, slightly elongate dorsal valve; note cracked traces of inner hinge plates (G). I–K, two paratypes, a dorsal valve (I, MGUH 34234) and a ventral valve (J, K, lateral and posterior views of MGUH 34235) preserved in a single block; note sulcus in umbonal area of ventral valve (K), bearing abraded costae. Scale bars represent 10 mm.

V. barrandei and *V. mayvillensis* is usually less than one-quarter of the valve length, confined to the umbonal area (Jin & Copper 2000; Jin *et al.* 2019). In the type species, the costae vary from moderately strong in some to very faint in other shells, as shown by Jin & Copper (2000, 2010), and its median septum is confined to the apical area and supports the posterior part of the spondylium, which becomes mostly free-hanging anteriorly.

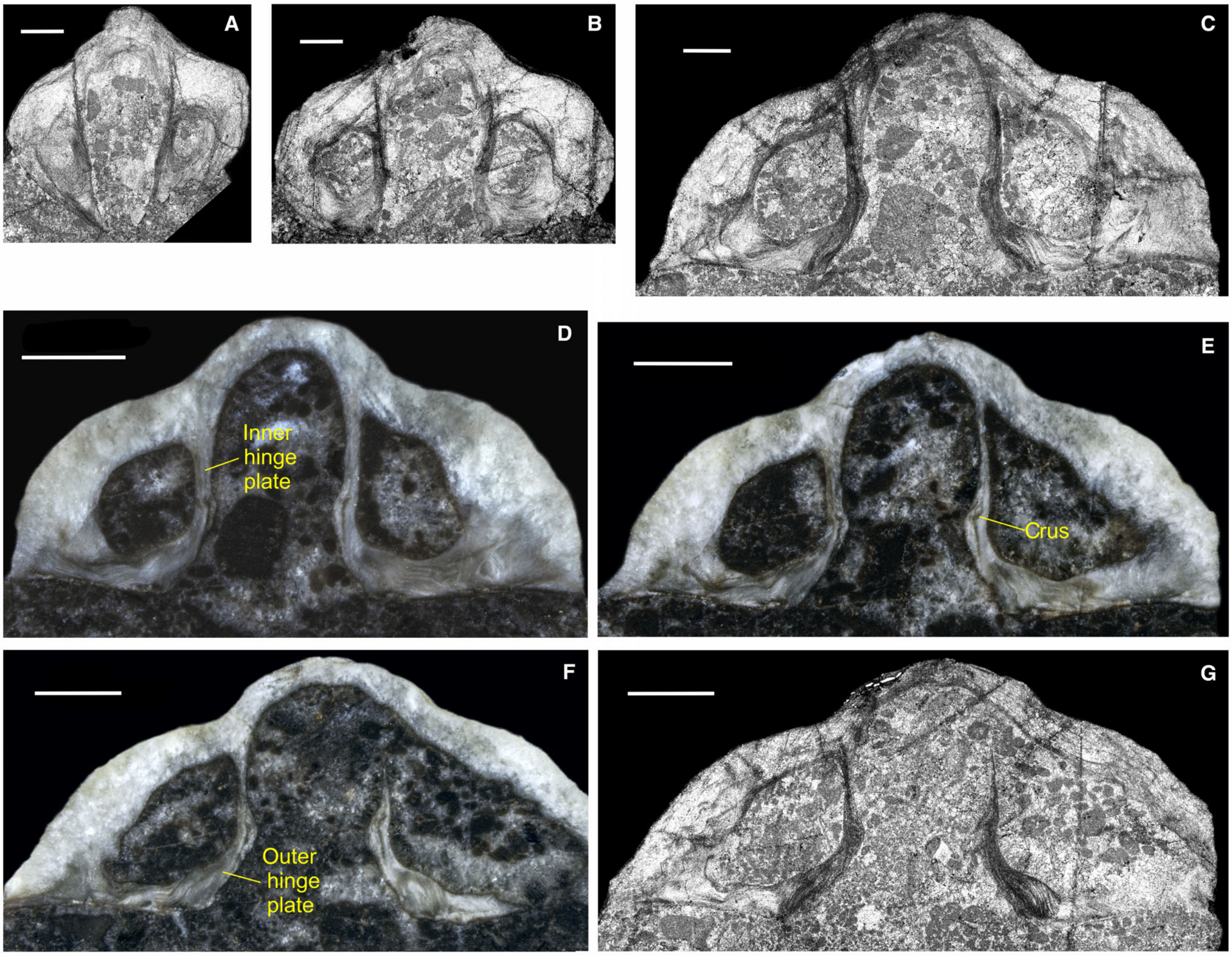

FIG. 14. *Virgiana hursti* sp. nov. Serial sections of specimen MGUH 34236, paratype, a dorsal valve from GGU 254760, Turesø Formation (Rhuddanian), Odins Fjord, Peary Land. A–C, G, acetate peels under transmitted light. D–F, polished rock surface under reflected light. Distance from valve apex: A, 1.2 mm; B, 4.8 mm; C, 2.8 mm; D, 2.8 mm; E, 3.0 mm; F, G, 3.5 mm. Scale bars represent 1 mm (A–C); 2 mm (D–G).

The large forms of *Virgiana hursti* sp. nov. resemble *V. decussata* (Whiteaves, 1891) from the Williston and Hudson basins of northern Manitoba, Canada in their numerous costae. *Virgiana decussata* also reaches a maximum shell length of 80 mm, but it has a flatter dorsal valve, especially in large shells, and its costae are weaker and finer, averaging 11 per 10 mm (Jin *et al.* 1993) compared with 8 per 10 mm in the Greenland species; *V. decussata* also has a much shorter ventral median septum (less than one-fifth valve length; Jin *et al.* 1993). Other common congeneric species from the Rhuddanian of Laurentia, such as *V. mayvillensis* Savage, 1916 from the Mayville Dolomite of Wisconsin and the Merrimack Formation of Anticosti Island (Jin & Copper 2000; Jin *et al.* 2019) and *V. utahensis* Sheehan, 1980 from the Tony Grove Member of the Laketown Dolomite of Nevada, have notably coarser and more sharply defined costae than *V. hursti*. Another commonly cited species, *Virgiana major* Savage, 1916, has been assigned as the type species for a new genus, *Virgianoides* Jin *et al.*, 2019 because of the presence of a cruralium supported anteriorly by a low median septum.

Genus PLEURODIUM Wang, 1955

Type species. Pentamerus (*Conchidium*) *tenuiplicatus* Grabau, 1925, upper Lojoping Formation (upper Aeronian), Yichang, Hubei, South China (Rong *et al.* 2017, p. 285).

Pleurodium sp.
Figure 15A–C

Material. GGU 82185–82187 (coquina); GGU 82191–82192 (coquina); GGU 82484 (vv); one conjoined shell, GGU 82485, Store Canyon Member, Alegatsiaq Fjord Formation.

Remarks. Among collections preserved mostly as coquina blocks, one well-preserved, conjoined shell in the North Greenland collection (GGU 82485) has several morphological features typical of *Pleurodium*. The dorsal valve of this specimen (Fig. 15A–C) is

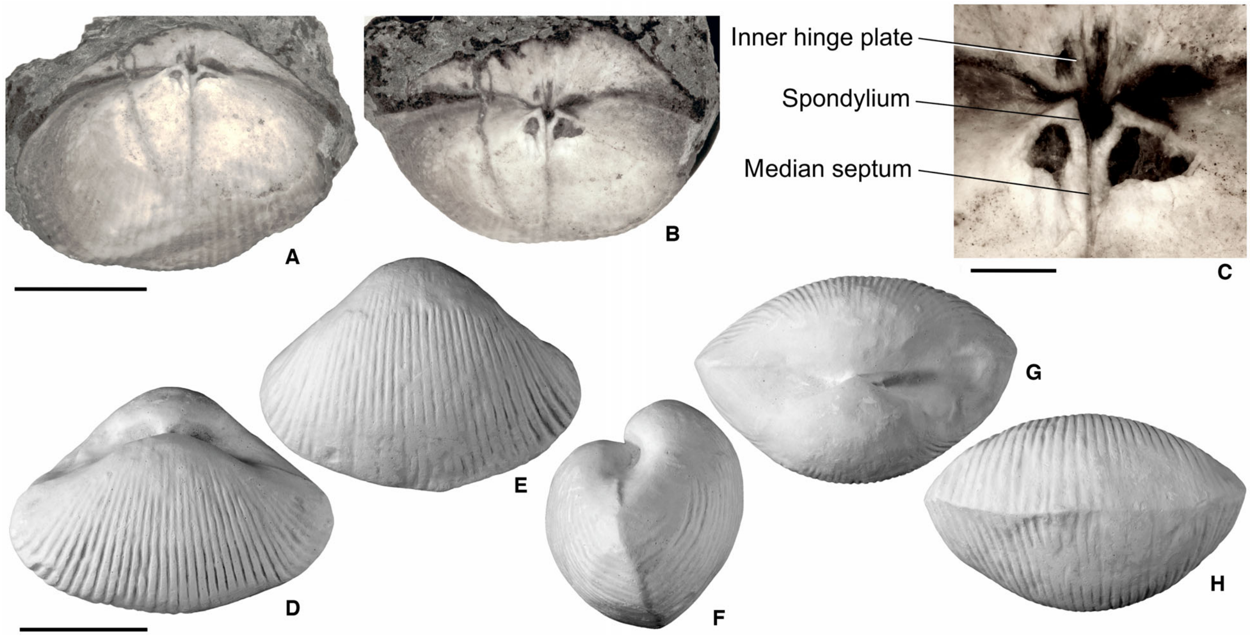

FIG. 15. *Pleurodium* sp. and comparison with type species. A–C, *Pleurodium* sp., MGUH 34237, oblique ventral, posterior, and further enlarged epical view of conjoined shell partly embedded in rock matrix, submerged in alcohol for imaging, showing median septum, spondylium and inner hinge plates in partly broken and abraded umbones of translucent shell, from GGU 82485, Kap Ammen, northern Hall Land, Store Canyon Member (Rhuddanian), Alegatsiaq Fjord Formation. D–H, *Pleurodium tenuiplicatum* (Grabau, 1925), plaster cast of paralectotype, NIGP 7440, dorsal, ventral, lateral, posterior and anterior views; note high and tumid ventral umbo; upper Lojoping Formation (upper Aeronian), Yichang, Hubei, South China. Scale bars represent: 20 mm (A, B, D–H); 5 mm (C).

mostly embedded in a dark-grey micrite matrix. The shell has a crushed (possibly broken) anterior, and the posterior–medial portion of the ventral valve is abraded, but the following characteristics can be observed.

Shell large, transversely subelliptical, strongly biconvex (length = 38.6 mm, width = 52.5 mm, thickness = 34.8 mm), with slightly deeper dorsal valve. Ventral umbo low (broken but estimated to be less than 4 mm above hinge line, only slightly higher than dorsal umbo), strongly convex; beak broken, exposing median septum and spondylium in apical area (Fig. 15C). Dorsal beak in-curved, arching ventrally beyond hinge line. Fold or sulcus absent, but weak medial furrow present in umbonal portion of ventral valve. Interareas or palintropes absent. Shell costate; costae in umbonal area weak to absent, becoming well defined in anterior two-thirds of shell; size and density of costae moderate, *c.* 3 per 5 mm, regularly spaced, straight as those in *Tcherskidium*; bifurcation of costae symmetrical, occasionally observed only in some costae, beginning at about mid-length in lateral parts, but at anterior one-quarter of ventral valve (dorsal valve embedded in matrix and its ribbing cannot be examined).

Median septum short, thick, with observable sagittal length of *c.* 9 mm. Inner hinge plates short, diverging slightly anteriorly to be 2 mm apart at their distal ends, with observable length of 5.7 mm. Other internal structures cannot be observed.

The Greenland specimen is similar to the type species, *Pleurodium tenuiplicatum* (Fig. 15D–H) in its notably wide and strongly biconvex shell, with straight, uniformly sized, relatively fine costae. A well-preserved paralectotype (Rong *et al.* 2017, pp. 332–333, pl. S6, figs 17–20; mislabelled as ×1.6, but should be ×1.0 (JY Rong pers. comm. 2022)) from the type locality reaches a length of 34.3 mm, width 50.5 mm, and thickness 32.1 mm. The conjoined shell from North Greenland resembles the paralectotype of *P. tenuiplicatus* also in its short, anteriorly divergent inner hinge plates along the valve floor (compare Fig. 15C with Rong *et al.* 2017, pl. S6, fig. 15).

Pleurodium sp. from North Greenland differs from the type species in its notably lower ventral umbo and occasional bifurcation of costae. *Pleurodium tenuiplicatum* has a high and obtuse ventral umbo, extending *c.* 10 mm above the hinge line, and its costae rarely bifurcate. The Greenland form, therefore, is most likely to be a new species, but its taxonomic assignment at the species level requires additional material for examination of its detailed internal structures.

The specimen appears to be from either the Store Canyon Member of the Alegatsiaq Fjord Formation or from the Petermann Halvø Formation. If the former is the case, this would extend the Alegatsiaq Fjord Formation into the upper Aeronian. However, Dawes (unpub. field notes, 1966) reported that the specimens were collected from calcareous shales and later wrote that samples GGU 82178–94 are from Unit 13B (Dawes & Peel 1984). When compared with the lithological descriptions of the Washington Land Group in Hurst (1980) and Sønderholm *et al.* (1987), Unit 13B probably encompasses both the uppermost member of the Alegatsiaq Fjord Formation and the lower part of the Petermann Halvø Formation. Therefore, it is most likely that *Pleurodium* occurs in the Petermann Halvø Formation and that this is of late Aeronian age.

Genus BOREALOIDES nov.

LSID. https://zoobank.org/nomenclaturalacts/6584DFA5-98A2-42E6-ABF5-10EE184CFCEA

Derivation of name. After *Borealis*, a virgianid genus, to which the new genus is similar in external morphology.

Type species. *Borealoides balderi* gen. et sp. nov. (see below).

Diagnosis. As for type (and only) species.

Remarks. The new genus shows certain similarity to *Virgianella* Nikiforova & Sapelnikov, 1971, especially in its prominently elongate, strongly ventribiconvex shell with a high and strongly arched ventral umbo, and internally in having a cruralium. In internal structures, however, it differs from *Virgianella* in having a relatively long median septum supporting the spondylium, variously developed ventral interarea, and faint ribbing in larger shells. In *Virgianella*, the ventral median septum is either absent or very short, and the inner hinge plates may unite to form an incipient cruralium posteriorly, but they are basomedially inclined yet discrete anteriorly (Nikiforova & Sapelnikov 1971, p. 50, fig. 1; Sapelnikov 1985, p. 29, fig. 10). The type species of *Virgianella* may have rarely developed faint ribbing in the anteromedial part of the ventral valve (Nikiforova & Sapelnikov 1971, pl. 5, figs 1a, 2b), although the genus was defined by the authors as being smooth. Three other genera of the Virgianidae are known to have a cruralium or incipient cruralium: *Peudoconchidium* Nikiforora & Sapelnikov, 1971, *Paraconchidium* Rong *et al*., 1974, and *Virgianoides* Jin *et al*., 2019; all of these have distinctly ribbed shells. *Paraconchidium* has a clearly defined ventral interarea (Jin *et al*. 2006, p. 74, fig. 2), as in the new genus.

In early Silurian pentameroids there was a remarkable evolutionary trend, repeated in separate lineages, from discrete hinge plates to cruralium in the dorsal valve, observed in the Rhuddanian *Virgiana*–*Virgianoides*, the Aeronian *Borealis*–*Borealoides*, and the Telychian *Pentamerus*–*Pentameroides* transitions (see also Johnson 1979; Jin & Copper 2000; Jin *et al*. 2019).

Borealoides balderi sp. nov.
Figures 16–20

LSID. https://zoobank.org/nomenclaturalacts/EAFB8D0F-40D3-4136-9FD6-7985827C112D

Derivation of name. After the Norse mythological god, *Balder*, the son of the chief god Odin. The name also coincides with Balder Glacier in the vicinity of Odins Fjord, where the new species occurs.

Holotype. MGUH 34240, ventral valve (Fig. 16E–I).

Paratypes. MGUH 34238, 34239, 34241–34252 (Figs 16A–D, 17–20).

Material. GGU 184102 (2 conjoined shells; 36 vv, 1 dv); GGU 184113 (4 conjoined shells; 64 vv, 7 dv); GGU 225777 (4 vv); GGU 254784 (8 vv, 2 dv); GGU 254792 (49 vv, 3 dv); GGU 270663 (6 vv, 1 dv); GGU 271634 (1 conjoined shell, 14 vv); GGU 270664 (1 conjoined shell, 3 vv); GGU 270688 (1 conjoined shell, 20 vv).

Type locality and stratum. The holotype and figured paratypes were collected from locality GGU 254792 (82.663055°N, 35.878887°W) by John Hurst in 1978 from the Odins Fjord Formation (Rhuddanian) at Odins Fjord, west-central Peary Land.

Diagnosis. Shell large, elongate, strongly ventribiconvex to nearly plano-convex with very deep ventral valve, smooth to faintly ribbed. Ventral interarea present but not always sharply delimited. Spondylium similar to that of *Borealis*, supported by high median septum extending for one-quarter to one-third of valve length. relatively long inner hinge plates basomedially united to form posteriorly sessile cruralium, anteriorly tapering onto low median ridge.

Description. Shell medium to very large, elongate-oval, or extremely elongate-elliptical in large forms (Figs 16–19), with largest ventral valve reaching a length of 58 mm, width 31 mm, and depth 38 mm; strongly ventribiconvex to nearly plano-convex, with ventral valves about fourfold as deep as the dorsal valves, and maximum width slightly anterior of mid-length of shell. Anterior commissure broadly sulcate as observed in rarely available conjoined shell (Fig. 18D). Shell usually smooth, but faint ribbing present in some specimens, especially in medial part of ventral valves (Figs 16A, C, E, J–L, 18I, K).

Ventral valve showing strong lateral compression, resulting in width/depth ratio of *c.* 0.83 in extremely deep valves (e.g. Fig. 16G, K). Ventral umbo high, helmet shaped, with apex being only slightly narrower than valve width, strong arched; beak prominently pointed and in-curved to point anteriorly (Fig. 16B, G, K). Delthyrium open. Ventral interarea high but narrow, well-delimited in well-preserved specimens (Fig. 16F, I). Sulcus-like medial furrow present in umbonal area, replaced anteriorly by broad, fold-like medial lobe in some specimens (Figs 16A, C, J, L, 17A, C, 18I, K).

Dorsal valve weakly convex in umbonal area, becoming nearly flat around mid-length, or even gently concave anteriorly, geniculating almost perpendicularly along each lateral margin to form vertical sides of 8–10 mm deep in valves of moderate to large size (Fig. 17D–F). Sulcus-like medial furrow present in some specimens (Fig. 17D).

Ventral interior. Shell wall strongly thickened during growth as indicated by rhythmic growth layers (Fig. 19D, E, H–J), Spondylium long, reaching *c.* 38% of valve length and 30% of valve depth (Figs 16D, F, 19B, H, I), with a narrow rounded basal portion and dorsolaterally deflected walls in the middle portion, thus becoming broadly V shaped in cross-section at its widest part. Median septum also strongly thickened by

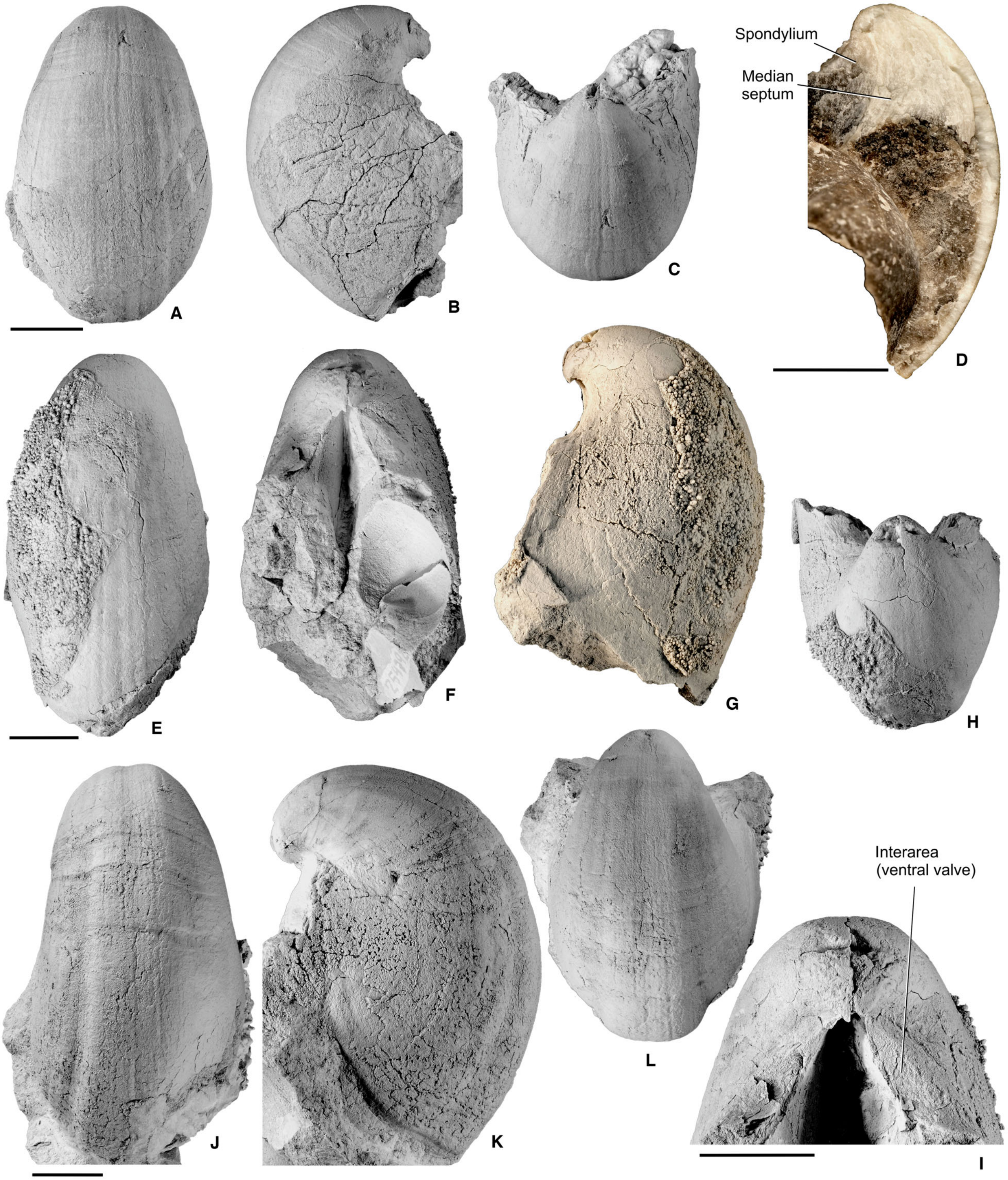

FIG. 16. *Borealoides balderi* gen. et sp. nov., four specimens from Odins Fjord Formation (Rhuddanian), GGU 254792, Odins Fjord, west-central Peary Land. A–C, MGUH 34238, paratype, ventral, lateral and posterior views of large, prominently elongate and rostrate ventral valve, with faint costae in medial part of valve. D, MGUH 34239, paratype, small, medially split ventral valve, showing relatively deep spondylium supported along its entire length and prominent median septum. E–I, MGUH 34240, holotype, ventral, interior, lateral and posterior views, and further enlarged umbonal area; note faint costae in medial part of valve (E), and relatively long, narrow-bottomed spondylium (F), and presence of interarea (F, I). J–L, MGUH 34241, paratype, ventral, lateral and posterior views of very large, trilobate valve, with fine and faint costae. Scale bars represent: 10 mm (A–C, E–I); 5 mm (D).

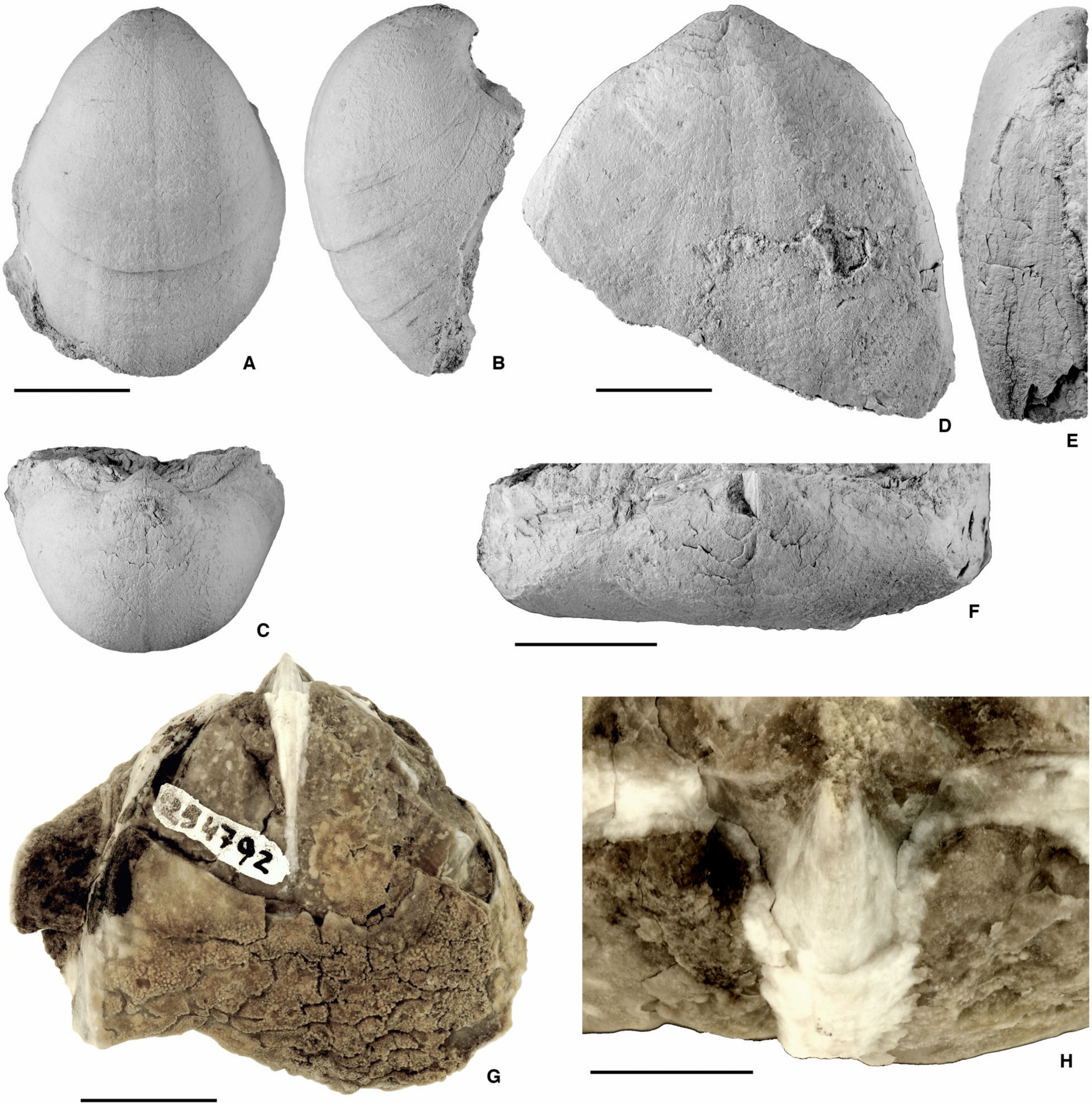

FIG. 17. *Borealoides balderi* gen. et sp. nov., three specimens from Odins Fjord Formation (Rhuddanian), GGU 254792, Odins Fjord, west-central Peary Land. A–C, MGUH 34242, paratype, ventral, lateral and posterior views of relatively small form. D–F, MGUH 34243, paratype, dorsal, lateral and posterior views of dorsal valve; note nearly flat profile, perpendicularly lateral margins, and partly exposed, sessile cruralium (F). G–H, MGUH 34244, paratype, dorsal and posterior views of partly exfoliated dorsal valve immersed in alcohol, showing posteriorly sessile cruralium supported anteriorly by median septum. Scale bars represent: 10 mm (A–G); 5 mm (H).

secondary shell substance during growth, supporting almost entire length (except for dorsally tilted distal end) of spondylium, anteriorly merged into extremely thickened valve floor (Figs 16D, 19D, E, H–J). Apical cavity on both sides of spondylium filled by secondary growth of shell material (Fig. 19D, E, J).

Dorsal interior. Inner hinge plates long, robust posteriorly, thinning anteriorly in comparison to consistently thick and strong outer hinge plates, extending for *c.* 14 mm from apex in a relatively large valve of 35 mm wide and 34 mm long, basomedially convergent along the posterior half of their length to form sessile, round-bottomed cruralium sitting directly on valve floor, supported distally by incipient median septum that tapers further anteriorly into a low median ridge (Fig. 17F–H). Outer hinge plates thick, strong, about same height as, but longer than, inner hinge plates (Fig. 20). Crural

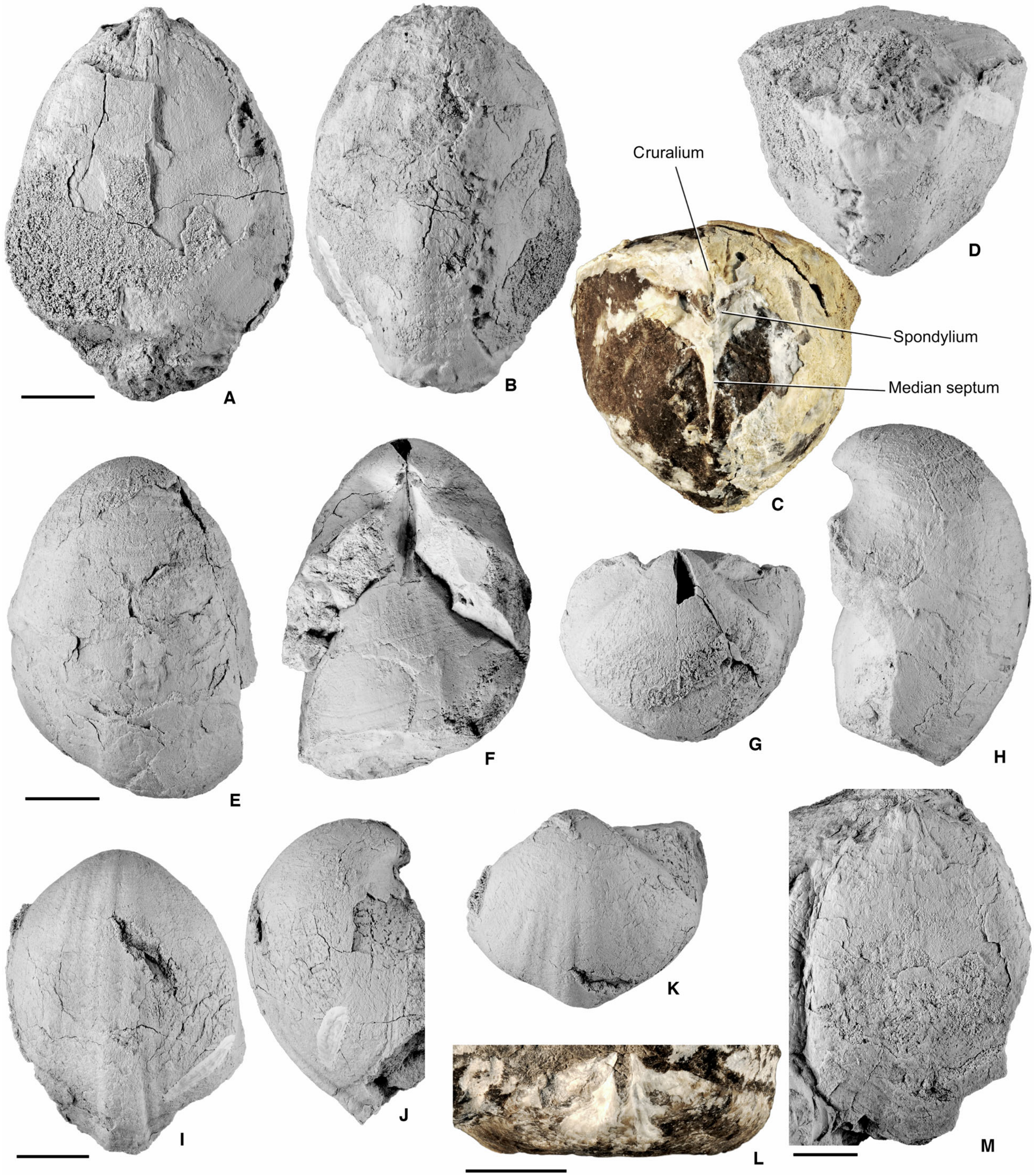

FIG. 18. *Borealoides balderi* gen. et sp. nov. A–D, MGUH 34245, paratype, dorsal, ventral, posterior (under alcohol), and anterior views of rare, conjoined shell; note presence of cruralium and long median septum; Odins Fjord Formation, hilltop between Bure Iskappe and Hans Tavsen Iskappe, Peary Land; GGU 271634. E–M, three specimens from Odins Fjord Formation, east side of Børglum Elv, southern Peary Land, GGU 184113: E–H, MGUH 34246, paratype, ventral, interior, posterior and lateral views of ventral valve, with another incomplete ventral valve attached (F); I–K, MGUH 34247, paratype, ventral, lateral and posterior views of medium-sized, slightly elongate, trilobate ventral valve with faint costae; L–M, MGUH 34248, paratype, posterior (under alcohol) and dorsal views of large, fairly flat dorsal valve. Scale bars represent 10 mm.

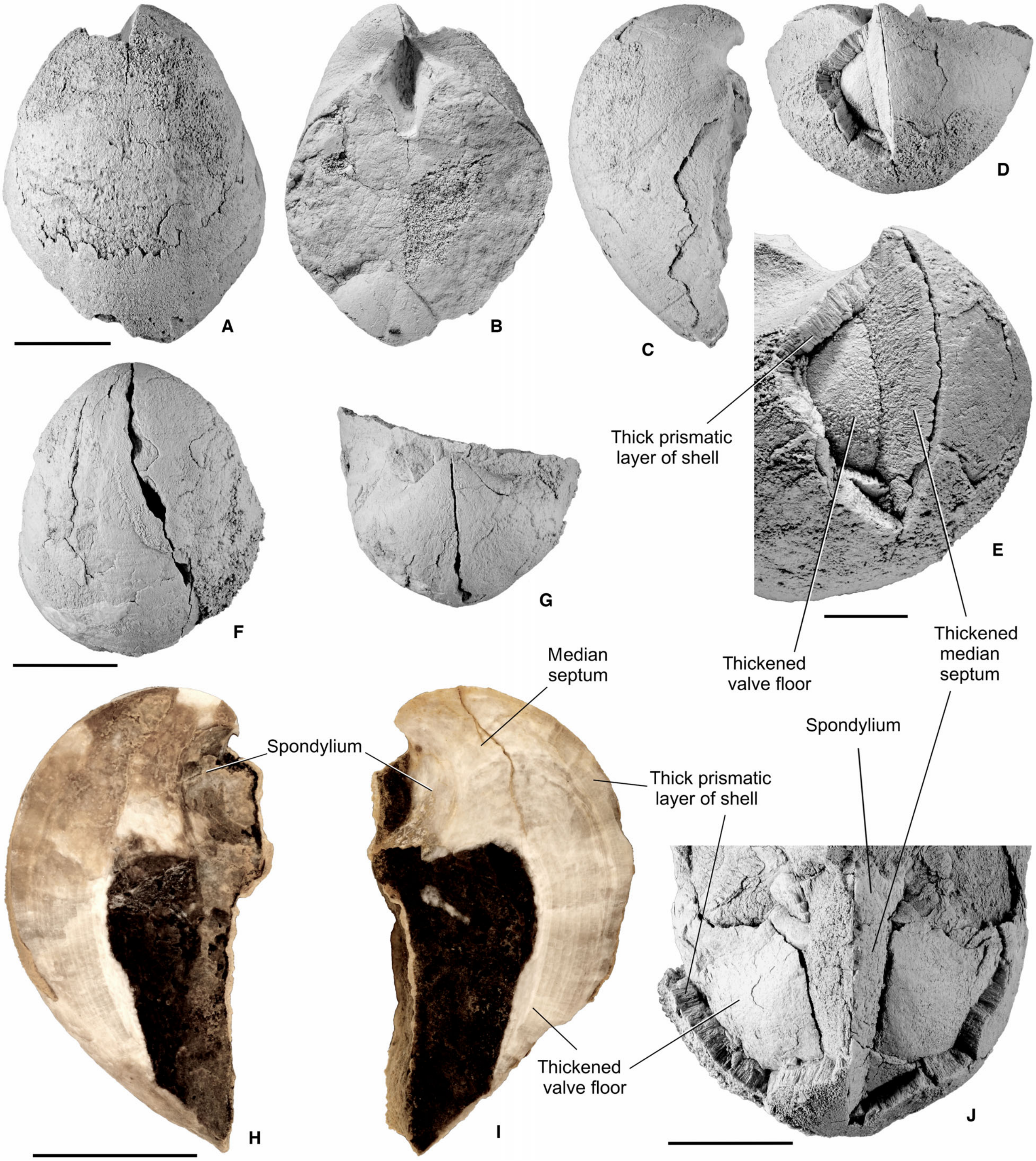

FIG. 19. *Borealoides balderi* gen. et sp. nov., three specimens from Odins Fjord Formation (Rhuddanian), GGU 184102, ‘Pentamerid bank’, central Peary Land. A–E, MGUH 34249, paratype, ventral, interior, lateral and posterior views, with further enlarged umbonal area (E) to show extreme thickening of median septum and valve floor. F–I, MGUH 34250, paratype, ventral and posterior views (F, G) of medially split ventral valve (H, I) showing extravagant thickening of umbonal cavity and valve floor. J, MGUH 34251, paratype, posterior view of exfoliated ventral valve; note thickened median septum and umbonal cavity. Scale bars represent: 10 mm (A–D, F–J); 5 mm (E).

base rounded in cross-section, forming fairly smooth junctions with outer and inner hinge plates, without notable flanges (Fig. 20, 4.1 mm from apex).

Remarks. As discussed above under the new genus, *Borealoides balderi* is unique in its combination of external and internal characters, such as its faintly ribbed, extremely

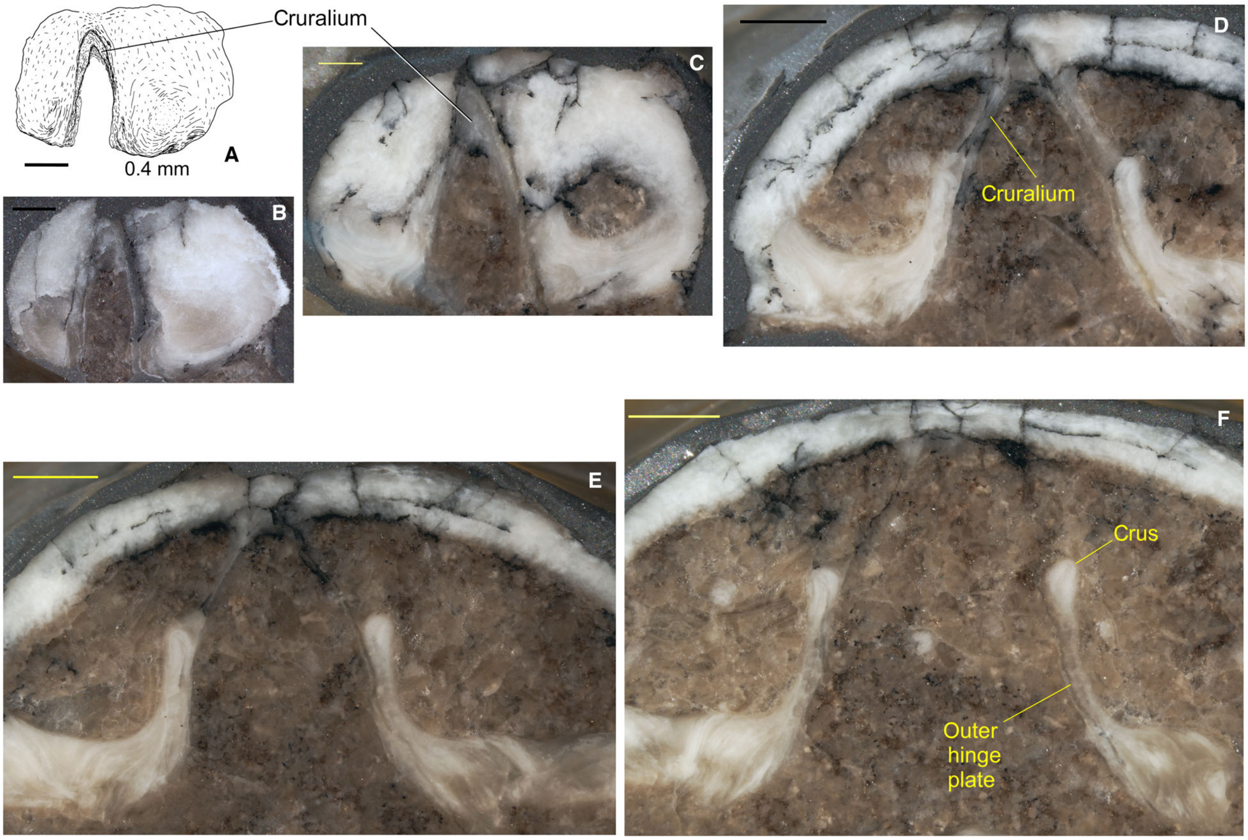

FIG. 20. *Borealoides balderi* gen. et sp. nov. Six selected (out of a total of 25) serial sections of dorsal valve, MGUH 34252, paratype, from four specimens from Odins Fjord Formation (Rhuddanian), GGU 254792, Odins Fjord, east-central Peary Land. Note development of cruralium. Distance from valve apex: A, 0.4 mm; B, 0.7 mm; C, 1.8 mm; D, 4.1 mm; E, 5.0 mm; F, 6.2 mm. Scale bars represent: 1 mm (A–C); 2 mm (D–F).

ventribiconvex shell, ventral interarea, long ventral median septum, and long dorsal cruralium supported anteriorly by a low median septum. In external morphology, the new species can be confused with the type species of *Virgianella* from the middle-upper Llandovery of Vaigach Island, Boreal Urals (e.g. Sapelnikov 1985, pl. 7, figs 5a, b) in its extreme elongation and lateral compression of the shell in large forms, and variously developed ventral interarea, although the internal structure of these two species are easily distinguishable by the much longer ventral median septum in *B. balderi*.

Genus HOLORHYNCHUS Kiær, 1902

Type species. Holorhynchus giganteus Kiær, 1902. Langåra Formation (uppermost Katian), Oslo Region, Norway (for more details see St. Joseph 1938; Cocks 1982; Brenchley *et al.* 1997).

Occurrence. Upper Katian to lower Llandovery; North Greenland, Baltoscandia, Urals, Kazakhstan, Tien Shan, North China (Ningxia and Inner Mongolia), Yukon, Alaska, and northeast Siberia (Kolyma).

Holorhynchus giganteus Kiær, 1902
Figure 21

[Selected synonymy]

1902 *Holorhynchus giganteus* Kiær, p. 63, figs 1–7.
1938 *Holorhynchus giganteus*; St. Joseph, p. 292, pl. 4, figs 1–5; text-fig. 9.
1971 *Holorhynchus giganteus*; Boucot *et al.*, p. 277, pl. 5, figs 1–9; pl. 6, figs 1–5.
1982 *Holorhynchus giganteus*; Cocks, p. 774, pl. 83, figs 12–17.
1983 *Holorhynchus* ex gr. *giganteus*; Oradovskaya, p. 53, pl. 9, fig. 1a, b.
2004 *Holorhynchus giganteus*; Rong *et al.*, p. 293, figs 5.1–5.18, 5.22–5.25, 6, 7 (and comprehensive synonymy therein up to 2004).
2009 *Holorhynchus giganteus*; Rasmussen, p. 48, *non* pl. 1, figs 10–11.
2015 *Holorhynchus giganteus*; Shiino *et al.*, p. 28, figs 3A–L, 4A–E.
2022 *Holorhynchus giganteus*; Jin *et al.*, p. 1475, fig. 9.1–9.9.

Lectotype. PMO 12431, selected and illustrated by St. Joseph (1938, pl. 4, figs 1–3), uppermost Katian, Oslo–Asker district, Norway.

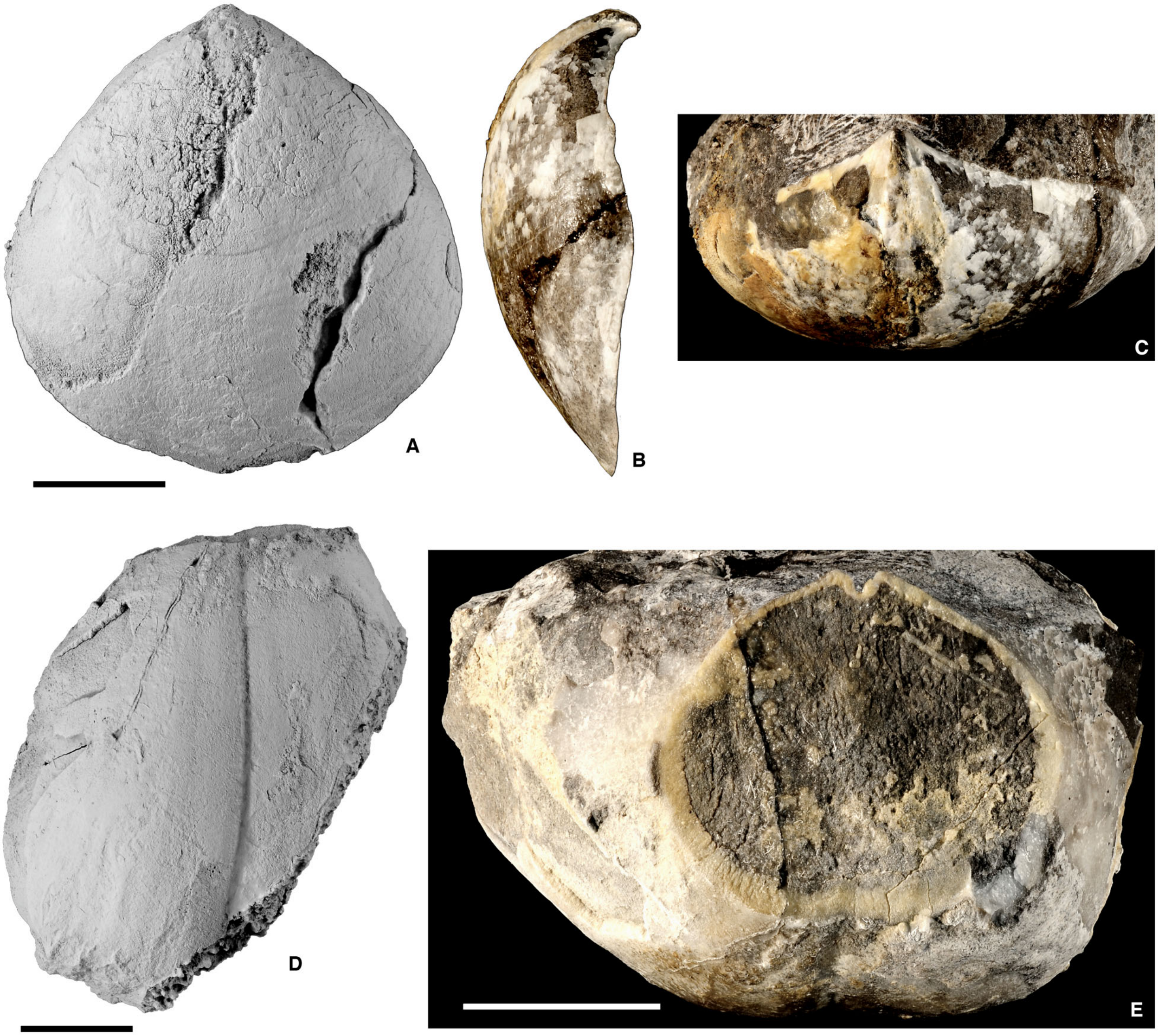

FIG. 21. *Holorhynchus giganteus* (Kiær, 1902). A–C, MGUH 34253, dorsal, lateral and posterior views (B, C under alcohol) of dorsal valve; note relatively long inner hinge plates visible through partly exfoliated, translucent shell material. D–E, MGUH 34254, ventral and posterior views of ventral valve, with natural broken umbo; note apical part of spondylium and lack of median septum. Scale bars represent 10 mm.

Material. GGU 82453 (1 vv); GGU 270643 (1 dv).

Remarks. An incomplete single ventral valve with a preserved length of 45 mm measured perpendicular to its medial line. The valve is smooth, with a moderately strong convexity, with very faint ribbing in its anterior left part. A sulcus-like, narrow medial furrow is present throughout the preserved valve length and, unlike a true sulcus, it does not increase in width anteriorly (Fig. 21D). A similar medial furrow and faint ribbing are present also in the topotype material of *H. giganteus* from Norway (Boucot *et al.* 1971) and in specimens of *H. giganteus* from the Siljan district of Sweden (Shiino *et al.* 2015). A minute posterior end of the spondylium is exposed in the naturally truncated cross-section of the umbonal portion, without any trace of a median septum (Fig. 21E). This shell was originally identified as *Holorhynchus* by Art Boucot (Dawes & Peel 1984, p. 27).

The dorsal valve is sub-oval in outline, weakly convex, reaching less than one-half of the depth of the ventral valve (Fig. 21A–C). The partly exfoliated umbo–beak area exposes a pair of discrete inner hinge plates, which are subparallel along the valve floor, extending for *c.* 10 mm from the valve apex, diverging only slightly from each other anteriorly.

Shell measurements (mm):

	Length	Width	Depth
GGU 82453 (vv)	45.1*	36.4*	25.9
GGU 270643 (dv)	35.5	35.1	9.4

* Preserved dimension of incomplete valve.

The incomplete ventral valve and the ovoid-shaped dorsal valve from North Greenland indicate a somewhat elongate shell, which differs from the mostly common, transversely extended form of *H. giganteus* from the type area (e.g. St. Joseph 1938; Cocks 1982). Variation in shell outline, however, has been noted in the Baltoscandian material. For example, a slightly elongate shell of *H. giganteus* was shown by Shiino *et al.* (2015, p. 28, fig. 3A) from the Boda Limestone of the Siljan district of Sweden (see also Rasmussen *et al.* 2010). The upper Rhuddanian virgianid *Nondia canadensis* Boucot & Chiang, 1974 may also have a smooth, elongate shell, as in the North Greenland specimens, but *N. canadensis* has a trilobate ventral valve and a short ventral median septum. Although *Nondia* has been commonly stated to be devoid of a ventral median septum, the 'median ridge' along the valve floor and the hanging 'ridge' from the spondylium base (see cross-sections in Boucot & Chiang 1974, pl. 2, fig. 6; text-fig. 3) would be the result of a planar cut through a short, posteriorly arched median septum. Such a short median septum is entirely absent in the Greenland specimen, even in the apical area (compare Fig. 21E with Boucot & Chiang 1974, pl. 2, fig. 6), thus precluding a *Nondia* affinity for the Greenland material.

Genus BREVILAMNULELLA Amsden, 1974

Type species. Clorinda? *thebesensis* Savage, 1913, Leemon Formation, Hirnantian, IL, USA.

Brevilamnulella sp.
Figure 22A–E

Material. DH02 (*c.* 20 shells embedded in small blocks of coquina); DH09 (*c.* 30 shells embedded in small blocks of coquina).

Remarks. Numerous shells from the lower Turesø Formation at the Børglum Elv section are assigned to *Brevilamnulella* based on their relatively small (usually <10 mm in length or width), moderately biconvex shell, with weak, rounded costae that become better defined anteriorly (Fig. 22E), broadly V-shaped spondylium that extends slightly anterior of the hinge line, and a short median septum confined to the apical area (Fig. 22A–C). In the dorsal valve, short hinge plates have been observed in medially split shells (Fig. 22D). The shells occur as a coquina, embedded in well-cemented, thick-bedded dolopackstone. It is extremely difficult, if not impossible, to extract shells from the rock without breaking them, thus hindering complete assessment of the morphological features and variations. For this reason this species is reported here under open nomenclature.

Genus VIRIDITA Jin & Copper, 2000

Type species. Camerella lenticularis Billings, 1866, uppermost Fox Point Member (basal Rhuddanian), Becscie Formation, Reef Point, Anticosti Island.

Viridita sp.
Figure 22F–I

Material. DH03 (*c.* 30 shells embedded in small blocks of coquina).

Remarks. This species occurs in great abundance as a *c.* 1.5-m-thick, packstone-grade coquinitic unit in the middle Turesø Formation, exposed as a carbonate ledge *c.* 700 m long in the Børglum Elv section, with bedding surfaces covered by shells of *Viridita* sp. (Fig. 22F, G). The coquina is virtually monospecific, and consists predominantly of ventral valves, as typical of virgianid shell beds of late Katian and Rhuddanian age. The shells are moderately to strongly biconvex, with nearly equal length and width, and an average diameter *c.* 10 mm, rarely exceeding 15 mm. The Greenland specimens are comparable in size to *Viridita lenticularis* from Anticosti Island but are more strongly convex, whereas they are similar to *Viridita glomerosa* Jin & Copper, 2010 from the lower Becscie Formation (basal Rhuddanian) in shell convexity, but are notably smaller in size. *Viridita glomerosa* has a size range of 13–28 mm in length or width. The Greenland species has shell structures similar to those of *V. glomerosa*, such as the posteriorly thickened shell wall, a short median septum confined to the apical area, small and shallow V-shaped spondylium (short arrows in Fig. 22F, G, I), and short hinge plates that extend barely anterior of the hinge line (long arrow in Fig. 22G). A more precise assignment at the species level awaits better-preserved (especially loose) specimens to determine detailed morphometrics.

Superfamily STRICKLANDIOIDEA Schuchert & Cooper, 1931
Family KULUMBELLIDAE Boucot *et al.*, 2002

Remarks. The subfamily Kulumbellinae of Boucot *et al.* (2002) was raised to family level by Rong *et al.* (2005) because of their distinct morphological characteristics in the superfamily Stricklandioidea. The family Kulumbellidae includes three genera: *Kulumbella* Nikiforova, 1960; *Rugolepyros* Lenz, 1989, and *Sinokulumbella* Rong *et al.*, 2005.

Genus KULUMBELLA Nikiforova, 1960

Type species. Kulumbella kulumbensis Nikiforova, 1960. Aeronian (middle Llandovery), Siberian Platform.

Remarks. Nikiforova & Andreeva (1961, p. 134) described the type species as having a plano-convex shell, although the holotype, an incomplete conjoined shell, shows a 'resupinate' profile,

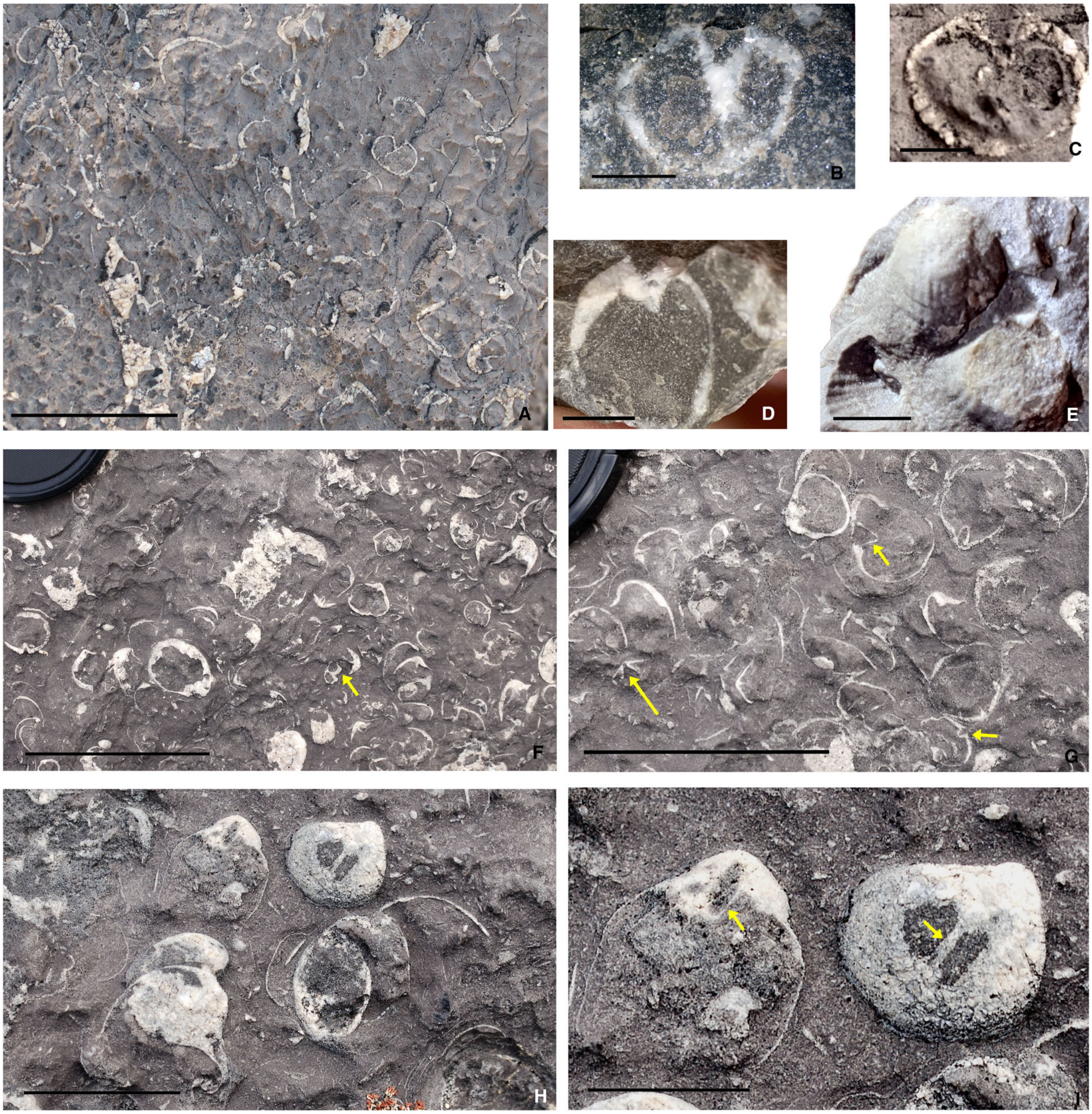

FIG. 22. A–E, *Brevilamnulella* sp. Børglum Elv section, lower Turesø Formation: A, field photograph of outcrop DH09 before it was sampled; B–D, MGUH 34255–34257, three specimens sampled from outcrop DH09; E, MGUH 34258, small block collected from outcrop DH02, showing moderately convex shells with rounded costae. F–I, *Viridita* sp. Børglum Elv section, middle Turesø Formation, field photographs of *Viridita* shell packstone beds exposed along a *c*. 700-m-long ledge (outcrop DH03); note very short hinge plates of dorsal valve (long arrow in G), short median septum, and distally free-hanging, broad V-shaped spondylium (short arrows in F, G, I). For stratigraphic positions of the samples see Harper *et al.* (2007, text-fig. 2). Scale bars represent: 40 mm (A, G); 5 mm (B–E); 50 mm (F); 20 mm (H); 10 mm (I).

similar to *Strophomena*. Of the 14 specimens illustrated by Nikiforova & Andreeva (1961, pl. 21, figs 5–7; pl. 22, figs 1–11), only two specimens have a concavo-convex or resupinate profile (e.g. Fig. 23A–C, holotype of *K. kulumbensis*). On examination of the type lot housed at VSEGEI, St Petersburg in 2019, JJ saw that the Siberian *Kulumbella* shells are similar to those from Anticosti Island in having a 'paper-thin' shell wall, which makes them easily bent or otherwise deformed during burial. These shells were interpreted to be originally biconvex based on the following observations: (1) some of the figured ventral valves of *K. kulumbensis* (e.g. Nikiforova & Andreeva 1961, pl. 22, fig. 1 = Fig. 23E herein) are normally convex and do not have

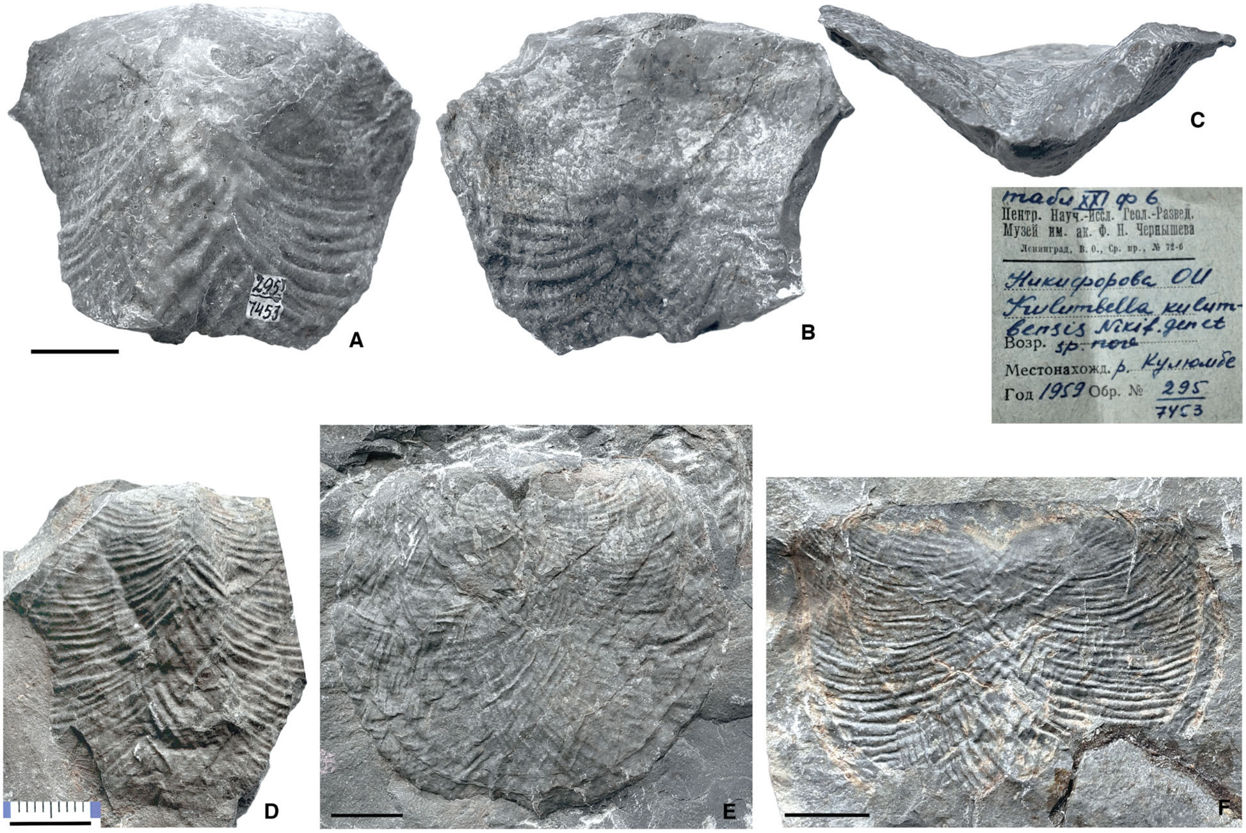

FIG. 23. *Kulumbella kulumbensis* Nikiforova, 1960, four re-photographed, original type specimens in the repository of the Geological Institute (VSEGEI), St. Petersburg, Russia, Aeronian (middle Llandovery), Siberian Platform. A–C, VSEGEI 295/7453, holotype (Nikiforova & Andreeva, 1961, pl. 21, fig. 6), dorsal, ventral and anterior views of convexo-concave shell (possibly due to taphonomic distortion); note predominantly chevron-patterned ribbing. D–F, three paratypes (without specific catalogue numbers at VSEGEI) indicating weakly biconvex shell profile (Nikiforova & Andreeva 1961, pl. 22, figs1, 5, 7). Scale bars represent 10 mm.

the anteromedially concave curvature seen in the holotype; (2) even the dorsal valve can have a ventrally bent lateral margin (Fig. 23F = Nikiforova & Andreeva 1961, pl. 22, fig. 7); and (3) *Kulumbella xacta* Jin & Copper, 1998 from Anticosti Island usually has a biconvex shell, but compaction of the thin valves resulted in most of them being preserved as flattened or variously bent valves, becoming slightly concave or convex, or even locally deformed around a small clast in the matrix (e.g. Jin & Copper 1998, fig. 4.1). These observations, therefore, suggest that the occasionally seen concave ventral valve is a taphonomic artefact: the ventral sulcus, which may have been prominent in some specimens, was enhanced during burial and compaction.

Jin & Copper (1998, 2000) confined *Kulumbella* to species with sharply and consistently developed, criss-cross, divaricate ribbing, whereas other species, which have been reported as *Kulumbella* but have faint or irregular development of divaricate ribbing, have been assigned to either *Chiastodoca* Jin & Copper, 1998, or *Sinokulumbella* Rong *et al.*, 2005 (for details see these publications). True *Kulumbella*, therefore, includes only the type species from Siberia, *K. xacta* from Anticosti Island, and the new species described below.

Kulumbella heimdali sp. nov.
Figure 24

LSID. https://zoobank.org/nomenclaturalacts/D42222BD-E82C-4EC4-B6DF-B2581BC0083A

1982 *Kulumbella* sp.; Hurst & Sheehan, p. 48 (no illustration).
1998 *Kulumbella* sp.; Jin & Copper, p. 445, figs 3.1–3.4 (= holotype designated below).

Derivation of name. Named after the Viking (Norse) god Heimdal, who possesses keen senses and keeps watch for invaders. The name coincides with Heimdal Icecap, which is next to the east side of Odins Fjord, where the new species occurs.

Holotype. MGUH 34259 (Fig. 24A–C), an incomplete, conjoined shell.

Paratypes. Five specimens, MGUH 34260–34265 (Fig. 24D–M).

Material. GGU 254795 (2 vv, 1 dv, 5 conjoined shells).

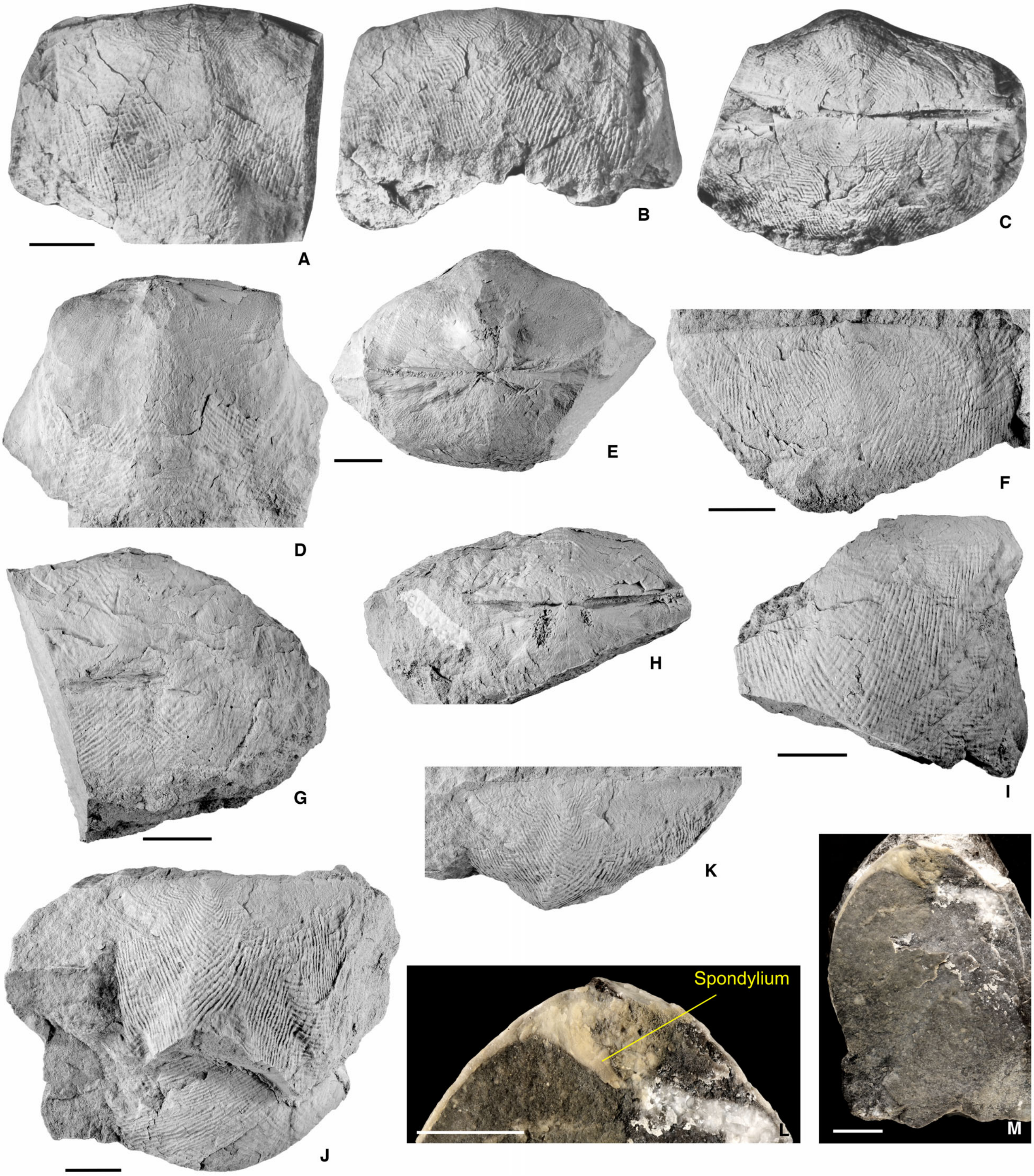

FIG. 24. *Kulumbella heimdali* sp. nov. Seven specimens from GGU 254795, Odins Fjord Formation (middle Aeronian), Odins Fjord, west-central Peary Land. A–C, MGUH 34259, holotype, dorsal, ventral and posterior views of anteriorly damaged, conjoined shell. D–E, MGUH 34260, paratype, dorsal and posterior views of strongly convex, conjoined shell with damaged anterior of posterolateral parts; note trilobed dorsal valve. F, MGUH 34261, paratype, incomplete dorsal valve, with gentle fold. G–H, MGUH 34262, paratype, dorsal and posterior views of incomplete, conjoined shell. I, MGUH 34263, paratype, incomplete ventral valve. J–K, MGUH 34264, paratype, dorsal and posterior views of anteriorly damaged, strongly trilobed dorsal valve. L–M, MGUH 34265, paratype, strongly convex, conjoined, (naturally) medially split shell, exposing relatively small, nearly sessile spondylium, confined mostly to the umbonal area, photographed under alcohol. Scale bars represent 10 mm.

Type locality and stratum. The holotype and paratypes are from GGU 254795, Odins Fjord Formation (middle Aeronian), Odins Fjord, east-central Peary Land.

Diagnosis. Large, equibiconvex shell with relatively strong convexity and semicircular to semi-ellipsoidal outline. Dorsal valve strongly trilobate in large shells, with fold-like medial lobe. Ventral sulcus weak. Criss-crossed divaricate ribs fine, sharply defined.

Description. Shell large, reaching a maximum length of 54 mm, width 68 mm, and thickness 46 mm (Fig. 24D, E), semicircular to semi-elliptical in outline, nearly equibiconvex with moderately strong convexity (Fig. 24C, E, L, M). Hinge line long, straight, terminating laterally in rounded-square or weak ear-like cardinal angles, slightly shorter than maximum shell width. Ventral umbo inconspicuous, hardly raised above overall contour of valve, extending only 2–3 mm posterior of hinge line, with a small beak in contact with a similarly small beak of dorsal valve. Weak, gentle sulcus present anteriorly *c.* 10–15 mm from apex. Ventral interarea as wide as hinge line, but only 2–3 mm in height, nearly orthocline to slightly tilted towards apsacline (Fig. 24C, H). Dorsal umbo and beak area similarly inconspicuous as those of the ventral valve, but may be slightly more noticeable due to development of fold (Fig. 24A, C–E, L). Dorsal interarea of similar height as ventral interarea, but more typically orthocline. Dorsal fold beginning at valve apex, widening anteriorly to reach about one-third valve width to make the valve appear trilobate (Fig. 24A, D, J). Exact anterior commissure not observed due to ubiquitously damaged shell anterior, but assumed to be gently uniplicate based on presence of development of dorsal fold. Divaricate, criss-cross ribs fine, sharply defined, slightly irregular in size and spacing, with various degrees of local distortion, averaging 15 per 10 mm throughout shell, somewhat finer in posteromedial areas of both valves.

Spondylium small, shallow, mostly sessile, confined to apical area of valve, extending anteriorly for *c.* 10 mm (Fig. 24L, M). Hinge plates also minute, extending anteriorly for *c.* 5 mm even in relatively large shells.

Remarks. The Greenland new species differs from the type species from Siberia and *Kulumbella xacta* from Anticosti Island in its markedly larger size and stronger convexity, which produces steeply sloping or perpendicular sides in some specimens (Fig. 24C). In *K. kulumbensis*, the ribbing in some shells can be much coarser (5 per 10 mm) and more chevron-like than criss-crossing (e.g. Fig. 24A, B, D), although in other specimens the ribbing is more similar to that in the Greenland and Anticosti species (Fig. 24E). *Kulumbella xacta* has divaricate ribs almost identical to those of the Greenland species in size and pattern, but differs from the Greenland form in having a weakly biconvex shell that lacks a fold or sulcus.

CONCLUSION

In this study, a total of 10 species representing 10 genera of Late Ordovician and early Silurian pentameride brachiopods (families Virgianidae and Kulumbellidae) were systematically described for the first time from the remote region of North Greenland. Among these brachiopods, the latest Katian virgianiads were part of the true warm-water *Tcherskidium* fauna (with such key taxa as *Tcherskidium* and *Proconchidium*) that thrived in, but were confined to, the palaeoequatorial and northern hemisphere palaeotropical regions during the pre-Hirnantian Late Ordovician. This warm-water fauna was represented during the early Silurian (Rhuddanian–Aeronian) by different genera of virgianid and kulumbellid pentamerides, notably *Virgiana* and *Kulumbella*. A striking palaeobiogeographic difference is that many of these taxa became much more cosmopolitan during the early Silurian and spread across the palaeotropics of the southern hemisphere, such as the occurrence of *Virgiana* in the Anticosti, Michigan, Williston and Hudson Bay basins of Canada. Most virgianids (e.g. *Tcherskidium*, *Proconchidium*, and *Borealoides*) from Northern Greenland show extravagant calcification, marked by generally large shells with an extremely thickened shell wall and enlarged internal skeletal structures, as typical for warm-water shelly faunas.

Acknowledgements. This is a much revamped study based partly on an earlier unfinished manuscript by PMS and J.M. Hurst in the 1980s. J.M. Hurst also collected a significant part of the North Greenland brachiopod material used in this study. We particularly thank Peter Dawes (GEUS), who collected some of the earliest material presented here, for performing, together with Simun D. Olsen, Stig A.S. Pedersen and Jon R. Ineson (GEUS) together with John Peel (Uppsala), the challenging tasks of retrieving locality data by looking through old archives, field notes and maps compiled before the age of the GPS in order to assign approximate coordinates to the oldest GGU localities collected. The Natural History Museum of Denmark provided access to the fossil material from North Greenland. The 2006 field work in North Greenland by three of the authors (JJ, DATH and CMØR) was funded by the Danish Natural Science Research Council (DATH), Natural Sciences and Engineering Research Council of Canada (JJ) and the University of Western Ontario (JJ). CMØR also acknowledges the Crown Prince Frederik Fund for funding his participation in the 2009 expedition to Kronprins Christian Land. DATH acknowledges support from the Leverhulme Trust (UK). Critical and constructive comments from journal reviewers L.E. Popov and J. Colmenar, and from the Editor L. Cherns, greatly improved this paper.

Author contributions. **Conceptualization** J Jin (JJ), CMØ Rasmussen (CMØR), DAT Harper (DATH); **Data Curation** JJ, PM Sheehan (PMS), CMØR, DATH; **Formal Analysis** CMØR, JJ, DATH; **Funding Acquisition** DATH, JJ, CMØR; **Investigation** CMØR, JJ, DATH; **Project Administration** DATH, JJ, CMØR; **Validation** CMØR, JJ, DATH; **Visualization** JJ, CMØR; **Writing – Original Draft Preparation** JJ, PMS, CMØR, DATH; **Writing – Review & Editing** JJ, DATH, CMØR, PMS.

DATA ARCHIVING STATEMENT

This published work and the nomenclatural acts it contains, have been registered in ZooBank: https://zoobank.org/References/72E2B511-02D4-43C3-BCDE-E24808C917CF

The faunal data used for cluster analysis in this study are available in the Dryad Digital Repository: https://doi.org/10.5061/dryad.0vt4b8h4g

Editor. Lesley Cherns

REFERENCES

ÁLVARO, J. J., GHOBADI POUR, M., SÁNCHEZ-GARCÍA, T., ZADEH, M. R. K. E., HAIRAPETIAN, V. and POPOV, L. E. 2022. Stratigraphic and volcanic signatures of Miaolingian–Late Ordovician rift pulses in the Alborz Mountains, northern Iran. *Journal of Asian Earth Sciences*, **233**, 105240.

AMSDEN, T. W. 1974. Late Ordovician and early Silurian articulate brachiopods from Oklahoma, southwestern Illinois, and eastern Missouri. *Oklahoma Geological Survey Bulletin*, **119**, 1–154.

ARMSTRONG, H. A. and LANE, P. D. 1981. The un-named Silurian(?) dolomite formation. Børglum Elv, central Peary Land. *Rapport Grønlands Geologiske Undersøgelse*, **106**, 29–34.

BERGSTRÖM, S. M., HUFF, W. D., SALTZMAN, M. R., KOLATA, D. R. and LESLIE, S. A. 2003. The greatest volcanic ash falls in the Phanerozoic: trans-Atlantic relations of the Ordovician Millbrig and Kinnekulle K-bentonites. *The Sedimentary Record*, **2**, 4–8.

BERGSTRÖM, S. M., CHEN, X. U., GUTIÉRREZ-MARCO, J. C. and DRONOV, A. 2009. The new chronostratigraphic classification of the Ordovician System and its relations to major regional series and stages and to δ^{13}C chemostratigraphy. *Lethaia*, **42**, 97–107.

BILLINGS, E. 1857. Report for year 1856. *Geological Survey of Canada, Report of Progress for the Years*, **1853-1854-1855-1856**, 247–345.

BILLINGS, E. 1866. Catalogues of the Silurian fossils of the island of Anticosti, with descriptions of some new genera and species. *Geological Survey of Canada, Separate Report*, **427**, 1–93.

BJERRESKOV, M. 1989. Ordovician graptolite biostratigraphy in North Greenland. *Rapport Grønlands Geologiske Undersøgelse*, **144**, 17–33.

BJERRESKOV, M. and POULSEN, V. 1973. Ordovician and Silurian faunas from northern Peary Land, North Greenland. *Rapport Grønlands Geologiske Undersøgelse*, **55**, 10–14.

BOUCOT, A. J. and AMSDEN, T. W. 1963. Virgianidae, a new family of pentameracean brachiopods. *Journal of Paleontology*, **37**, 296.

BOUCOT, A. J. and CHIANG, K. K. 1974. Two new Lower Silurian virginianinid brachiopods from the Nonda Formation, northern British Columbia. *Journal of Paleontology*, **48**, 63–73.

BOUCOT, A. J. and HURST, J. M. 1979. Silurian biogeography: revision of the North Atlantic realm in the Llandovery. *Rapport Grønlands Geologiske Undersøgelse*, **91**, 57–60.

BOUCOT, A. J., JOHNSON, J. G. and RUBEL, M. 1971. Descriptions of brachiopod genera of subfamily Virgianinae Boucot and Amsden 1963. *Easti NSV Teaduste Akadeemia Toimetised, Keemia Geoloogia*, **20**, 271–281.

BOUCOT, A. J., RONG, J. Y. and BLODGETT, R. B. 2002. Pentameridina. 960–1026. *In* KAESLER, R. L. (ed.) *Treatise on invertebrate paleontology. Part H. Brachiopoda (revised). Vol. 4*. Geological Society of America & University of Kansas.

BRENCHLEY, P. J., MARSHALL, J. D., HINTS, L. and NOLVAK, J. 1997. New isotopic data solving an old biostratigraphic problem: the age of the upper Ordovician brachiopod *Holorhynchus giganteus*. *Journal of the Geological Society of London*, **154**, 335–342.

CANDELA, Y. 2014. Evolution of Laurentian brachiopod faunas during the Ordovician Phanerozoic sea level maximum. *Earth-Science Reviews*, **141**, 27–44.

COCKS, L. R. M. 1982. The commoner brachiopods of the latest Ordovician of the Oslo-Asker district, Norway. *Palaeontology*, **25**, 755–781.

COCKS, L. R. M. and TORSVIK, T. H. 2021. Ordovician palaeogeography and climate change. *Gondwana Research*, **100**, 53–72.

COLMENAR, J. and RASMUSSEN, C. M. Ø. 2018. A Gondwanan perspective on the Ordovician Radiation constrains its temporal duration and suggests first wave of speciation, fuelled by Cambrian clades. *Lethaia*, **51**, 286–295.

COPPER, J. and JIN, J. 2017. Early athyride brachiopod evolution through the Ordovician–Silurian mass extinction and recovery, Anticosti Island, eastern Canada. *Journal of Paleontology*, **91**, 1123–1147.

DAWES, P. R. and PEEL, J. S. 1984. Biostratigraphic reconnaissance in the Lower Palaeozoic of western North Greenland. *Rapport Grønlands Geologiske Undersøgelse*, **121**, 19–31.

DENG, Y., FAN, J., ZHANG, S., FANG, X., CHEN, Z., SHI, Y., WANG, H., WANG, X., YANG, J., HOU, X., WANG, Y., ZHANG, Y., CHEN, Q., YANG, A., FAN, R., DONG, S., XU, H. and SHEN, S. 2021. Timing and patterns of the Great Ordovician Biodiversification Event and Late Ordovician mass extinction: perspectives from South China. *Earth-Science Reviews*, **220**, 103743.

DERAKHSHI, M., ERNST, R. E. and KAMO, S. L. 2022. Ordovician-Silurian volcanism in northern Iran: implications for a new Large Igneous Province (LIP) and a robust candidate for the Late Ordovician mass extinction. *Gondwana Research*, **107**, 256–280.

ETHERIDGE, R. 1878. Palæontology of the coasts of the Arctic Lands visited by the late British expedition under Captain Sir George Nares, R.N., K.C.B., F.R.S. *Quarterly Journal of the Geological Society of London*, **34**, 568–639.

FAN, J.-X., SHEN, S.-Z., ERWIN, D. H., SADLER, P. M., MacLEOD, N., CHENG, Q.-M., HOU, X.-D., YANG, J., WANG, X.-D., WANG, Y., ZHANG, H., CHEN, X., LI, G.-X., ZHANG, Y.-C., SHI, Y.-K., YUAN, D.-X., CHEN, Q., ZHANG, L.-N., LI, C. and ZHAO, Y.-Y.

2020. A high-resolution summary of Cambrian to Early Triassic marine invertebrate biodiversity. *Science*, **367**, 272–277.

FINNEGAN, S., BERGMANN, K., EILER, J. M., JONES, D. S., FIKE, D. A., EISENMAN, I., HUGHES, N. C., TRIPATI, A. K. and FISCHER, W. W. 2011. The magnitude and duration of Late Ordovician–Early Silurian glaciation. *Science*, **331**, 903–906.

FORTEY, R. A. and COCKS, L. R. M. 2005. Late Ordovician global warming: the Boda Event. *Geology*, **33**, 405–408.

GRABAU, A. W. 1925. Summary of the faunas from the Sintan Shale. *Bulletin of the Geological Survey of China*, **7**, 77–85.

HANKEN, N.-M., UCHMAN, A., NIELSEN, J. K., OLAUSSEN, S., EGGEBØ, T. and STEINSLAND, R. 2016. Late Ordovician trace fossils from offshore to shallow water mixed siliciclastic and carbonate facies in the Ringerike Area, Oslo Region, Norway. *Ichnos*, **23**, 189–221.

HARPER, D. A. T. and RONG, J.-Y. 2001. Palaeozoic brachiopod extinctions and recoveries. *Geological Journal*, **36**, 317–328.

HARPER, D. A. T., JIN, J., RASMUSSEN, C. M. Ø., RASMUSSEN, J. A. and STOUGE, S. 2007. Overview of the pentameride brachiopod succession (Upper Ordovician–Lower Silurian) in Børglum Elv and GB Schley Fjord, Peary Land, North Greenland. *Acta Palaeontologica Sinica*, **46** (Suppl), 176–180.

HARPER, D. A. T., RASMUSSEN, C. M. Ø., LILJEROTH, M., BLODGETT, R. B., CANDELA, Y., JIN, J., PERCIVAL, I. G., RONG, J.-Y., VILLAS, E. and ZHAN, R.-B. 2013. Biodiversity, biogeography and phylogeography of Ordovician rhynchonelliform brachiopods. *Geological Society London Memoirs*, **38**, 127–144.

HARPER, D. A. T., HAMMARLUND, E. U. and RASMUSSEN, C. M. Ø. 2014a. End Ordovician extinctions: a coincidence of causes. *Gondwana Research*, **25**, 1294–1307.

HARPER, D. A. T., JIN, J. and RASMUSSEN, C. M. Ø. 2014b. Late Ordovician carbonate mounds from North Greenland: a peri-Laurentian dimension to the Boda Event? *GFF*, **136**, 95–99.

HIGGINS, A. K., INESON, J. R., PEEL, J. S., SURLYK, F. and SØNDERHOLM, M. 1991. Lower Palaeozoic Franklinian Basin of North Greenland. *Bulletin Grønlands Geologiske Undersøgelse*, **160**, 71–139.

HUANG, B., CHEN, D., HARPER, D. A. T. and RONG, J. 2023. Did the Late Ordovician mass extinction event trigger the earliest evolution of ‘strophodontoid’ brachiopods? *Palaeontology*, **66**, e12642.

HURST, J. M. 1980. Silurian stratigraphy and facies distribution in Washington Land and western Hall land, North Greenland. *Bulletin Grønlands Geologiske Undersøgelse*, **138**, 1–95.

HURST, J. M. 1981. Platform edge and slope relationships: Silurian of Washington Land, North Greenland and comparison to Arctic Canada. *Bulletin of Canadian Petroleum Geology*, **29**, 408–419.

HURST, J. M. 1984. Upper Ordovician and Silurian carbonate shelf stratigraphy, facies and evolution, eastern North Greenland. *Bulletin Grønlands Geologiske Undersøgelse*, **148**, 1–73.

HURST, J. M. and SHEEHAN, P. M. 1982. Pentamerid brachiopod relationships between Siberia and east north Greenland in the Late Ordovician and Early Silurian. 482. *In* MAMET, B. L. and COPELAND, M. J. (eds) *Third North American Paleontological Convention, Proceedings, Vol. 2.*

HURST, J. M. and SURLYK, F. 1982. Stratigraphy of the Silurian turbidite sequence of North Greenland. *Bulletin Grønlands Geologiske Undersøgelse*, **145**, 1–121.

JIN, J. and BLODGETT, B. R. 2020. Late Ordovician brachiopods from east-central Alaska, northwestern margin of Laurentia. *Journal of Paleontology*, **94**, 637–652.

JIN, J. and COPPER, P. 1998. *Kulumbella* and *Microcardinalia* (*Chiastodoca*) new subgenus, Early Silurian divaricate stricklandiid brachiopods from Anticosti Island, eastern Canada. *Journal of Paleontology*, **72**, 441–453.

JIN, J. and COPPER, P. 2000. Late Ordovician and Early Silurian pentamerid brachiopods from Anticosti Island, Québec. *Palaeontographica Canadiana*, **18**, 1–140.

JIN, J. and COPPER, P. 2010. Origin and evolution of the Early Silurian (Rhuddanian) virgianid pentameride brachiopods: the extinction recovery fauna from Anticosti Island, eastern Canada. *Bollettino della Società Paleontologica Italiana*, **49**, 1–11.

JIN, J. and ZHAN, R. 2008. *Late Ordovician orthide and billingsellide brachiopods from Anticosti Island, eastern Canada: Diversity change through mass extinctions*. NRC Research Press, Ottawa, 159 pp.

JIN, J., CALDWELL, W. G. E. and NORFORD, B. S. 1993. Early Silurian brachiopods and biostratigraphy of the Hudson Bay Lowlands, Manitoba, Ontario, and Quebec. *Geological Survey of Canada Bulletin*, **457**, 1–220.

JIN, J., ZHAN, R. B. and RONG, J. Y. 2006. Taxonomic reassessment of two virgianid brachiopod genera from the Upper Ordovician and Lower Silurian of South China. *Journal of Paleontology*, **80**, 72–82.

JIN, J., HARPER, D. A. T. and RASMUSSEN, C. M. Ø. 2009. *Sulcipentamerus* (Pentamerida, Brachiopoda) from the Lower Silurian Washington Land Group, North Greenland. *Palaeontology*, **52**, 385–399.

JIN, J., HARPER, D. A. T., RASMUSSEN, J. A. and SHEEHAN, P. M. 2012. Late Ordovician massive-bedded *Thalassinoides* ichnofacies along the palaeoequator of Laurentia. *Palaeogeography, Palaeoclimatology, Palaeoecology*, **367–368**, 73–88.

JIN, J., HARPER, D. A. T., COCKS, L. R. M., McCAUSLAND, P. J. A., RASMUSSEN, C. M. Ø. and SHEEHAN, P. M. 2013. Precisely locating the Ordovician equator in Laurentia. *Geology*, **41**, 107–110.

JIN, J., SOHRABI, A. and SPROAT, C. 2014. Late Ordovician brachiopod endemism and faunal gradient along palaeotropical latitudes in Laurentia during a major sea level rise. *GFF*, **136**, 125–129.

JIN, J., ZHAN, R. B. and WU, R. C. 2018. Equatorial cold-water tongue in the Late Ordovician. *Geology*, **46**, 759–762.

JIN, J., MIKULIC, D. and KLUESSENDORF, J. 2019. Virgianid brachiopods of the Michigan Basin, and its implications for post-extinction diversification of the Silurian pentameride fauna in Laurentia. *Revista Italiana di Paleontologia e Stratigrafia*, **125**, 637–649.

JIN, J., BLODGETT, R. B., HARPER, D. A. T. and RASMUSSEN, C. M. Ø. 2022. Warm-water *Tcherskidium* Fauna

(Brachiopoda) in the Late Ordovician northern hemisphere of Laurentia and peri-Laurentia. *Journal of Paleontology*, **96**, 1461–1478.

JIN, J., RASMUSSEN, C. M. Ø., SHEEHAN, P. M. and HARPER, D. A. T. 2023. Data from: Late Ordovician and Early Silurian virgianid and stricklandioid brachiopods from North Greenland: implications for a warm-water faunal province. Dryad Digital Repository. https://doi.org/10.5061/dryad.0vt4b8h4g

JOHNSON, M. E. 1979. Evolutionary brachiopod lineages from the Llandovery Series of eastern Iowa. *Palaeontology*, **22**, 549–567.

KIÆR, J. 1897. Faunistische Uebersicht der Etage 5 des norwegischen Silursystems. *Videnskabsselskabets Skrifter Christiana I Matemastisk-Naturvitenskabelig Klasse*, **3**, 1–76.

KIÆR, J. 1902. Etage 5 i Asker ved Kristiana. *Norges Geologiske Undersøgelse, Aarbog for 1902*, **1**, 1–111.

KOCH, L. 1920. Stratigraphy of Northwest Greenland. *Meddelelser fra Dansk Geologisk Forening*, **5**, 1–78.

KOCH, L. 1925. The geology of North Greenland. *American Journal of Science*, **9**, 271–285.

KOCH, L. 1928. Stratigraphy of Greenland. *Meddelelser om Grønland*, **73**, 205–320.

KOVALEVSKIY, O. P., KOLOBOVA, I. M., KOREN, T. N., MODZALEVSKAYA, T. L., POPOV, L. E., SOBOLEVSKAYA, R. F. and STUKALINA, G. A. 1991. *Biozonalnoe raschlenenie ashgilla i nizhnego llandoveri v SSSR*. Vsegei, Leningrad, 44 pp.

LENZ, A. C. 1989. Silurian (Wenlockian) brachiopods from the southern Mackenzie Mountains, Northwest Territories. *Canadian Journal of Earth Sciences*, **26**, 1220–1233.

LING, M. X., ZHAN, R.-B., WANG, G.-X., WANG, Y., AMELIN, Y., TANG, P., LIU, J. B., JIN, J., HUANG, B., WU, R. C., XUE, S., FU, B., BENNETT, V. C., WEI, X., LUAN, X.-C., FINNEGAN, S., HARPER, D. A. T. and RONG, J.-Y. 2019. An extremely brief end Ordovician mass extinction linked to abrupt onset of glaciation. *Solid Earth Sciences*, **4**, 190–198.

LIU, D.-Y., XU, H.-K. and LIANG, W.-P. 1983. Brachiopoda. 254–286. *In* NANJING INSTITUTE OF GEOLOGY AND MINERAL RESOURCES (ed.) *Palaeontological atlas of East China (1): Early Palaeozoic volume*. Geological Publishing House, Beijing. [in Chinese]

M'COY, F. 1844. *A synopsis of the characters of the Carboniferous Limestone fossils of Ireland*. University Press, Dublin, 207 pp.

MODZALEVSKAYA, T. L. 2018. Upper Ordovician–Silurian brachiopods. 61–198, 202–203, 228–231. *In* NEKHOROSHEVA, L. V. and SOBOLEVSKAYA, R. F. (eds) *The Ordovician, Silurian, and Devonian stratigraphy and fauna of Kotelny Island (New Siberian Islands)*. FSBI VNIIOkeangeologia, St Petersburg.

NIKIFOROVA, O. I. 1960. Order Pentamerida. 197–205. *In* SARYCHEVA, T. G. (ed.) *Osnovy Paleontologii*. Izdadelstvo Akademii Nauk SSSR, Moscow.

NIKIFOROVA, O. I. 1989. Pozdneordovikskie pentameridy (brakhiopody) Tsentralnogo Taymyra. *Ezhegodnik Vsesoyuznogo Paleontologicheskogo Obshchestva*, **32**, 77–87.

NIKIFOROVA, O. I. and ANDREEVA, O. N. 1961. Stratigrafiya ordovika i silura Sibirskoi platformy i ee paleontologicheskoe obosnovanie (Brakhiopody). *Trudy Vsegei, nov. ser.*, **56**, 1–412.

NIKIFOROVA, O. I. and SAPELNIKOV, V. P. 1971. Novye rannesiluriyskie Virgianidae (Brachiopoda). *Paleontologicheskiy Zhurnal*, **2**, 47–56.

NIKOLAEV, A. A. 1968. *Conchidium*? *unicum* sp. nov. 30–53. *In* Balashov, Z. G. and Russian S.F.S.R. Ministerstvo geologii (collective authors) *Polevoy atlas ordovikskoi fauny Severa-Vostoka SSSR*. Magadanskoe Knuzhnoe Izdatelstvo, Magadan.

NIKOLAEV, A. A. 1974. Nadsemeistvo Pentameracea. 65–72, 129–131. *In* SEVERO-VOSTOCHNOE KOMPLEKCNYY NAUCHNO-ISSLEDOBATELSKIY INSTITUT, AKADEMIYA NAUK SSSR (ed.) *Opornye razrezy Paleozoya Severo-Vostoka SSSR*. Svknii, Magadan.

NIKOLAEV, A. A. and SAPELNIKOV, V. P. 1969. Dva novykh roda pozdneordovikskikh Virgianidae. *Trudy Sverdlovskogo Ordena Trudovogo Krasnogo Znameni Gornogo Instituta*, **63**, 11–17.

ORADOVSKAYA, M. M. 1983. Opisanie fauny. Zamkovye brakhiopody. 35–73. *In* SOKOLOV, B. S. (ed.) *Granitsa Ordovika i Silura na Severo-vostoke SSSR*. Nauka, Leningrad.

PEEL, J. S. and HURST, J. M. 1980. Late Ordovician and early Silurian stratigraphy of Washington Land, western North Greenland. *Rapport Grønlands Geologiske Undersøgelse*, **100**, 18–24.

POHL, A., NARDIN, E., VANDENBROUCKE, T. R. A. and DONNADIEU, Y. 2016. High dependence of Ordovician ocean surface circulation on atmospheric CO_2 level. *Palaeogeography, Palaeoclimatology, Palaeoecology*, **458**, 39–51.

POHL, A., NARDIN, E., VANDENBROUCKE, T. R. A. and DONNADIEU, Y. 2023. The Ordovician ocean circulation: a modern synthesis based on data and models. *Geological Society of London Special Publications*, **532**, SP532–2022–1.

POULSEN, C. 1934. The Silurian faunas of North Greenland. I. The fauna of the Cape Schuchert Formation. *Meddelelser om Grønland*, **72**, 1–46.

POULSEN, C. 1943. The Silurian faunas of North Greenland. II. The fauna of the Offley Island Formation. Part 2, Brachiopoda. *Meddelelser om Grønland*, **72** (3), 1–60.

RASMUSSEN, C. M. Ø. 2009. A palaeoecological and biogeographical investigation of the Ordovician–Silurian boundary based on brachiopods. Unpub. PhD thesis, University of Copenhagen, Denmark, 311 pp.

RASMUSSEN, C. M. Ø. 2013. Late Ordovician brachiopods from eastern north Greenland: equatorial offshore migration of the Red River fauna. *Palaeontology*, **56**, 359–379.

RASMUSSEN, C. M. Ø. 2014. Phylogeography of Ordovician–Silurian rhynchonelliformean brachiopods: tracking higher order distributional patterns, radiations and extinctions in 4D. *GFF*, **136**, 223–228.

RASMUSSEN, C. M. Ø., EBBESTAD, J. O. and HARPER, D. A. T. 2010. Unravelling a Late Ordovician pentameride (Brachiopoda) hotspot from the Boda Limestone, Siljan district, central Sweden. *GFF*, **132**, 133–152.

RASMUSSEN, C. M. Ø., KRÖGER, B., NIELSEN, M. L. and COLMENAR, J. 2019. Cascading trend of Early Paleozoic marine radiations paused by Late Ordovician extinctions. *Proceedings of the National Academy of Sciences*, **116**, 7207–7213.

RASMUSSEN, C. M. Ø., VANDENBROUCKE, T. R. A., NOGUES-BRAVO, D. and FINNEGAN, S. 2023. Was the Late Ordovician mass extinction truly exceptional? *Trends in Ecology & Evolution*, **38**, 812–821.

RONG, J.-Y. and BOUCOT, A. J. 1998. A global review of the Virgianidae (Ashgill-Llandovery, Brachiopods, Pentameroidea). *Journal of Paleontology*, **72**, 457–465.

RONG, J.-Y., XU, H.-K. and YANG, X.-C. 1974. Silurian brachiopods. 195–208. *In* NIGP (ed.) *Atlas of stratigraphy and paleontology of southwest China*. Science Press, Beijing. [in Chinese]

RONG, J.-Y., JONES, B. and NENTWICH, F. W. 1989. *Proconchidium* from Late Ordovician strata of Brodeur Peninsula, Baffin Island, Arctic Canada. *Journal of Paleontology*, **63**, 25–33.

RONG, J.-Y., ZHAN, R.-B. and JIN, J. 2004. The Late Ordovician and Early Silurian pentameride brachiopod *Holorhynchus* from North China. *Journal of Paleontology*, **78**, 287–299.

RONG, J.-Y., JIN, J. and ZHAN, R.-B. 2005. Two new genera of Early Silurian stricklandioid brachiopods from South China and their bearing on stricklandioid classification and paleobiogeography. *Journal of Paleontology*, **79**, 1143–1156.

RONG, J.-Y., HUANG, B., ZHAN, R.-B. and FU, L.-P. 2017. Silurian brachiopod genera on type species of China. 245–341. *In* RONG, J.-Y., JIN, Y. G., SHEN, S. Z. and ZHAN, R. B. (eds) *Phanerozoic brachiopod genera of China*. Science Press, Beijing.

RONG, J., HARPER, D. A. T., HUANG, B., LI, R., ZHANG, X. and CHEN, D. 2020. The latest Ordovician Hirnantian brachiopod faunas: new global insights. *Earth-Science Reviews*, **208**, 103280.

RUKAVISHNIKOVA, T. B. and SAPELNIKOV, V. P. 1973. Novye pozdneashgilskie Pentameracea Kazakhstana. *Instituta Geologii i Geokhimii, Uralskiy Nauchnyy Tsentr, AN SSSR, Trudy*, **99**, 89–114.

SALTZMAN, M. R. and YOUNG, S. A. 2005. A long-lived glaciation in the Late Ordovician? Isotopic and sequence-stratigraphic evidence from western Laurentia. *Geology*, **33**, 109–112.

SAPELNIKOV, V. P. 1985. *Sistema i stratigraficheskoe znachenie brakhiopod podotryada pentameridin*. Nauka, Moskva, 206 pp.

SAPELNIKOV, V. P. and RUKAVISHNIKOVA, T. B. 1975. *Verkhneordovikskie, siluriyskie i nizhnedevonskie pentameridy Kazakhstana*. Akademiya Nauk SSSR, Uralskiy Nauchnyy Tsentr, Nauka, Moskva, 227 pp.

SAVAGE, T. E. 1913. Alexandrian series in Missouri and Illinois. *Geological Society of America Bulletin*, **24**, 351–376.

SAVAGE, T. E. 1916. Alexandrian rocks of northeastern Illinois and eastern Wisconsin. *Geological Society of America Bulletin*, **27**, 305–324.

SCHUCHERT, C. and COOPER, G. A. 1931. Synopsis of the brachiopod genera of the suborders Orthoidea and Pentameroidea, with notes on the Telotremata. *American Journal of Science*, **22**, 241–251.

SEPKOSKI, J. J. Jr 1995. The Ordovician Radiations: diversification and extinction shown by global genus level taxonomic data. 393–396. *In* COOPER, J. D., DROSER, M. and FINNEY, S. C. (eds) *Ordovician odyssey: Short Papers for the 7th International Symposium on the Ordovician System*. Society for Sedimentary Geology SEPM.

SEPKOSKI, J. J. Jr and SHEEHAN, P. M. 1983. Diversification, faunal change, and community replacement during the Ordovician radiations. 673–717. *In* TEVESZ, M. J. S. and McCALL, P. L. (eds) *Biotic interactions in recent and fossil benthic communities*. Springer.

SHEEHAN, P. M. 1980. The Late Ordovician and Silurian of the eastern Great Basin. Part 3: brachiopods of the Tony Grove Lake Member of the Laketown Dolomite. *Milwaukee Public Museum, Contributions in Biology & Geology*, **30**, 23 pp.

SHEEHAN, P. M. and COOROUGH, P. J. 1990. Brachiopod zoogeography across the Ordovician–Silurian extinction event. *Geological Society Memoir*, **12**, 181–187.

SHIINO, Y., SUZUKI, Y., HARPER, D. A. T., MORI, H. and BERGSTRÖM, J. 2015. Late Ordovician Holorhynchus succession in the Siljan district, Sweden: facies, faunas and a latest Katian event. *GFF*, **137**, 25–35.

SMITH, M. P., SØNDERHOLM, M. and TULL, S. J. 1989. The Morris Bugt Group (Middle Ordovician–Silurian) of North Greenland and its correlatives. *Rapport Grønlands geologiske Undersøgelse*, **143**, 5–20.

SMITH, M. P., RASMUSSEN, J. A., ROBERTSON, S., HIGGINS, A. K. and LESLIE, A. G. 2004. Lower Palaeozoic stratigraphy of the East Greenland Caledonides. *Geological Survey of Denmark and Greenland Bulletin*, **6**, 5–28.

SØNDERHOLM, M., HARLAND, T. L., DUE, P. H., JØRGENSEN, L. N. and PEEL, J. S. 1987. Lithostratigraphy and depositional history of Upper Ordovician–Silurian shelf carbonates in central and western North Greenland. *Rapport Grønlands Geologiske Undersøgelse*, **133**, 27–41.

SPROAT, C. and JIN, J. 2017. Paleobiogeography of the Late Ordovician brachiopod fauna during a major marine transgression and initial colonization of the epicontinental seas in Laurentia. *Palaeogeography, Palaeoclimatology, Palaeoecology*, **487**, 105–117.

STIGALL, A. L. 2023. A review of the Late Ordovician (Katian) Richmondian Invasion of eastern Laurentia. *Palaeogeography, Palaeoclimatology, Palaeoecology*, **618**, 111520.

ST. JOSEPH, J. K. S. 1938. The Pentameracea of the Oslo region being a description of the Kiaer collection of pentamerids. *Norsk Geologisk Tidsskrift*, **17**, 225–336.

STOUGE, S., RASMUSSEN, C. M. Ø. and HARPER, D. A. T. 2023. The Ordovician System in Greenland. 27–64. *In* SERVAIS, T., HARPER, D. A. T., LEFEBVRE, B. and PERCIVAL, I. G. (eds) *A global synthesis of the Ordovician System: Part 2*. Geological Society, London, Special Publications, **533**.

SURLYK, F. and HURST, J. M. 1984. The evolution of the early Paleozoic deep-water basin of North Greenland. *Bulletin of the Geological Society of America*, **95**, 131–154.

TORSVIK, T. H. and COCKS, L. R. M. 2013. New global palaeogeographical reconstructions for the Early Palaeozoic and their generation. *Geological Society, London, Memoirs*, **38**, 5–24.

TORSVIK, T. H. and COCKS, L. R. M. 2016. Ordovician. 101–123. *In Earth History and Palaeogeography*. Cambridge University Press.

TROEDSSON, G. T. 1928. On the Middle and Upper Ordovician faunas of northern Greenland, part 2. *Meddelelser om Grønland*, **72**, 1–197.

TWENHOFEL, W. H. 1914. The Anticosti Island faunas. *Geological Survey of Canada, Museum Bulletin*, **3**, 1–35.

TWENHOFEL, W. H. 1928. Geology of Anticosti Island. *Geological Survey of Canada Memoir*, **154**, 1–481.

WANG, Y. 1955. New genera of brachiopods. *Academia Sinica, Scientia Sinica*, **4**, 327–357.

WHITEAVES, J. F. 1891. Descriptions of four new species of fossils from the Silurian rocks of the southeastern portion of district of Saskatchewan. *Canadian Record of Science*, **4**, 293–303.

ZHAN, R. B. and COCKS, L. R. M. 1998. Late Ordovician brachiopods from the South China Plate and their palaeogeographical significance. *Special Papers in Palaeontology*, **59**, 1–70.